Aerobic Alcohol and Amine Oxidations Catalyzed by *Trans*-Dioxo(porphyrinato)ruthenium(VI) Complexes

by

Heather K. Dobson
B.Sc., University of Waterloo, 1996

A THESIS SUBMITTED IN PARTIAL FULFILLMENT OF
THE REQUIREMENTS FOR THE DEGREE OF
MASTER OF SCIENCE

in

THE FACULTY OF GRADUATE STUDIES
(Department of Chemistry)

We accept this thesis as conforming
to the required standard.

THE UNIVERSITY OF BRITISH COLUMBIA
September 1998

In presenting this thesis in partial fulfilment of the requirements for an advanced degree at the University of British Columbia, I agree that the Library shall make it freely available for reference and study. I further agree that permission for extensive copying of this thesis for scholarly purposes may be granted by the head of my department or by his or her representatives. It is understood that copying or publication of this thesis for financial gain shall not be allowed without my written permission.

Department of Chemistry

The University of British Columbia
Vancouver, Canada

Date Oct 8/98

DE-6 (2/88)

ABSTRACT

The stoichiometric and aerobic catalytic oxidations of amines and benzhydrols by *trans*-Ru(porp)$(O)_2$ complexes (porp = TMP, OCP, OCP-Cl_8, see Figure) in benzene under mild conditions are described.

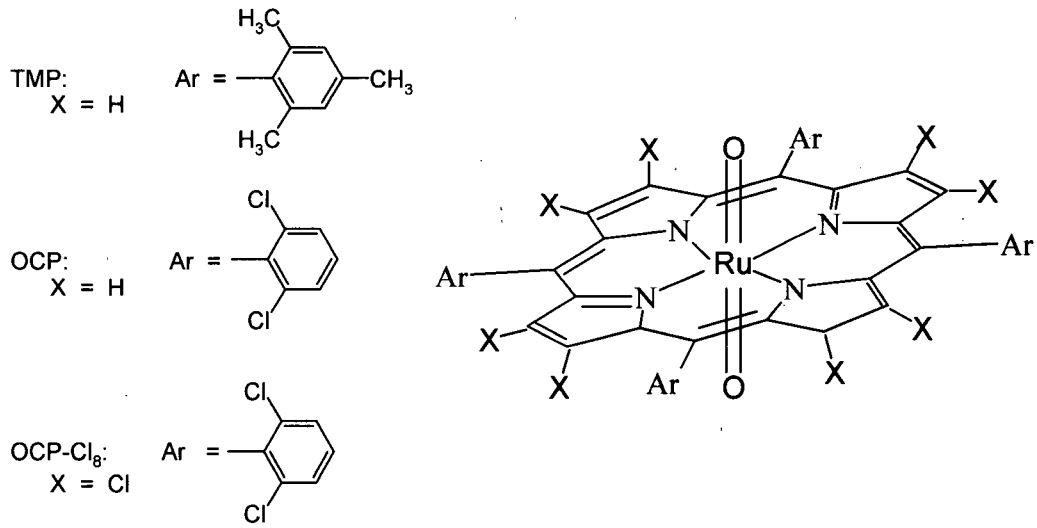

Figure: *Trans*-dioxo(porphyrinato)ruthenium(VI) complexes. TMP, OCP and OCP-Cl_8 are the dianions of *meso*-tetramesitylporphyrin, *meso*-tetra(2,6-dichlorophenyl)porphyrin and *meso*-tetra(2,6-dichlorophenyl)-β-octachloroporphyrin, respectively.

Kinetic data, determined by UV-VIS and ^{1}H-NMR spectroscopic analyses, for the stoichiometric oxidation of *p*-substituted benzhydrols indicate that the oxidation mechanism proceeds through the formation of a {Ru-alcohol} adduct (governed by an equilibrium constant K) which subsequently decomposes in a slower step (with rate constant k_1) leading to ketone formation. Isotope effects of $K^H/K^D \sim 0.6$ and $k_1{}^H/k_1{}^D \sim 15$ for α-deuteration of the alcohol indicate that the adduct is formed through hydrogen-bonding interactions probably between the Ru=O and the α-CH with cleavage of this C-H

bond occurring in the rate-determining step. Electron-donating substituents favour alcohol oxidation, as illustrated by a limited linear Hammett relationship of k_1 with $2\sigma_p$ for di-*p*-substituted benzhydrols. The {Ru-alcohol} adduct formation is essentially isenthalpic, while the k_1 activation parameters are $\Delta H_1^{\ddagger} = 58 \pm 10$ kJ/mol and $\Delta S_1^{\ddagger} = -120 \pm 30$ J/(mol K). *Trans*-Ru^{IV}(TMP)(alkoxo)$_2$ complexes have been isolated from the stoichiometric oxidation reactions and characterized by ^{1}H-NMR, UV-VIS and IR spectroscopies.

Aerobic oxidation of benzhydrols is catalyzed by *trans*-Ru(porp)$(O)_2$ at 50°C in benzene; ketones are the only organic products of the reaction. Water is essential for higher catalytic activity and turnovers of up to 24 (98% conversion) are seen at 50°C after 19 h. Under these conditions, the catalyst activities follow the trend: *trans*-Ru(OCP-Cl_8)$(O)_2$ > *trans*-Ru(TMP)$(O)_2$ > *trans*-Ru(OCP)$(O)_2$. Limited linear Hammett relationships, based on % conversion after 45 h at 50°C, indicate that catalytic oxidation is also favoured by the *p*-substitution of electron-donating substituents on the benzhydrols. Catalytic activity is limited by the rate of Ru(VI)-dioxo regeneration.

Stoichiometric amine oxidation by *trans*-Ru(OCP)$(O)_2$ and *trans*-Ru(TMP)$(O)_2$ studied by UV-VIS spectroscopy gives irreproducible results. The source of the irreproducibility is not determined, though it is not from trace oxygen, the amine, the catalyst, trace acid or water in the system. The reactions, however, are light-sensitive. Aerobic oxidation of amines is catalyzed by *trans*-Ru(porp)$(O)_2$ at 50°C under 1 atm of air; however, turnovers greater than 3 are only seen after 90 h in biphasic benzene/water systems, a result that contradicts a previous report.

TABLE OF CONTENTS

LIST OF TABLES

Table A.5. - A.52. Relative Intensity of ^{1}H-NMR Signals of *Trans*-Ru(TMP)$(O)_2$ as a Function of Time

LIST OF FIGURES

LIST OF ABBREVIATIONS

% conversion$_H$	% conversion of benzhydrol
% conversion$_X$	% conversion of a *p*-X substituted benzhydrol
δ	chemical shift
ε	extinction coefficient
ρ	Hammett factor
$\Delta H_1^{\ddagger}$	enthalpy of activation
λ_{max}	wavelength of maximum absorbance
σ_p	Hammett factor
$\Delta S_1^{\ddagger}$	entropy of activation
14-TMC	1,4,8,11-tetramethyl-1,4,8,11-tetra-azacyclotetradecane
15-TMC	1,4,8,12-tetramethyl-1,4,8,12-tetra-azacyclopentadecane
16-TMC	1,4,8,13-tetramethyl-1,4,8,13-tetra-azacyclohexadecane
A	absorbance
A_∞	absorbance at t = ∞
A_o	absorbance at t = 0 s
atm	atmosphere(s)
BHT	2,6-di(*t*-butyl)-4-methylphenol
bpy	bipyridine
br	broad
conc.	concentrated
d	doublet

dd	doublet of doublets
DMSO	dimethylsulfoxide
expt.	experiment(s)
eq.	equation(s)
equiv.	equivalent(s)
FAB	fast atom bombardment
FID	flame ionization detector
GC	gas chromatography
GC-MS	gas chromatography coupled with a mass spectrometer as a detector
HPLC	high performance liquid chromatography
Hz	Hertz
IR	infrared
K	equilibrium constant
k_1	rate constant for the rate determining step
k_{obs}	pseudo-first order rate constant
L	ligand
m	multiplet
M^-	negative ion parent peak
M^+	positive ion parent peak
m-CPBA	*m*-chloroperbenzoic acid
m.p.	melting point
MeOTPP	*meso*-tetra(3,4,5-trimethoxyphenyl)porphyrin (dianion)

MS	mass spectrometry
NADPH	nicotinamide adenine dinucleotide phosphate (reduced form)
NMO	N-methylmorpholine N-oxide
NMR	nuclear magnetic resonance
OAc	acetate
OCP	*meso*-tetra(2,6-dichlorophenyl)porphyrin (dianion)
OCP-Cl_8	*meso*-tetra(2,6-dichlorophenyl)-β-octachloroporphyrin (dianion)
OEP	β-octaethylporphyrin (dianion)
PhINTs	(4-methylphenyl)sulfonyliminoiodobenzene
porp	porphyrin dianion
R	alkyl or aryl group
r.t.	room temperature
rac-	racemic
Ru	Ru(porp)
s	second(s) or singlet
salen	bis(salicylaldehyde)ethylenediamine
t	triplet or time
$t_{1/2}$	half-life
TBAP	tetra(*n*-butyl)ammonium perruthenate
TBHP	*t*-butylhydrogen peroxide
TBPP	*meso*-tetra(4-*t*-butylphenyl)porphyrin (dianion)
TLC	thin layer chromatography

TMP	*meso*-tetramesitylporphyrin (dianion)
TMS	tetramethylsilane
TPAP	tetra(*n*-propyl)ammonium perruthenate
TPP	*meso*-tetraphenylporphyrin (dianion)
Ts	4-methylphenylsulfonyl or tosyl
UV-VIS	ultraviolet-visible
X	*p*-substituent

ACKNOWLEDGMENTS

Well it has been two years of hard work and I definitely would not have made it without some help. I would like to thank both Liane and Marietta who gave invaluable tips to make life easier in running the NMR spectrometers. Thanks also go to all of the James Gang for aiding me when the research was not going quite as planned! The final copy of my thesis would not have been quite so polished if it had not been for the work of my supervisor, who also deserves commendation for being so patient with my many mistakes. Finally...thanks Craig for keeping me sane!!

CHAPTER I

INTRODUCTION

The oxidation of organic substrates is a fundamental reaction in organic chemistry, whether it is performed on an industrial or laboratory scale.[1] At present, however, many reactions commonly use stoichiometric amounts of toxic metal oxidants, high temperatures and are plagued by low selectivities.[1,2,3] Due to environmental demands and the need for efficient, highly selective product formation, performing these reactions catalytically, under mild conditions and using inexpensive oxidants has become a important objective. Since the first use of RuO_4 as an oxidant in 1953,[4] Ru-oxo complexes have gained attention as versatile compounds for the oxidation of a wide range of substrates including, olefins, hydrocarbons, sulfides, alcohols and amines.[1,5-8] This versatility coupled with the fact that the oxidation reactions can be made catalytic under mild conditions[6] has stimulated efforts to develop Ru-oxo complexes as the ideal oxidation catalyst. The following chapter presents a brief review on the application of Ru-oxo complexes to oxidation reactions, focusing on recent developments in alcohol and amine catalytic oxidations.

Alcohol Oxidations

Ruthenium oxo species are well known for their ability to oxidize primary and secondary alcohols to aldehydes, carboxylic acids and ketones, as is evidenced by their inclusion in several reviews written on oxidation chemistry.[6,7] In most cases Ru-oxo species are the active catalysts although the pre-catalysts may be non-oxo ruthenium

complexes.[8] Often a stoichiometric amount of an oxygen atom donor such as: amine N-oxide, iodosobenzene, peroxide or dioxygen and a 2-equivalent reductant like an aldehyde, is required for catalysis; however, catalytic aerobic oxidation using only pure dioxygen or air as the co-oxidant is also possible. Alcohol oxidations by Ru complexes are discussed in the following sections according to the nature of the Ru complex and the type of co-oxidant used.

Non-porphyrin Ruthenium Oxidants

Reactions Catalytic in the Presence of NMO (N-methylmorpholine-N-oxide)

Some of the best known Ru-oxo complexes involved in alcohol oxidation are the perruthenates, TBAP (tetra-*n*-butylammonium perruthenate) and its more easily prepared TPAP (tetra-*n*-propylammonium perruthenate) analogue. In the presence of NMO these $[Ru^{VII}(O)_4]^-$ species will oxidize primary and secondary alcohols to aldehydes and ketones without affecting allylic, epoxy, lactone, indole, acetal and ether functionalities. Molecular sieves (4 Å) are required to absorb any water present in the reaction mixture. The reactions occur at room temperature (r.t.) and yield a maximum 500 turnovers (moles of substrate consumed per mole of catalyst used).[6] Mechanistic studies, in acetonitrile, show the reaction to be first-order in both the catalyst and alcohol and fractional order in NMO.[6,9] The reaction is thought to proceed via the initial formation of a catalyst-substrate complex which then undergoes a rate determining reaction with NMO to yield a second complex which rapidly forms the ketone products. Oxidation of cyclobutanol

yields mainly cyclobutanone indicating a 2-electron oxidation process occurs in the rate-determining step.[6]

Two of the oxygen atoms of perruthenate can be replaced with chlorine or nitrogen donors, without the loss of catalytic activity for alcohol oxidation. In addition, the chlorinated complex, $[Ru(O)_2Cl_3]^-$, will oxidize phosphines, thioethers, alkenes and phenols. These complexes function stoichiometrically as 2- or 4-electron oxidants (with halogen and nitrogen donors, respectively) and will oxidize alcohols to aldehydes or ketones with up to 135 turnovers. The use of chelating nitrogen donors, such as bipyridine, limits the use of the complex to stoichiometric oxidation only. Of note, the majority of the halogenated or nitrated dioxo complexes have *trans*-oxo ligands. When a carboxylate group is incorporated amongst the ligands a *cis*-dioxo orientation is exhibited. These $[Ru^{VII}(O)_2(OCOR)Cl_2]^-$ complexes selectively oxidize alcohols to aldehydes and ketones in the presence of double bonds. Oxidation of phosphines and thioethers also occurs.[6] Mechanistic studies show conflicting results, indicating a first-order dependence on the catalyst and either fractional or first-order dependence on each of the alcohol and NMO.[9,10] Tony *et al.* have proposed that the varying alcohol dependence results from the pre-association of the catalyst and alcohol.[9]

A few monooxoruthenium(IV) complexes are known; however, they are poorer oxidants than their corresponding dioxo analogues and will only catalytically oxidize activated benzylic alcohols.[6]

Reactions Catalytic in the Presence of TBHP (t-Butyl Hydrogen Peroxide)

With a three-fold excess of TBHP over the substrate, commercially available $RuCl_3 \cdot nH_2O$ will oxidize secondary alcohols to ketones with up to 550 turnovers at 80°C.[11] A Ru(III) N,N',N''-trimethyl-1,4,7-triazacyclononane derivative is capable of oxidizing activated allylic and benzylic alcohols to the corresponding aldehydes or ketones at r.t. Secondary aliphatic alcohols are also oxidized though only with 1/10 of the turnovers for the activated alcohols. Mechanistic studies indicate that the oxidation is probably a 2-electron process in that cyclic alcohols were oxidized to cyclic ketones; a Ru-O-O-*t*Bu complex was proposed as the active species.[12]

Reactions Catalytic in the Presence of Halogenated Co-oxidants: ClO_4^-, BrO_3^- and IO_4^-

The well-defined RuO_4 complex will catalytically oxidize a host of substrates in the presence of halogenated co-oxidants. Studies have indicated that the complex is a stoichiometric 5-electron acceptor, forming Ru(III) final products, with hydride transfer proposed as the rate-determining step.[6] In the presence of bromate, RuO_4^- will oxidize alcohols to acids and ketones in good yields and turnovers, though the reaction is non-selective and any double bonds present are cleaved.[6]

The perchlorate salts of several cationic *trans*-$[Ru(L)_2(O)_2]^{2+}$ and *trans*-$[RuL'(O)_2]^{2+}$ complexes, where L and L' are aromatic, 2- or 4-atom nitrogen donor ligands, respectively, have been studied as stoichiometric oxidants. A large amount of

work has been focused, in particular, on the use of cyclic tetra-aza ligands (Figure I.1).[6,13] Tellurato or iodato *trans*-$Ru(O)_2(bpy)$ complexes will catalyze the formation of aldehydes and ketones from alcohols at r.t., with up to 113 turnovers.[14]

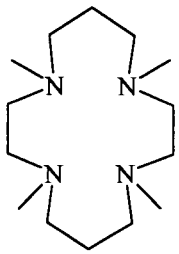

14-TMC
1,4,8,11-tetramethyl-1,4,8,11-tetra-azacyclotetradecane

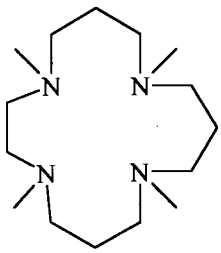

15-TMC
1,4,8,12-tetramethyl-1,4,8,12-tetra-azacyclopentadecane

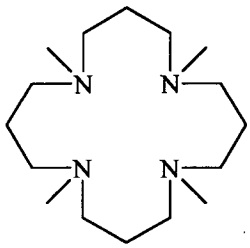

16-TMC
1,4,8,13-tetramethyl-1,4,8,13-tetra-azacyclohexadecane

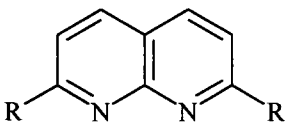

1,8-naphthyridines:
R = H, Cl, OMe, NH_2, N=N-Ph

Figure I.1. Cyclic tetra-aza and naphthyridine ligands.[6,15]

Recently, Boelrijk *et al.* have shown that the binuclear $[\{Ru(H_2O)L_2\}_2O]$ complexes, where L is 1,8-naphthyridine or its derivatives (Figure I.1), are capable of catalyzing oxidations of primary and secondary alcohols in aqueous solution. With a BrO_3^- co-oxidant, turnovers of 800-900 are achieved at r.t. Unfortunately the selectivity of the system is low as acid, aldehyde and double-bond cleavage products are obtained for the oxidation of allylic alcohols.[15]

Using O_2 as the Co-oxidant

Air or O_2 is the ideal oxygen source as it is inexpensive, readily available and only generates water as the reduced by-product, in contrast to the previously discussed co-oxidants. Unfortunately, the number of non-porphyrin systems that will catalytically oxidize alcohols using dioxygen as the co-oxidant is limited. One of the first reported was by Tang and co-authors, in 1978, when they determined that $RuCl_3$ would catalyze ketone formation from secondary alcohols under of 2-3 atm of O_2 at 100°C. The reactions, however, take 95-100 h and do not go to completion, forming olefin side-products in up to 50% yield. A maximum of 44 turnovers is achieved for the oxidation of octan-2-ol.[16] Subsequent studies by Matsumoto and Watanabe[17] and Drago's group[18] indicate that aerobic alcohol oxidation also occurs with $RuO_2 \cdot H_2O$ and the trinuclear ruthenium carboxylate complexes $[Ru_3O(O_2CR)_6L_3]^n$ (R = CH_3, C_2H_5; L = H_2O, PPh_3; and n = 0, 1+). In both cases temperatures of 65-70°C are required. Low turnovers of ~ 4 are achieved with $RuO_2 \cdot H_2O$, while 1000 turnovers are possible with the trinuclear ruthenium species under 3 atm of O_2 after 143 h. *Trans*-dioxoruthenium(VI) complexes with pyridine or TMC ligands will also promote aerobic oxidation of alcohols, though with low turnovers of 12 and 2.8, respectively, at r.t. over 18 h.[6] More recently, it was determined that TPAP would also catalyze the aerobic oxidation of alcohols in 60-99% yield at r.t. in CH_2Cl_2 over 30-60 min.[19,20] Catalyst concentrations of 5-10 mol% give optimum yields, lower concentrations resulting in deactivation of the catalyst after 10-20 turnovers. Switching the solvent to toluene allows oxidation at a catalyst concentration of 1 mol%; however, the reaction now takes 18 h to reach an equivalent, optimum,

conversion. As with TPAP oxidations with NMO, 4 Å molecular sieves are required to absorb the H_2O co-product for the oxidation of secondary alcohols. In contrast, primary alcohols are oxidized to aldehydes in higher yields in the absence of sieves.[19,20]

Other non-oxo Ru complexes have also been investigated for aerobic alcohol oxidation. In some tri-component systems, a Co-salen complex acts as the oxygen activating complex while a Ru complex is used to dehydrogenate the alcohol. The two components link the dehydrogenation of the substrate to the reduction of dioxygen to water using a quinone co-catalyst (Figure I.2). Reaction temperatures range from 20°C with $RuCl(OAc)(PPh_3)_2$ to 65-100°C with a binuclear Ru-carbonyl derivative. Turnovers of 70 and up to 200 based on Ru, respectively, are achieved.[21]

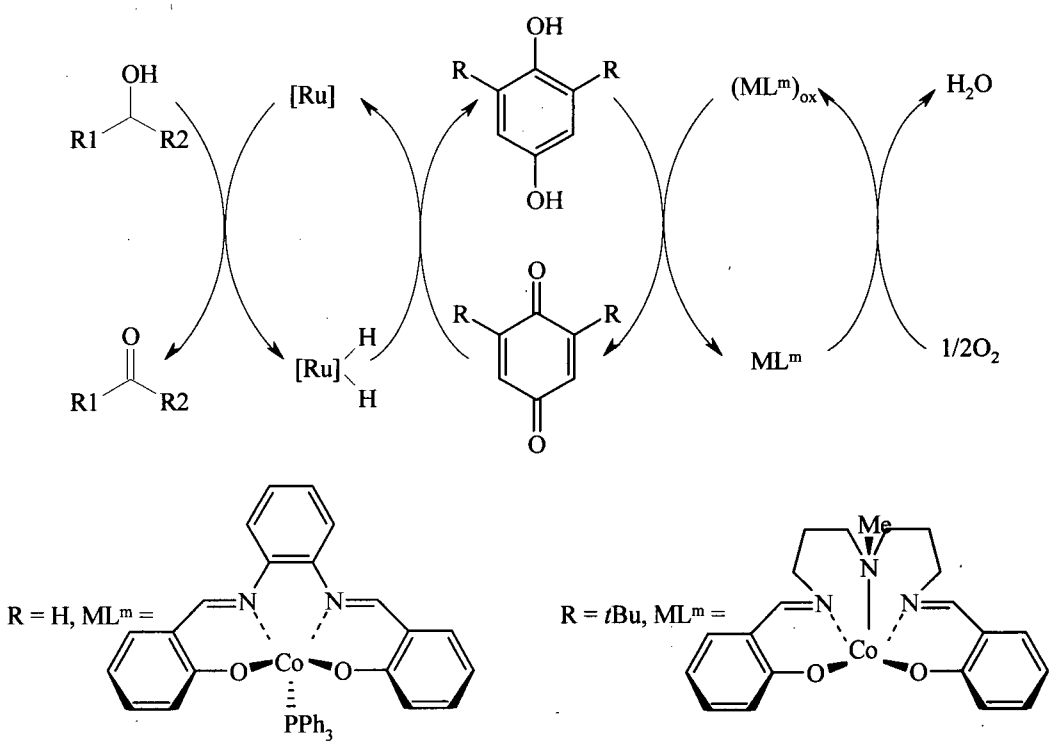

Figure I.2. Aerobic alcohol oxidation using a tri-component system.[21]

Ruthenium Porphyrin Oxidants

Cytochrome P-450: Nature's Oxidant

Metalloporphyrins have received attention as oxidation catalysts based on a relation to cytochrome P-450, an enzyme able to catalyze selectively the O_2-oxidation of a range of organic compounds under ambient conditions. This monooxygenase enzyme, first isolated from bacteria in 1970, has been found in a wide range of organisms from bacteria to humans, and functions as a catalyst in the oxidation of substrates under aerobic conditions in the presence of an electron source (NADPH). The active oxidation site in cytochrome P-450 is an iron(III) protoporphyrin IX (FePpIX) complex that is bound to the protein through the sulfur atom of a cysteine thiolate residue (Figure I.3).[22a]

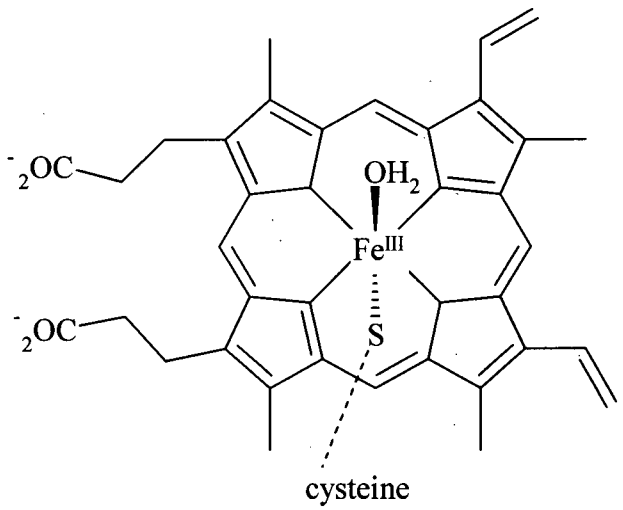

Figure I.3. Iron protoporphyrin IX prosthetic group in cytochrome P-450.[22]

Oxygen binds to the metal centre and leads to the formation of the active oxidizing species $(PpIX^{\bullet+})Fe^{IV}(O)$, which transfers the oxygen atom to a substrate to regenerate the starting $Fe^{III}(PpIX)$ moiety.[22b] The substrate itself is not bound directly to the iron

centre but is held within the hydrophobic pocket formed by the amino acid residues that surround the active site.[22c] The proposed catalytic cycle for substrate oxidation is shown below; however, only the first three steps of the mechanism have been spectroscopically verified while the remaining steps occur too rapidly to be distinguished (Figure I.4).[22]

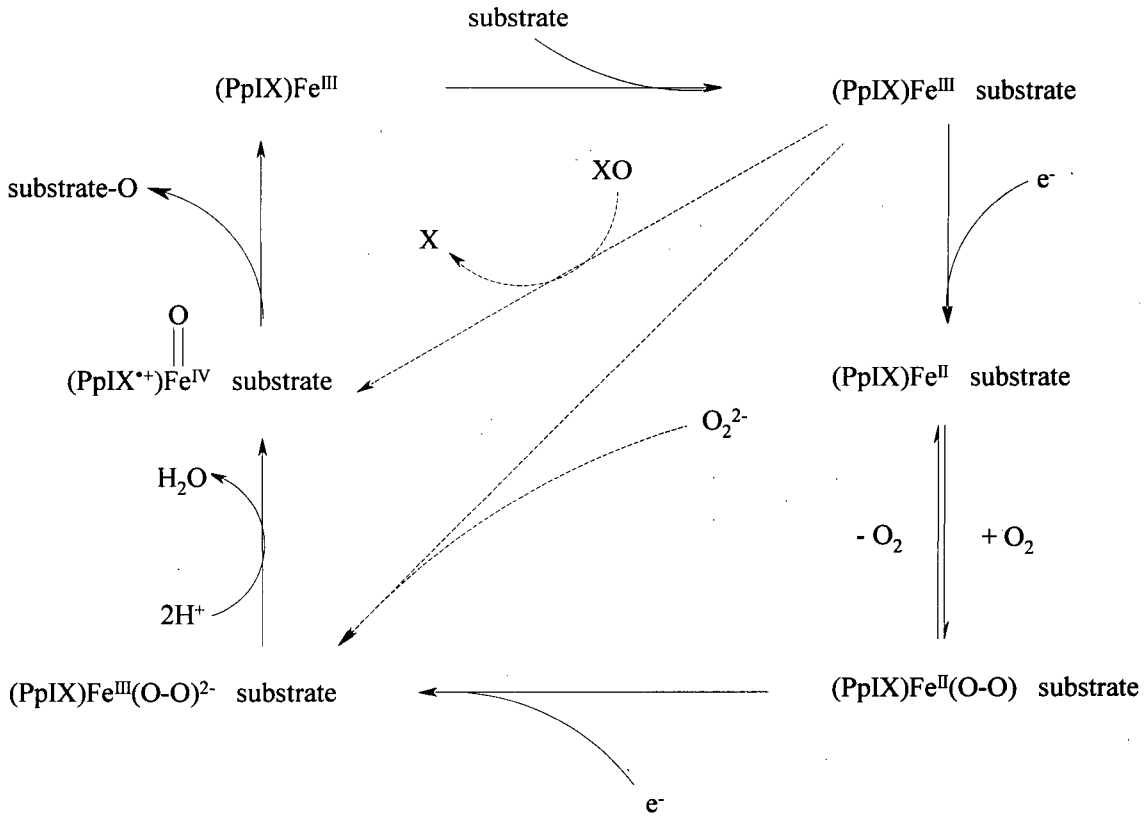

Figure I.4. Mechanism for substrate oxidation catalyzed by cytochrome P-450; the alternate pathways utilizing (i) an O-atom donor (XO) and (ii) a peroxide are also shown.[22]

Synthetic Ruthenium Porphyrins

Several metal based porphyrin systems, including Fe, Mn and Ru have been studied in an effort to simulate the activity of cytochrome P-450 *in vitro*.[23] Ruthenium has the distinction of forming metalloporphyrin oxidation catalysts that exhibit true dioxygenase character and transfers both oxygen atoms of O_2 to the substrate without the use of additional co-reductants. Fe- and Mn-based systems will also oxidize substrates under O_2; however, only in the presence of an electron source such as $NaBH_4$ or ascorbate.[23]

Synthetic porphyrins, in contrast to naturally occurring porphyrins such as protoporphyrin IX, are generally substituted at the bridging carbon rather than on the pyrrole rings (octaethylporphyrin, H_2OEP, is one exception). Three generations of porphyrin molecules have been described when their use as ligands in Ru porphyrin oxidations are discussed.[23] The first generation is *meso*-tetraphenylporphyrin (H_2TPP) and its alkyl-derivatives. Unfortunately, Ru(TPP) species are unstable under oxidizing conditions and decompose to form the μ-oxo 'dimer' $[Ru(TPP)(OH)]_2O$. Methyl group substitution at the *ortho* and *para* positions on the *meso*-phenyl rings forms the more stable *meso*-tetramesitylporphyrin (H_2TMP), allowing isolation of a *trans*-dioxoruthenium(VI) (*trans*-$Ru(TMP)(O)_2$) complex (Figure I.5).[24a] The second and third generation of porphyrins have halogenated phenyl substituents and pyrrole rings, respecitively.[24] Like H_2TMP, these porphyrins, such as *meso*-tetra(2,6-dichlorophenyl)porphyrin (H_2OCP) and *meso*-tetra(2,6-dichlorophenyl)-*β*-octachloroporphyrin ($H_2OCP\text{-}Cl_8$), form isolable *trans*-dioxo complexes (Figure I.5).[24]

Interestingly, chlorinating the pyrrole positions of the porphyrin leads to saddle and ruffle distortions of the porphyrin plane in both the free-base and the corresponding Ru(porp)CO complexes.[25]

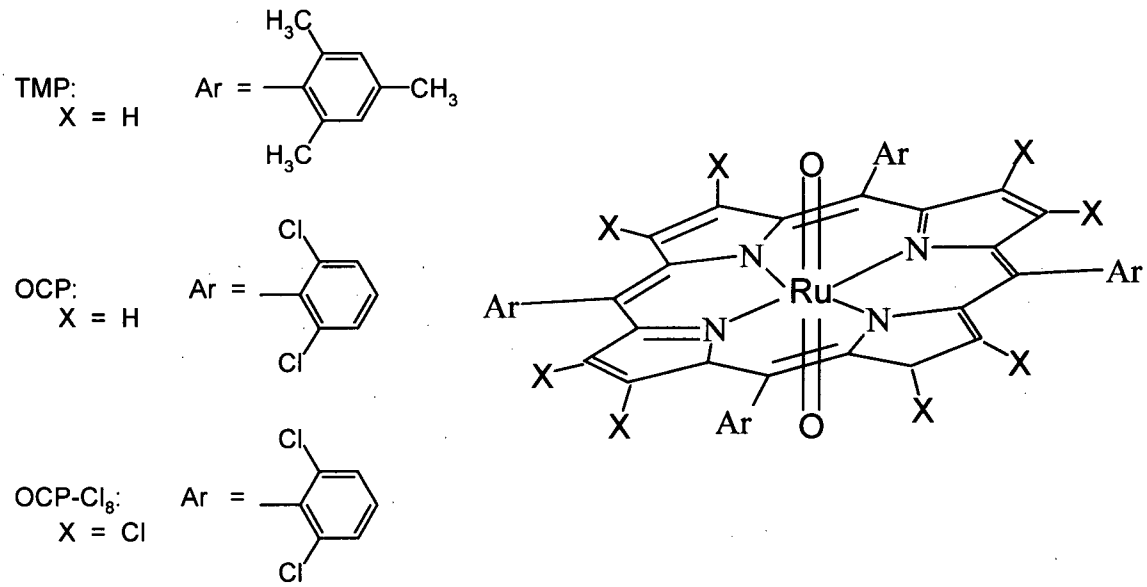

Figure I.5. *Trans*-dioxo(porphyrinato)ruthenium(VI) complexes.

Trans-dioxo(porphyrinato)ruthenium(VI) complexes (porp = TMP, OCP, OCP-Cl_8), synthesized from *m*-CPBA oxidation of Ru(porp)(CO) complexes, aerobic oxidation of *trans*-Ru(porp)$(L)_2$ complexes (L = MeCN,[5,26] THF,[27] or N_2[28]), or oxidation of *trans*-Ru(porp)$(THF)_2$ with N_2O,[29] exhibit rich oxidation chemistry. The dioxo complexes will catalytically oxidize olefins to epoxides,[5,24] thioethers to sulfoxides,[5] tertiary arylphospines, $AsPh_3$ and $SbPh_3$ to the corresponding oxides,[30] alcohols to aldehydes and ketones,[31,32] Ph_3CH to Ph_3COH,[32] and amines to imines and nitriles.[33] The stoichiometric oxidation of phenols to quinones is also possible.[24]

Reactions Catalytic in the Presence of Amine N-oxides

The first highly efficient oxidation of alcohols to aldehydes and ketones catalyzed by Ru porphyrin complexes was published by Ohtake *et al.* in 1991.[34] Heteroaromatic amine N-oxides are used as the co-oxidants to oxidize primary allylic and benzylic alcohols to aldehydes in 65-90% yield (non-activated alcohols gave only 2% yield of the corresponding aldehyde) at r.t. Catalyst turnovers are within the range of 110-150. Subsequent research by the same authors indicates that the addition of concentrated HBr or HCl and molecular sieves to the reaction mixture allows even non-activated secondary alcohols to be readily oxidized.[35] After 24 h at r.t., ketones are formed selectively in 80-90% yield, with catalyst turnovers of 160-180. Interestingly, hydroxylation of alkanes, using N-oxide co-oxidants, is also catalyzed by $Ru(TMP)(O)_2$, Ru(TMP)(CO) and Ru(TPP)(CO) with turnovers up to 120000 over a period of 6 h at 40°C (5.6/s). Under these conditions, Ru(TPP)(CO) is actually the best catalyst. The acid is thought to react with the Ru porphyrin precursors to form bromo/chloro species; the acid then, perhaps, accelerates the deoxygenation of the N-oxide co-oxidant by the Ru porphyrins to form the proposed active catalytic species *trans*-Ru(porp)(O)(X) (X = Cl, Br),[35] although other formulations are feasible.[24]

Catalytic Aerobic Oxidations with Ruthenium Porphyrins

At 50°C under 1 atm of air, *trans*-$Ru(porp)(O)_2$, where porp = TMP or OCP, catalyze the aerobic oxidation of alcohols to aldehydes and ketones.[31,32,36] Water or KOH (3 M) is essential for the catalytic activity of the complexes in 2-phase aqueous/benzene

media. Complete conversion occurs for benzylic alcohols after 16 h, showing catalyst turnovers of 200; however, the oxidation of inactivated alcohols is much slower and shows only 8-20% conversion and 16-40 turnovers after 16 h. Both the TMP- and OCP-based complexes are equally active towards alcohol oxidation, though bleaching of the OCP system occurs after 16 h indicating catalyst deactivation. In contrast, the TMP-based system still shows some catalytic activity after 10 days. Kinetic studies for the stoichiometric oxidation of *i*PrOH with *trans*-Ru(TMP)$(O)_2$ (eq. 1.1) indicate that the reaction is first-order in both the catalyst (10^{-4}-10^{-3} M) and substrate (up to 0.3 M). A paramagnetic (S = 1), *trans*-Ru(TMP)$(OCH(CH_3)_2)_2$ complex, isolated from the stoichiometric reactions and characterized by NMR, IR, UV-VIS spectroscopies and X-ray crystallography, is proposed to be an intermediate in the aerobic oxidation of the alcohol. Finally, kinetic isotope labeling studies on the stoichiometric reaction show an intramolecular isotope effect of ~ 2 attributed to α-CH bond cleavage which, when combined with an increased rate of reaction in the presence of added base, indicates that hydride transfer is probably the rate-controlling step. Of note, at high concentrations of *i*PrOH (1-2 M) the k_{obs} vs. [*i*PrOH] plot levels off, where k_{obs} is the measured pseudo first-order rate constant for loss of *trans*-Ru(TMP)$(O)_2$ in eq. 1.1.

$$Ru(TMP)(O)_2 + 3\ i\text{PrOH} \rightarrow Ru(TMP)(O i\text{Pr})_2 + Me_2C{=}O + 2\ H_2O \qquad (1.1)$$

These results were attributed to solvent effects, rather than saturation kinetics, as the oxidation of *i*PrOH in the presence of high concentrations of *t*BuOH (an alcohol inert to oxidation) had a lower k_{obs} than the oxidation of *i*PrOH in the absence of *t*BuOH.[31,32,36] Further work, in this thesis, has attempted to confirm these results and study the effect of changing steric and electronic factors of the substrate on the rate of alcohol oxidation.

Amine Oxidations

Amine oxidations are important reactions from both synthetic and metabolic perspectives. In living systems, amines are oxidized by a variety of enzymes, including cytochrome P-450, amine oxidase and flavoenzymes.[1] Cytochrome P-450, in particular, will catalyze the formation of N-oxides and N-dealkylated or N-dehydrogenated products from amines.[37] Understanding the mechanisms of these reactions is important in the metabolism of both naturally occurring amines and xenobiotics.[38] Amine oxidations are also important in the synthesis of biologically active compounds, including antibiotics.[39] Because of the versatility of Ru complexes in the catalytic oxidation of a variety of organic substrates, extending their application to amine oxidation was a logical step.

Non-Porphyrin Ruthenium Oxidants

Reactions Catalytic in the Presence of NMO, PhIO and Peroxides

Tertiary amines are oxidatively N-demethylated by Ru catalysts, at r.t., in the presence of peroxides, TBHP[40] and H_2O_2.[41] The reactions are thought to proceed through the formation of an iminium intermediate which is then trapped to give the corresponding

α-substituted alkylamine (Figure I.6). In the presence of TBHP (2-3 equiv.), a $RuCl_2(PPh_3)_3$ catalyst (3 mol%) will oxidize a range of tertiary N-methylanilines to N-*t*-butyldioxymethylanilines in 80-95% yield. With H_2O_2 (1.5-4 equiv.), the reactions are performed in MeOH with $RuCl_2(PPh_3)_3$ or $RuCl_3 \cdot nH_2O$ (5 mol%) to yield 55-87% of the tertiary N-methoxymethylanilines. In both systems, treatment of the trapped products with aqueous HCl results in the formation of N-demethylated amines.

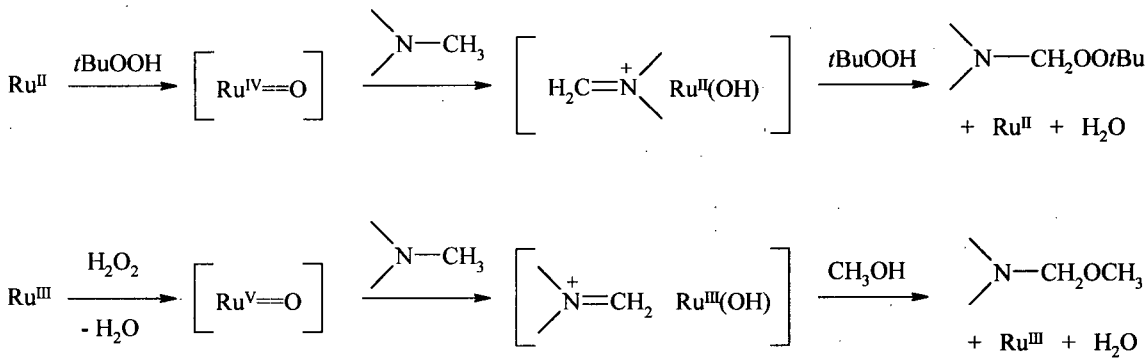

Figure I.6. Mechanism of amine oxidation with peroxide co-oxidants.[1,41]

The same catalyst, $RuCl_2(PPh_3)_3$, will oxidize activated secondary amines to imines in 55-98% yield. Both TBHP[42] and PhIO[43] co-oxidants have been used. In the absence of an activating phenyl ring or double bond, α to the C-H bond being cleaved, oxidation does not occur. Activated primary amines are also oxidized by the catalyst and PhIO, though, in low yields, 15-40%. In these reactions, the imine intermediate is hydrolyzed to give aldehyde and ketone products.[43]

More recently, Goti and co-workers[44] have determined that the use of TPAP in oxidation reactions may also be extended to include amine substrates. Tertiary

hydroxylamines are oxidized to nitroenes, in 75-100% yield, using NMO co-oxidant. The reactions occur at r.t., in the presence of 4 Å molecular sieves, with 1-5 mol% of the catalyst and a minimum of 1 equiv. of NMO. Under similar reaction conditions, TPAP will oxidize activated secondary amines to imines in 52-95% yield.[45] Imine formation by TPAP-catalyzed amine oxidation has recently been applied to the synthesis of pyrrolo[2,1-*c*][1,4]benzodiazepine antibiotics.[39] The mild conditions, absence of side-product formation, non-aqueous work up and minimized racemization during the reaction were the main advantages for the use of this method of imine synthesis.

Aerobic Amine Oxidations

In 1978, Tang *et al.* first reported that aerobic oxidation of amines was possible using Ru catalysts.[16] Under 2-3 atm of O_2 at 100°C in toluene, $RuCl_3 \cdot nH_2O$ oxidizes benzyl- and *n*-butylamines to the corresponding nitriles and amides with 90-100% conversion. Ketones, N-alkylimines and uncharacterized high boiling compounds are the products of the oxidation of 2-aminoalkanes, in 70% conversion. The reaction is thought to proceed through the formation a Ru(III) hydride species created from β-hydride elimination within a Ru(III) amine complex.[16] (The first example of β-hydride elimination from an amine was recently demonstrated within an Ir complex.)[46] Aerobic oxidation of benzyl- and *n*-butylamine is also effected by a $RuCl_2(PhCH_2NH_2)_2(PPh_3)_2$ catalyst to form the corresponding nitriles at r.t. under 1 atm of O_2; based on a study of these reactions it is proposed that O_2 oxidizes the Ru(II) to Ru(III), with subsequent dehydrogenation of the amine and regeneration of Ru(II).[47] Secondary amines are

oxidized to imines and imine hydrolysis products by $RuCl_2(PPh_3)_3$ and *cis*-$RuCl_2(DMSO)_4$ at 80°C in toluene under a constant flow of O_2; these catalysts are not very active and only oxidize dibenzylamine in 35% conversion.[48]

Tertiary amines are stoichiometrically N-demethylated by cationic $[Ru(bpy)_2(O)(PR_3)](ClO_4)_2$ complexes (bpy = 2,2'-bipyrindine, R = Ph or Et) under an inert atmosphere to form N-methylaniline and formaldehyde;[49] the kinetics of the reaction with N,N-dimethylaniline indicate a first-order dependence on both the complex and substrate, and in MeCN a $[Ru(bpy)_2(PR_3)(MeCN)]^{2+}$ complex is formed. The reaction is assumed to proceed through the transfer of an oxygen atom from the Ru(IV) complex to the substrate, with the final inclusion of oxygen in the formaldehyde co-product. Under 1 atm of O_2 in non-coordinating solvents, the reaction is catalytic with $[Ru(OH_2)(bpy)_2(PPh_3)](ClO_4)_2$; at r.t. with 0.1 mol% of the catalyst, N,N-dimethylaniline is demethylated to form N-methylaniline and formaldehyde exclusively. As the stoichiometric and catalytic reactions generated the same products, it was proposed that the (oxo)ruthenium(IV) complex, formed from the reaction of the Ru(II) precursor with O_2, is the active catalyst.[49]

Ruthenium Porphyrin Oxidants

Despite the well known use of Ru porphyrins as oxidants of organic substrates,[24] little work has been published on their use in the dehydrogenation of amines. The first example was reported in 1992 by Huang *et al.* who found that *trans*-

dioxo(*meso*-tetra(3,4,5-trimethoxyphenyl)porphyrinato)ruthenium(VI) complexes (*trans*-Ru(MeOTPP)$(O)_2$) would dehydrogenate diphenylamine 'stoichiometrically' to form a bis(diphenylamido)ruthenium(IV) complex.[50] This complex is stable in solution, can be purified by column chromatography and recrystallized from CH_2Cl_2 and heptane solvents. The complex was characterized by UV-VIS, IR and ^{1}H-NMR spectroscopies. Elemental analysis was also performed on the complex, but was not reported. Interestingly, in contrast to known paramagnetic dihalogeno-[51] and dialkoxoruthenium(IV)[31] complexes, the bis(diphenylamido) complex is diamagnetic, similar to dialkyl- and diaryl(porphyrinato)ruthenium(IV)[52] complexes. The absence of N-H stretches and a band at 1012 cm^{-1} in the Ru oxidation state region[26,27] confirms the amido and Ru(IV) nature of the complex.[50]

More recently, Morice *et al.* have reported the stoichiometric dehydrogenation of amino esters by *trans*-dioxoruthenium(VI) picket-fence type porphyrin complexes.[38] In this case, Ru(II) imino ester complexes are isolated in 44-55% yields (Figure I.7). The reactions are performed in an excess of amino ester at r.t. under an inert atmosphere. The resulting imino ester complexes can be purified by column chromatography and are characterized by IR, UV-VIS and ^{1}H-NMR spectroscopies, the NMR data indicating two different axial ligands. The presence of the imino ester ligand is confirmed by the presence of a singlet for the N-H proton and one for the α-Me substituent within the alanine methyl ester species, and two doublets (J = 20 Hz, NH and CH) for the corresponding glycine methyl ester complex, in the ^{1}H-NMR data.[38]

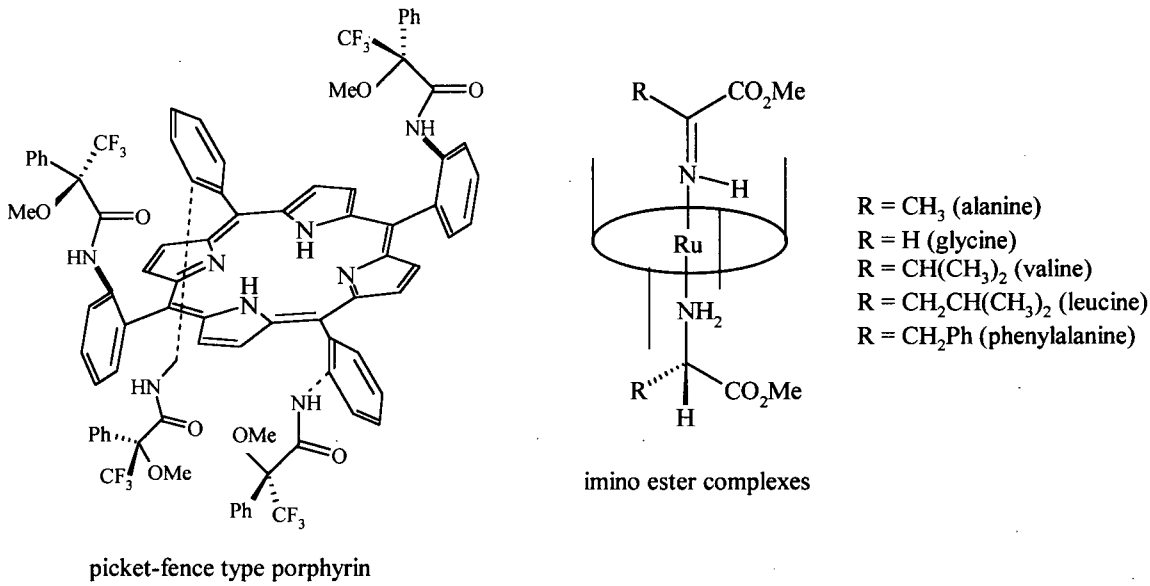

Figure I.7. Ruthenium imino ester complexes.[38]

The first dehydrogenation of amines catalyzed by Ru porphyrins was reported by Bailey and James.[33] Primary amines of the form RCH_2NH_2 (R = aryl or alkyl) are quantitatively converted to nitriles at 50°C under 1 atm of air in benzene after 24 h. In contrast, primary, of the type R_2CHNH_2 (R = aryl), and secondary amines are oxidized to imines in 75-90% yield, whereas R_2CHNH_2 amines (R = alkyl) form imines only in low yields of 10-20%. With the exception of the synthesis of nitriles, all of the reactions show side-products due to imine hydrolysis. The three dioxo complexes, *trans*-Ru(TMP)$(O)_2$, *trans*-Ru(OCP)$(O)_2$ and *trans*-Ru(OCP-Cl_8)$(O)_2$, were used in the investigation, with the chlorinated catalysts showing faster rates of reaction and deactivation. A bis(benzylamine) complex, isolated from the *trans*-Ru(TMP)$(O)_2$-catalyzed oxidation of benzylamine and characterized by X-ray crystallography, UV-VIS, IR and ^{1}H-NMR spectroscopies, indicates bis(amino)ruthenium(II) complexes are the final Ru products.

The observation of N-H stretches at 3028 cm^{-1} and a Ru(II) oxidation state marker[26,27] at 1000 cm^{-1} in the IR spectrum confirm the presence of the amine ligands.[33] Kinetic and mechanistic details of these reactions are unknown and were sought as a part of this work.

Ruthenium porphyrin imido complexes can be synthesized directly from (i) the reaction of PhINTs ((4-methylphenyl)sulfonyliminoiodobenzene) with Ru(porp)(CO)(MeOH) (porp = TPP or OEP),[53] (ii) the reaction of Ru(porp)$(Cl)_2$ (porp = *meso*-tetra(4-*t*-butylphenyl)porphyrin, TBPP) with *para*-substituted anilines,[54] and (iii) by the bromine oxidation of Ru(porp)$(t\text{BuNH}_2)_2$ (porp = TPP or MeOTPP).[55] In the first case, a bis(tosyl)imidoruthenium(VI) complex was isolated and characterized. The NTs group can be transferred to alkenes to form aziridines and the complex will oxidize benzyl alcohol to benzaldehyde in 95% yield. The Ru(IV) complex Ru(TBPP)(NR) isolated from the second reaction will react with PPh_3 to give $RN{=}PPh_3$ and the bis(phosphine)ruthenium(II) complex. This imido complex is paramagnetic, with a magnetic moment corresponding to two unpaired electrons. In the presence of PhIO, the imido complex will also catalyze the epoxidation of styrene in 25% yield. The third reaction forms diamagnetic *trans*-Ru(porp)(O)(N*t*Bu) complexes that will react with PPh_3 to form $O{=}PPh_3$, $t\text{BuN}{=}PPh_3$ and Ru(porp)$(PPh_3)_2$. The corresponding bis(imido) complexes were not formed, possibly due to hydrolysis to form the more stable oxoimido complexes.

Goals of this Thesis

This thesis is an extension of the work recently done in this laboratory on alcohol and amine oxidation reactions catalyzed by Ru porphyrin complexes.[31-33,36] The goals set for this thesis were:

1. To investigate the kinetics of the stoichiometric oxidation of *para*-substituted benzhydrols with *trans*-Ru(porp)$(O)_2$ oxidants, to help establish the mechanism of alcohol oxidation (porp = TMP, OCP or OCP-Cl_8).
2. As a subsection of goal 1, to determine the role that electronic changes in the alcohol have on the rate of stoichiometric and catalytic oxidations effected by *trans*-Ru(porp)$(O)_2$.
3. To investigate the mechanism of amine oxidation by *trans*-Ru(porp)$(O)_2$.

CHAPTER II

EXPERIMENTAL

General

Gases [CO, N_2, Ar, and O_2 (99+% pure)] were supplied by Linde Gas, Union Carbide Inc. The Ar used in photolysis was passed through a Ridox column (Fisher Scientific) to remove trace O_2. Trace moisture present in Ar and N_2 was removed by passing the gases through a column of $CaSO_4$ (Fisher Scientific).

The solvents used for synthetic or purification purposes, such as CH_2Cl_2, benzene, toluene, and CH_3CN, were supplied by Fisher Scientific as spectroscopic grade. When dry benzene was required, the solvent was dried over Na/benzophenone and stored under N_2. All other solvents, required to be moisture-free, were dried over CaH_2 and stored under N_2. Decalin, purchased from Aldrich, was used without further purification. Deuterated solvents (C_6D_6, $CDCl_3$, CD_3CN, DMSO-d_6 and D_2O, all 99.6+% deuterated) were purchased from Cambridge Isotope Laboratories. When needed to be used under anaerobic conditions, the solvents were degassed using three freeze-pump-thaw cycles or sparged with dry Ar or N_2 for 20-30 min

Fine chemicals were purchased either from Fisher Scientific or Aldrich, while $RuCl_3 \bullet 3H_2O$ was obtained on loan from Johnson Matthey Ltd. or Colonial Metals Inc. Dodecacarbonyltriruthenium, $Ru_3(CO)_{12}$, was prepared according to a published procedure and recrystallized from benzene to yield a bright orange crystalline solid.[56]

Pyrrole was distilled from CaH_2 prior to use and stored at 4°C under N_2. BF_3 etherate and MeOH complexes were stored in a vacuum desiccator. Benzhydrols were purified by recrystallization from hexanes and Et_2O prior to use. Amines were purified by distillation (under vacuum where necessary) and stored over molecular sieves (5 Å, BDH) under N_2.

All reactions involving air- or moisture-sensitive reagents were performed under an atmosphere of Ar or N_2 on the bench using standard Schlenk techniques. Reactions were monitored by thin layer chromatography (TLC) using pre-coated, aluminum backed, silica and neutral alumina sheets (Fisher Scientific). Flash chromatographic purification was carried out on silica gel 60 (220-400 mesh ASTM), neutral alumina (activity I), or basic alumina (activity I) purchased from Fisher Scientific.

The NMR-spectra were measured on Varian XL-300 (300 MHz), Bruker AC-200E (200 MHz) or Bruker WH-400 (400 MHz) FT spectrometers. Proton chemical shifts are given as δ in parts per million (ppm) against the residual solvent as the internal standard (7.15 ppm for C_6H_6, 7.24 ppm for $CHCl_3$ and 2.49 ppm for DMSO), relative to TMS. Fluorine chemical shifts are given as δ referenced to CF_3CO_2H in C_6D_6 or $CDCl_3$ and were obtained on the Bruker AC-200E (188.31 MHz) spectrometer. The ^{1}H-NMR chemical shift multiplicities are denoted as follows:

s: singlet dd: doublet of doublets

d: doublet m: multiplet

t: triplet br: broad

Variable temperature experiments were performed on the Varian XL-300 spectrometer using C_6D_6 and $CDCl_3$ solvents. The temperature of the probe was allowed to equilibrate for at least 15 min before analysis of a reaction commenced. In anaerobic experiments, a pulse delay of 2 s was incorporated into all of the experiments to ensure complete relaxation of the porphyrin ^1H resonances. The procedure used to measure the kinetics of alcohol oxidations by ^1H-NMR spectroscopy is detailed at the start of Chapter III.

The infrared spectra, over the range of 4000-600 cm^{-1}, were recorded on a ATI Mattson Genesis Series FTIR instrument. Samples were prepared as: (a) a Nujol mull between two KBr plates, or (b) a solid dispersed within a compressed KBr pellet. Only the relevant absorptions are listed.

Spectroscopic UV-Visible data were collected on a Hewlett-Packard 8452A Diode-Array Spectrophotometer (resolution 2 nm) equipped with a thermoelectric temperature controller. Extinction coefficients, ε, are given in units of M^{-1} cm^{-1} in parentheses following the reported wavelength maximum, λ_{max}. Anaerobic kinetic studies followed by UV-VIS were obtained using an anaerobic cell having a 1.0 or 0.1 cm path length

(Figure II.1). The procedures used in these studies are presented at the beginnings of Chapters III and IV.

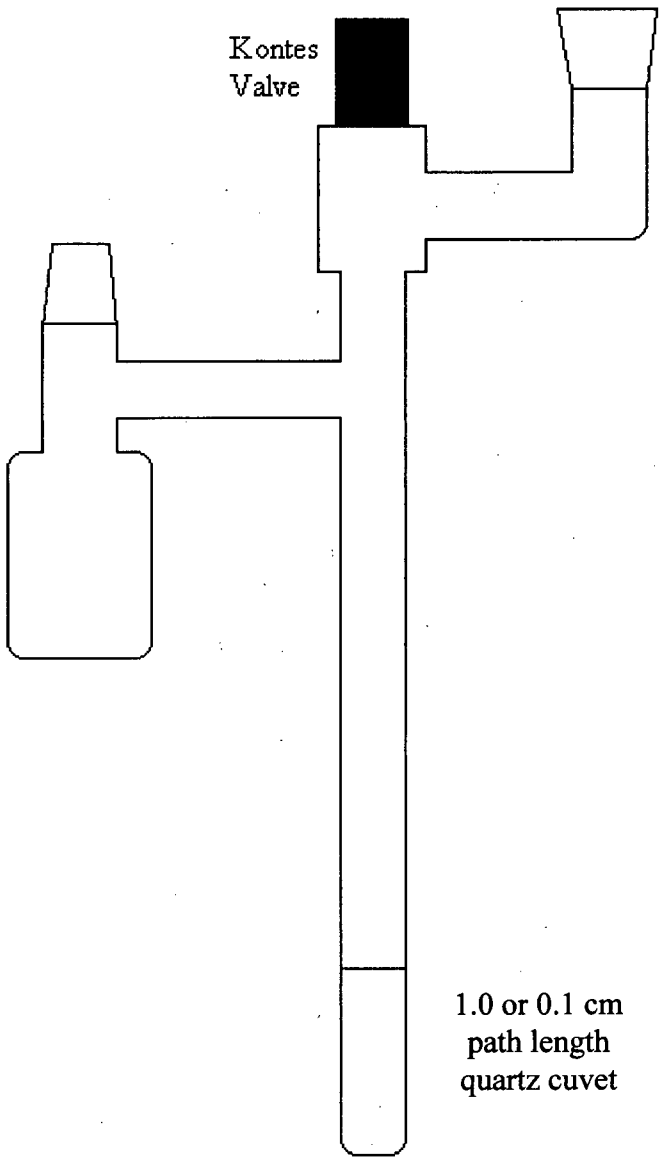

Figure II.1. Anaerobic UV-VIS spectroscopic cell.

Elemental analyses were obtained by Mr. P. Borda of this department. Mass spectral analyses were performed in this department in a facility headed by Dr. G. Eigendorf. A fast atom bombardment (FAB) on thioglycerol and 3-nitrobenzylalcohol matrices method of ionization was used.

Melting points were obtained from samples placed between glass plates using a Fisher-Johns apparatus. The experimental values were not corrected.

Samples were analyzed by gas chromatography on an HP 5891A instrument, using He as the carrier gas, equipped with a hydrogen-flame ionization detector (FID). All of the gases were purified with Supelco gas-purifier systems (HC 2-2445). Separation of the sample components was obtained using a medium polarity HP-17 column (cross-linked 50%-Ph-50%-Me silicon capillary column, 25 m in length, 0.32 mm inner diameter, 0.26 μm thick column coating) or a polar Carbowax 20 column (polyethylene glycol stationary phase, 25 m in length, 0.2 mm inner diameter, 0.1 μm thick column coating). Injection volumes of 0.5 - 1 μL were used with sample concentrations of the order of 10^{-2} to 10^{-1} M. The column head pressure was maintained at 15.5 psi and a split-gas flow rate of ~ 70 mL/min was used to ensure that the sample would not overload the column. A chromosorb W-HP precolumn was used to ensure that all of the metal was removed from the sample before it reached the start of the column. The conditions for separation of the amine and alcohol standards are listed in Table II.1 and Table II.2, respectively. Calibration curves of concentration versus peak area were measured over four

concentrations for each of the samples to determine the ratio of substrate/product detector response for each column.

Table II.1. Conditions for Amine Separation by GC.

Substrate/Product [Column][a]	**Temperature Program[b]**	**Retention Times (min)**	**Detector Response Ratio (Substrate/Product)**
Ph_2CHNH_2/ $Ph_2C{=}NH$ [Carbowax 20M]	80°C (2 min) 10°C/min to 220°C (10 min)	17.38 17.63	0.75/1
Ph_2CHNH_2/ $Ph_2C{=}NH$, Ph_2CO [HP-17]	150°C (5 min) 2°C/min to 180°C	12.69 13.58 13.10	1/1/1
$Ph(Me)CHNH_2$/ $Ph(Me)C{=}NH$[c] [Carbowax 20M]	80°C (2 min) 10°C/min to 220°C (10 min)	7.36 8.43	1/1
$PhCH_2NH_2$/ benzonitrile [Carbowax 20M]	same as above	7.67 7.97	0.6/1
$(PhCH_2)NH$/ $PhCH_2N{=}CHPh$, benzonitrile, PhCHO [Carbowax 20M]	60°C (2 min) 20°C/min to 220°C (10 min)	16.54 17.25 10.32 9.60	2.2/1/1.2/2.3

[a] Compounds were standards, obtained commercially from Aldrich. Concentrations ranged from 10^{-2} to 10^{-1} M in benzene.

[b] Injector and detector ports were maintained at 220°C.

[c] Determined by GC-MS.

Table II.2. Conditions for Alcohol Separation by GC.

Substrate/Product [Column][a]	**Temperature Program[b]**	**Retention Times (min)**	**Detector Response Ratio (Substrate/Product)**
Ph_2CHOH/ Ph_2CO [HP-17]	150°C (5 min) 2°C/min to 175°C	13.44 12.99	1/1
(p-MeO-C_6H_4)$_2$CHOH/ (p-MeO-C_6H_4)$_2$CO [HP-17]	150°C (2 min) 10°C/min to 220°C (5 min)	12.07 15.14	1/1
(p-F-C_6H_4)$_2$CHOH/ (p-F-C_6H_4)$_2$CO [HP-17]	same as above	7.25 6.47	1/1
(p-Cl-C_6H_4)PhCHOH/ (p-Cl-C_6H_4)PhCO [HP-17]	same as above	9.99 9.39	1/1
(p-MeO-C_6H_4)PhCHOH/ (p-MeO-C_6H_4)PhCO [HP-17]	same as above	11.20 11.75	1/1

[a] Compounds were standards, obtained commercially from Aldrich or synthesized (see below). Concentrations ranged from 10^{-2} to 10^{-1} M in benzene.

[b] Injector and detector ports were always maintained at 220°C.

Synthesis of Benzhydrol Substrates

Benzhydrol, 4,4'-dimethoxybenzhydrol and 4,4'-difluorobenzhydrol were purchased from Aldrich and recrystallized from hexanes and Et_2O. The remaining substituted benzhydrols, 4-chlorobenzhydrol, 4-methoxybenzhydrol, 4,4'-N,N'-dimethylaminobenzhydrol and α-deuterobenzhydrol were synthesized as follows.

General Procedure

Dry Et_2O (125 mL) was added to a 3-necked round-bottomed flask containing lithium aluminum hydride (500 mg, 12 mmol) under N_2. The mixture was cooled to 0°C in an ice-bath and the corresponding benzophenone (5 g, 18 - 27 mmol) in dry Et_2O (50 mL) was added dropwise via syringe. The resulting mixture was warmed to r.t. and stirred overnight under N_2. Analysis by TLC indicated that no starting material remained. The mixture was cooled again to 0°C, and the reaction quenched dropwise with water (50 mL). The aqueous layer was acidified with conc. HCl and the benzhydrol product extracted with Et_2O (2 x 20 mL). The Et_2O layers were combined, washed with water and brine and dried over $MgSO_4$. Evaporation of the solvent on a rotary evaporator yielded the crude benzhydrol as a pale yellow solid. Recrystallization in hexanes and Et_2O yielded the pure substituted benzhydrols as crystalline, white needles.

4,4'-Dimethoxybenzhydrol [(p-MeO-C_6H_4)$_2$CHOH]

^{1}H-NMR (300 MHz, $CDCl_3$, 20°C):

7.24 (d, 4H, *o*-H); 6.83 (d, 4H, *m*-H); 5.73 (d, 1H, CH); 3.75 (s, 6H, *p*-OMe) 2.04 (d, 1H, OH)

Analysis: Calculated: C, 73.74; H, 6.61

Found: C, 73.65; H, 6.57

m.p.: 69-70°C[57]

4,4'-Difluorobenzhydrol [(p-F-C_6H_4)$_2$CHOH]

^{1}H-NMR (300 MHz, $CDCl_3$, 20°C):

7.30 (dd, 4H, *o*-H); 7.01 (t, 4H, *m*-H); 5.79 (d, 1H, CH); 2.20 (d, 1H, OH)

^{19}F-NMR (188.31 MHz, C_6D_6, 20°C):

-38.96 (s)

Analysis: Calculated: C, 70.89; H, 4.58

Found: C, 71.01; H, 4.55

m.p.: 45-46°C[58]

Benzhydrol [Ph_2CHOH]

^{1}H-NMR (300 MHz, $CDCl_3$, 20°C):

7.33 (m, 10H, phenyl H); 5.95 (d, 1H, CH); 2.29 (d, 1H, OH)

Analysis: Calculated: C, 84.75; H, 6.57

Found: C, 84.60; H, 6.53

m.p.: 65-66°C[57]

4-Chlorobenzhydrol [(p-Cl-C_6H_4)PhCHOH]

Yield: 55%

^{1}H-NMR (200 MHz, $CDCl_3$, 20°C):

7.30 (m, 9H, phenyl H); 5.75 (d, 1H, CH); 2.92 (br d, 1H, OH)

Analysis: Calculated: C, 71.54; H, 5.08

Found: C, 71.70; H, 5.06

m.p.: 58-59°C[57]

4-Methoxybenzhydrol [(p-MeO-C_6H_4)PhCHOH]

Yield: 79%

^{1}H-NMR (200 MHz, $CDCl_3$, 20°C):

7.30 (m, 7H, phenyl H); 6.80 (d, 2H, *m*-H); 5.70 (d, 1H, CH); 2.25 (br d, 1H, OH)

Analysis: Calculated: C, 78.47; H, 6.59

Found: C, 78.30; H, 6.52

m.p.: 64-65°C

4,4'-N,N'-Dimethylaminobenzhydrol [(p-Me_2N-C_6H_4)$_2$CHOH][ζ]

Yield: 52%

^{1}H-NMR (200 MHz, $CDCl_3$, 20°C):

7.15 (d, 4H, *o*-H); 6.65 (d, 4H, *m*-H); 5.55 (d, 1H, CH); 2.81 (s, 12H, $N(CH_3)_2$); 2.35 (br d, 1H, OH)

Analysis: Calculated: C, 75.51; H, 8.21; N, 10.37

Found: C, 75.79; H, 8.34; N, 10.42

m.p.: 102-104°C[57]

[ζ] This compound was retained by the pre-column in GC analysis and is not listed in Table 2. Conversion and turnovers for catalytic reactions involving this substrate were determined by ^{1}H-NMR analysis (based on *o*-H and N-Me integration of the benzhydrol and benzophenone species).

α-Deuterobenzhydrol [Ph_2CDOH]

This compound was synthesized according to the general procedure listed above, but using lithium aluminum deuteride in place of lithium aluminum hydride.

Yield: 55%

^{1}H-NMR (300 MHz, $CDCl_3$, 20°C):

7.33 (m, 10H, phenyl H); 2.19 (s, 1H, OH)

Analysis: Calculated: C, 84.28; H, 6.57

Found: C, 84.18; H, 6.53

m.p.: 65-66°C

*Benzhydrol-O-*d *[Ph_2CHOD]*

Benzhydrol was heated to reflux in a biphasic C_6H_6/D_2O system for 24 h. The C_6H_6 layer was dried over Na_2SO_4, and removed under vacuum to yield a pale yellow solid. The compound was purified by sublimation under vacuum to give white needles in 75% yield. Analysis of the product by ^{1}H-NMR indicated 55% incorporation of deuterium.

Synthesis of Porphyrins

General Procedure

The porphyrins H_2TMP and H_2OCP were prepared at r.t. in dry CH_2Cl_2 using BF_3•MeOH as the catalyst following the procedure determined by Lindsey and Wagner.[59] The products were purified by column chromatography through silica gel, and then

through basic alumina. The product purity was determined by ^{1}H-NMR, UV-VIS spectroscopies, and TLC analysis. The data agree with previously reported analyses.[59]

Meso-*Tetramesitylporphyrin [H_2TMP]*

Yield: 20%

^{1}H-NMR (400 MHz, $CDCl_3$, 20°C):

8.59 (s, 8H, *β*-pyrrole); 7.24 (s, 8H, *m*-H); 2.60 (s, 12H, *p*-CH_3); 1.83 (s, 24H, *o*-CH_3); -2.51 (s, 2H, N-H)

UV-VIS (C_6H_6): 420, 514, 550, 590, 648 nm

Meso-*Tetra(2,6-dichlorophenyl)porphyrin [H_2OCP]*

Yield: 8%

^{1}H-NMR (400 MHz, $CDCl_3$, 20°C):

8.64 (s, 8H, *β*-pyrrole); 7.75 (d, 8H, *m*-H); 7.68(t, 4H, *p*-H); -2.54 (s, 2H, N-H)

UV-VIS (C_6H_6): 420, 514, 590, 650, 706 nm

Synthesis of Ruthenium Porphyrin Complexes

Synthesis of Carbonyl(porphyrinato)ruthenium(II) Complexes [Ru(porp)(CO), porp = TMP or OCP]

Ruthenium was inserted into the centre of the porphyrins according to a modified Tsutsui procedure.[60a] A 200 mL solution of the porphyrin in decalin (0.003 M) was

heated to reflux in a 3-necked round-bottomed flask equipped with a condenser. The solution was kept under an atmosphere of CO by bubbling the gas through the solution. When the solution had reached reflux, solid $Ru_3(CO)_{12}$ to generate a 0.005 M solution was added. The reaction was monitored by TLC (toluene eluant on a silica plate) over 4 h. At this time, if the reaction was incomplete by TLC, additional portions of $Ru_3(CO)_{12}$ (the same quantity as previously used) were added. When no free-base porphyrin was visible by TLC, the reaction mixture was cooled to r.t. and passed through a column of silica gel using decalin and then toluene as the eluant. Once all of the free-base porphyrin had eluted as a dark purple band, the eluant was changed to 1% MeCN in toluene and the Ru porphyrin complex was eluted as a bright red band. A second purification of the porphyrin complex through basic alumina with a toluene eluant yielded the product in approximately 75% yield. The purities of the complexes were established by ^{1}H-NMR, UV-VIS and TLC analysis, and the data agreed with previously determined results.[5]

Ru(TMP)(CO)

Yield: 70%

^{1}H-NMR (400 MHz, $CDCl_3$, 20°C):

8.46 (s, 8H, *β*-pyrrole); 7.24 (s, 8H, *m*-H); 2.59 (s, 12H, *p*-CH_3); 1.86 (br s, 24H, *o*-CH_3); water is seen as a broad singlet at δ 1.6.

UV-VIS (C_6H_6): 414, 530 nm

IR (KBr): ν_{CO} = 1940 cm^{-1}

Analysis: Calculated: C, 75.22; H, 5.76; N, 6.26

+ H_2O C, 73.76; H, 6.04; N, 5.86

Found: C, 74.14; H, 5.99; N, 5.94

Ru(OCP)(CO)

Yield: 75%

^{1}H-NMR (400 MHz, $CDCl_3$, 20°C):

8.50 (s, 8H, *β*-pyrrole); 7.75 (br t, 8H, *m*-H); 7.65 (t, 4H, *p*-H)

UV-VIS (C_6H_6): 410, 530, 556 (shoulder) nm

IR (KBr): ν_{CO} = 1950 cm^{-1}

M.S. (FAB): $[Ru(OCP)(CO)]^-$, 1053 (M^- + Cl), 1018 (M^-), 990 (M^- - CO), 956 (M^- - CO - Cl)

Synthesis of Carbonyl(meso-tetra(2,6-dichlorophenyl)-β-octachloroporphyrinato)ruthenium(II) [Ru(OCP-Cl_8)(CO)]

Chlorinating the *β*-pyrrole positions of the porphyrin was accomplished using a modified procedure of a published preparation.[32] A round-bottomed flask was charged with Ru(OCP)(CO) (100 mg, 0.098 mmol), N-chlorosuccinimide (300 mg, 2.96 mmol) and CH_2Cl_2 (50 mL). The mixture was heated to reflux under air for 24 h and evaporated to dryness. The resulting brown solid was sonnicated in *i*PrOH, and the mixture filtered to yield a dark purple solid. Further purification by sonnicating the purple solid in MeOH, followed by filtration gave a bright red solid.

Yield: 47%

^{1}H-NMR (200 MHz, DMSO-d_6, 20°C):

7.93 (m, *m*-H and *p*-H)

UV-VIS (CH_2Cl_2):

418, 544 nm

IR (KBr): ν_{CO} = 1965 cm^{-1}

M.S. (FAB): $[Ru(OCP\text{-}Cl_8)(CO)]^-$, 1330 ($M^-$ + Cl), 1266 (M^- - CO), 1231 (M^- - CO - Cl), 1195 (M^- - CO - 2Cl), 1162 (M^- - CO - 3Cl)

Synthesis of* Trans-*bis(acetonitrile)*(meso-*tetramesitylporphyrinato)ruthenium (II)

[Ru(TMP)(MeCN)$_2$]

The title complex was synthesized following a standard photolysis procedure.[5,26,32] During the course of experimentation, however, it was determined that the complex could be synthesized in a Schlenk tube, rather than a photolysis tube. Ru(TMP)(CO) (40 mg, 0.043 mmol) was dissolved in a 3:5 $MeCN/C_6H_6$ mixture (HPLC grades, 80 mL) in a Schlenk tube equipped with a condenser. A stainless steel needle (26 gauge) was inserted through a rubber septum into the Schlenk tube, and the solution was purged with dry Ar for 30 min. The solution was irradiated with a 450 W Hanovia-Hg vapour lamp for 7 h. Analysis by ^{1}H-NMR spectroscopy of a withdrawn sample indicated that no starting material remained. The solvent was removed under vacuum to yield the acetonitrile complex as a dark purple solid. Purity of the complex was determined by ^{1}H-NMR, UV-VIS and IR spectroscopic analysis, and the data agreed with previously determined results.[5,26,32]

Yield: 80%

^{1}H-NMR (300 MHz, C_6D_6, 20°C):

8.65 (s, 8H, β-pyrrole); 7.30 (s, 8H, *m*-H); 2.55 (s, 12H, *p*-CH_3); 2.20 (s, 24H, *o*-CH_3); -1.35 (s, 6H, CH_3CN)

UV-VIS (C_6H_6): 410, 508 nm

IR (KBr): $\nu_{CN} = 2270\ cm^{-1}$

Synthesis of* Trans-*dioxo(porphyrinato)ruthenium(VI) Complexes

[Ru(porp)(O)$_2$, porp = TMP, OCP and OCP-Cl$_8$]

The dioxo complexes were prepared *in situ* by *m*-CPBA oxidation of the corresponding Ru(porp)(CO) compounds in benzene or chloroform.[5] The excess acids were removed by column chromatography through silica or basic alumina, the dioxo-complex was the first band that eluted. *In situ* synthesis of *trans*-Ru(TMP)$(O)_2$ was also possible by aerobic oxidation of *trans*-Ru(TMP)$(MeCN)_2$ in benzene.[5,26] Solid *trans*-Ru(porp)$(O)_2$ complexes were isolated by removing the benzene or chloroform solvents under vacuum to yield dark purple solids (75-98% isolated yield). Analysis of the dioxo complexes by ^{1}H-NMR, UV-VIS, and IR spectroscopies gave data that agreed with those previously reported.[5,26]

Ru(TMP)(O)$_2$

^{1}H-NMR (300 MHz, C_6D_6, 20°C):

9.02 (s, 8H, β-pyrrole); 7.10 (s, 8H, *m*-H); 2.42 (s, 12H, *p*-CH_3); 1.83 (s, 24H, *o*-CH_3)

UV-VIS (C_6H_6): 422, 516 nm

IR (KBr): $\nu_{Ru=O}$ = 820 cm^{-1}

Ru(OCP)(O)$_2$

^{1}H-NMR (400 MHz, $CDCl_3$, 20°C):

8.90 (s, 8H, β-pyrrole); 7.65 (m, 16H, *m*-H and *p*-H)

UV-VIS (C_6H_6): 422, 512, 580 nm

IR (KBr): $\nu_{Ru=O}$ = 820 cm^{-1}

Ru(OCP-Cl$_8$)(O)$_2$

^{1}H-NMR (400 MHz, $CDCl_3$, 20°C):

7.75 (m, *m*-H and *p*-H)

UV-VIS (CH_2Cl_2):

430, 522 nm

IR (KBr): $\nu_{Ru=O}$ = 820 cm^{-1}

Synthesis of* Trans-*bis(alkoxo)*(meso-*tetramesitylporphyrinato)ruthenium(IV)

Complexes

[Ru(TMP)(OR)$_2$]

A solution of *trans*-Ru(TMP)(O)$_2$, prepared from Ru(TMP)(CO) (40 mg, 0.044 mmol) and *m*-CPBA (40 mg, 0.23 mmol) in benzene (10 mL), was purified by column chromatography through basic alumina, and sparged with N_2 for 30 min. Meanwhile, a Schlenk tube containing a substituted benzhydrol (50 mg, 0.2-0.3 mmol) was evacuated and flushed with N_2. The *trans*-Ru(TMP)(O)$_2$ solution (8 mL) was transferred to the Schlenk tube using a syringe, and the resulting solution stirred under N_2 for 12 h. An aliquot, transferred via canula to an NMR tube under N_2, indicated the absence of any dioxo starting material. Subsequently, the dark brown solution was passed quickly through two pipette columns of basic alumina and evaporated to dryness by blowing N_2 through the solution. A dark purple solid was collected and analyzed by ^{1}H-NMR, UV-VIS, IR, and MS. Extinction coefficients were determined in the presence of a slight excess of the alcohol, the solution concentrations being determined from integration of the *o*- and *p*-CH_3 protons versus a CH_2Cl_2 internal standard in ^{1}H-NMR spectra. Elemental analysis could not be obtained on the complexes as decomposition of the complexes occurred in solution during elution from the columns. The complexes were unstable in solution under air and regenerated *trans*-Ru(TMP)(O)$_2$ in the absence of excess alcohol.

Ru(TMP)(OCHPh$_2$)$_2$

Yield: 50%

^{1}H-NMR (200 MHz, C_6D_6, 20°C):

10.81 (d, 8H, *m*-H); 7.67 (s, 8H, *m*-H); 4.39 (t, 4H, *p*-H); 3.01 (s, 12H, *p*-CH_3); 2.83 (s, 24H, *o*-CH_3); -22.49 (s, 8H, β-pyrrole)

UV-VIS (C_6H_6): 406 (130000), 522 (15000) nm

IR (KBr): $\nu_{C\text{-}N}$ = 1009 cm^{-1} Ru(IV) oxidation state marker[26,27]

$\nu_{Ru\text{-}O}$ = 764 cm^{-1} (tentative assignment)

Ru(TMP)(OCH(p-MeO-C$_6$H$_4$)$_2$)$_2$

Yield: 45%

^{1}H-NMR (200 MHz, C_6D_6, 20°C):

9.74 (s, 8H, *m*-H); 7.58 (s, 8H, *m*-H); 2.96 (s, 12H, *p*-CH_3); 2.85 (s, 24H, *o*-CH_3); 2.78 (s, 12H, *p*-OMe); -24.23 (s, 8H, β-pyrrole)

UV-VIS (C_6H_6): 408 (100000), 524 (12000) nm

IR (KBr): $\nu_{C\text{-}N}$ = 1010 cm^{-1} Ru(IV) oxidation state marker[26,27]

$\nu_{Ru\text{-}O}$ = 699 cm^{-1} (tentative assignment)

Ru(TMP)(OCH(p-F-C_6H_4)$_2$)$_2$

Yield: 53%

^{1}H-NMR (200 MHz, C_6D_6, 20°C):

9.83 (d, 8H, *m*-H); 7.67 (s, 8H, *m*-H); 3.01 (s, 12H, *p*-CH_3); 2.78 (s, 24H, *o*-CH_3); -24.23 (s, 8H, *β*-pyrrole)

^{19}F-NMR (188.31 MHz, C_6D_6, 20°C):

-37.50 (s)

UV-VIS (C_6H_6): 408 (100000), 524 (12000) nm

IR (KBr): ν_{C-N} = 1009 cm^{-1} Ru(IV) oxidation state marker[26,27]

ν_{Ru-O} = 673 cm^{-1} (tentative assignment)

CHAPTER III

OXIDATION OF ALCOHOLS

Introduction

A variety of Ru complexes can be used to catalyze the conversion of alcohols to aldehydes and ketones; the more recent applications are discussed in Chapter I. The number of non-porphyrin systems that function with O_2 as the oxygen source is limited. Work in this laboratory has shown that *trans*-Ru(porp)$(O)_2$ complexes (porp = TMP, OCP and OCP-Cl_8) will catalytically oxidize primary and secondary alcohols to aldehydes and ketones in the presence of water or a base.[5,31,32,36] The mechanisms of both the stoichiometric and catalytic alcohol oxidations by *trans*-Ru(porp)$(O)_2$ are not well understood. In order to increase the knowledge of these mechanisms and to evaluate the electronic and steric influence of the alcohol on its reactivity, the kinetics and activity of *p*-substituted benzhydrols toward oxidation by Ru(VI)-dioxo porphyrin complexes were investigated.

Sample Preparation and Data Analysis

Stoichiometric Reactions

The stoichiometric oxidation of benzhydrol was followed by ^{1}H-NMR and UV-VIS spectroscopies, while that of (p-MeO-$C_6H_4)_2$CHOH and (p-F-$C_6H_4)_2$CHOH were followed by UV-VIS spectroscopy only. The kinetic data from both ^{1}H-NMR and UV-VIS spectroscopic analysis of the reactions are tabulated in Appendix A.

UV-VIS Spectroscopic Experiments

Solid benzhydrol (0.016-1 g, 0.087-5.4 mmol) was placed in the flask of an anaerobic cell (Figure II.1, p.25), and the system evacuated and flushed 3 times with N_2. Meanwhile, a solution of *trans*-Ru(TMP)$(O)_2$ (5×10^{-5}-7×10^{-4} M), synthesized from *m*-CPBA oxidation of Ru(TMP)(CO) in benzene and purified by column chromatography through basic alumina, was purged with N_2 for 20 min. Using a syringe, 4 mL of the Ru-solution was transferred to the cuvet of the anaerobic cell and monitored by UV-VIS spectroscopy to determine the Ru concentration. The two components were mixed for 1 min and then the reaction was monitored by UV-VIS spectroscopy over the range of 450-820 nm. The temperature of the sample holder was maintained at 25°C during the course of the reaction and a filter, placed between the light source and sample, was used to prevent 200-450 nm light from reaching the sample.

The kinetics of alcohol oxidation were followed, over 3-12 h, by monitoring the changes in absorbance at 490 nm. Pseudo first-order rate constants, k_{obs}, were determined from non-linear regression analysis of absorbance versus time plots (not weighted) where A_∞ was a variable (Figure III.1). Values for k_{obs} determined from these plots were verified by comparison with the values obtained from a Guggenheim analysis of the data (see Figure A.2, Appendix A).

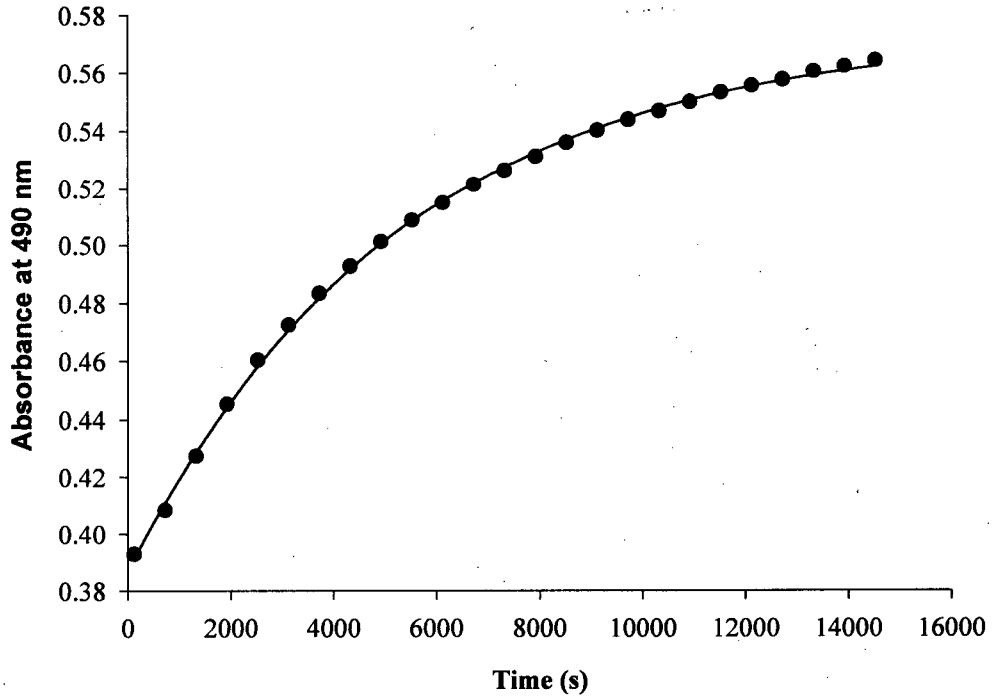

Figure III.1. A typical absorbance versus time plot for stoichiometric benzhydrol oxidation by *trans*-Ru(TMP)$(O)_2$. The line, $A = A_\infty + (A_o - A_\infty)\exp(-k_{obs}t)$, was fit to the data using non-linear regression analysis, A_∞ and k_{obs} being variables.

^{1}H-NMR Spectroscopic Experiments

A solution of *trans*-Ru(TMP)$(O)_2$ (5×10^{-4}-5×10^{-3} M) was made by *m*-CPBA oxidation of *trans*-Ru(TMP)(CO) in C_6D_6. The solution was passed through a pipette column of basic alumina to remove any excess acids and purged with N_2 for 20 min. Benzhydrol (1-135 mg, 0.0054-0.73 mmol) was added to an NMR tube that was capped with a septum, and the system evacuated and flushed 3 times with N_2. The N_2-saturated *trans*-Ru(TMP)$(O)_2$ solution (0.5 mL) was added to the alcohol in the NMR tube under

N_2, *via* syringe, and the resulting solution mixed for 20 s. The reaction was then monitored by ^{1}H-NMR spectroscopy over the next 20 min - 12 h. In experiments run at 35 and 50°C, the ^{1}H-NMR probe was equilibrated at the desired temperature for a minimum of 15 min prior to the start of the experiment. The solution of *trans*-Ru(TMP)$(O)_2$ and the NMR tube containing the solid alcohol were also heated to the desired temperature prior to the start of the reaction.

The kinetics of the stoichiometric benzhydrol oxidation were followed by measuring the loss of β-H signal intensity of the *trans*-Ru(TMP)$(O)_2$ oxidant using the intensity of the alcohol α-CH (δ 5.50) as an internal standard. Based on this ratio and the known 'practically constant' alcohol concentration, the concentration of *trans*-Ru(TMP)$(O)_2$ in solution at a given time was calculated. When the ratio of alcohol to Ru was $\leq$ 30:1 the concentration of *trans*-Ru(TMP)$(O)_2$ could also be determined by comparing the integration of the β-H signal to that of the alcohol α-CH. However, at alcohol to Ru ratios $\geq$ 100:1 the error in determining the β-H integration relative to that of the alcohol α-CH was too large to give an accurate *trans*-Ru(TMP)$(O)_2$ concentration. At low alcohol concentrations ($\leq$ 30:1 compared to Ru), k_{obs} values determined from measuring changes in both the intensity and integration of the β-H signal were the same, 1.7×10^{-4} s^{-1}. The loss of the dioxo-species could not be followed by monitoring changes in the signal intensity of the *o*- and *p*-CH_3 groups of the TMP as, in many cases, these peaks were obscured by the OH signal of the alcohol. In experiments where this was not the case, the same k_{obs} values were obtained for the loss of *trans*-Ru(TMP)$(O)_2$ monitored

at both the *o*- or *p*-CH_3 and β-H positions; 1.3 x 10^{-4} s^{-1} for the oxidation of Ph_2CHOH (0.015 M) with *trans*-Ru(TMP)$(O)_2$ (^{1}H-NMR spectral changes seen during this reaction are illustrated in Figure III.2 and Figure III.3). The natural logarithm of the [*trans*-Ru(TMP)$(O)_2$] was plotted against time to determine the value of the pseudo first-order rate constant, k_{obs} (Figure III.3). The oxidation of Ph_2CDOH was monitored using the intensity of the alcohol OH signal as the internal standard.

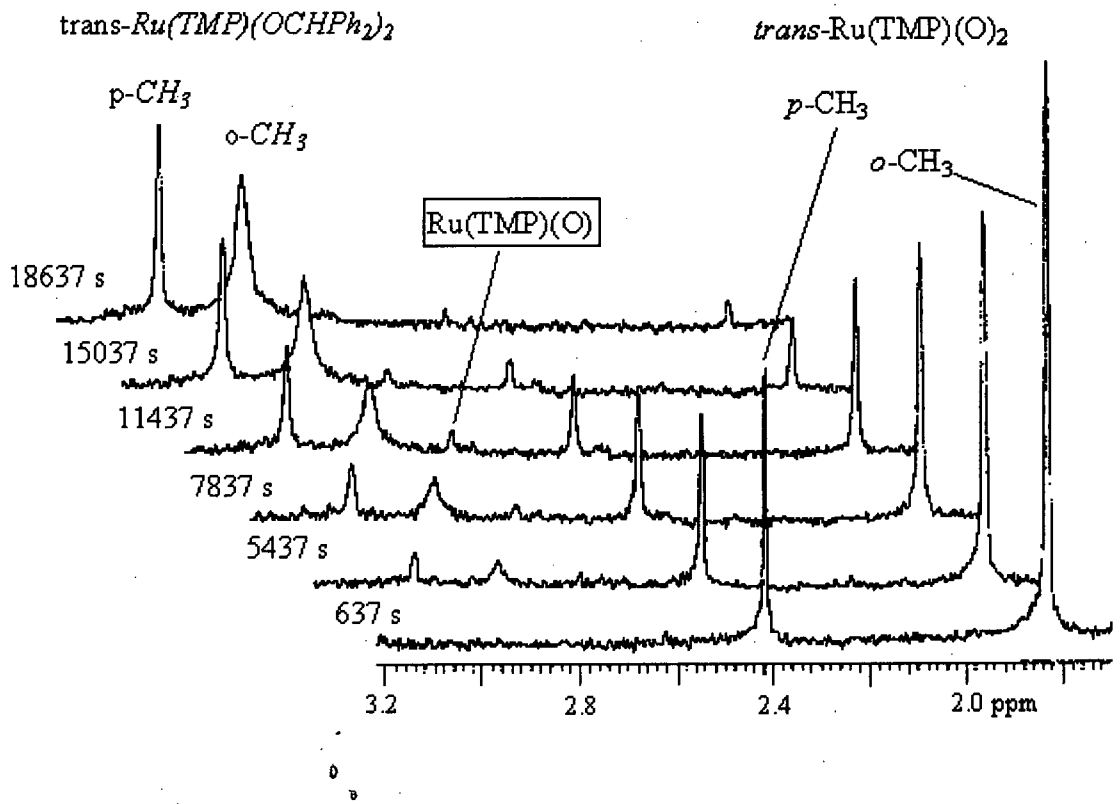

Figure III.2. ^{1}H-NMR spectral changes in the *o*- and *p*- CH_3 signals for the TMP during the stoichiometric oxidation of Ph_2CHOH by *trans*-Ru(TMP)$(O)_2$. ([*trans*-Ru(TMP)$(O)_2]_o$ ~ 5 x 10^{-4} M and [Ph_2CHOH] = 0.015 M). Peaks identified in regular font correspond to *trans*-Ru(TMP)$(O)_2$ with those labeled in italics corresponding to the *trans*-Ru(TMP)$(OCHPh_2)_2$ product.

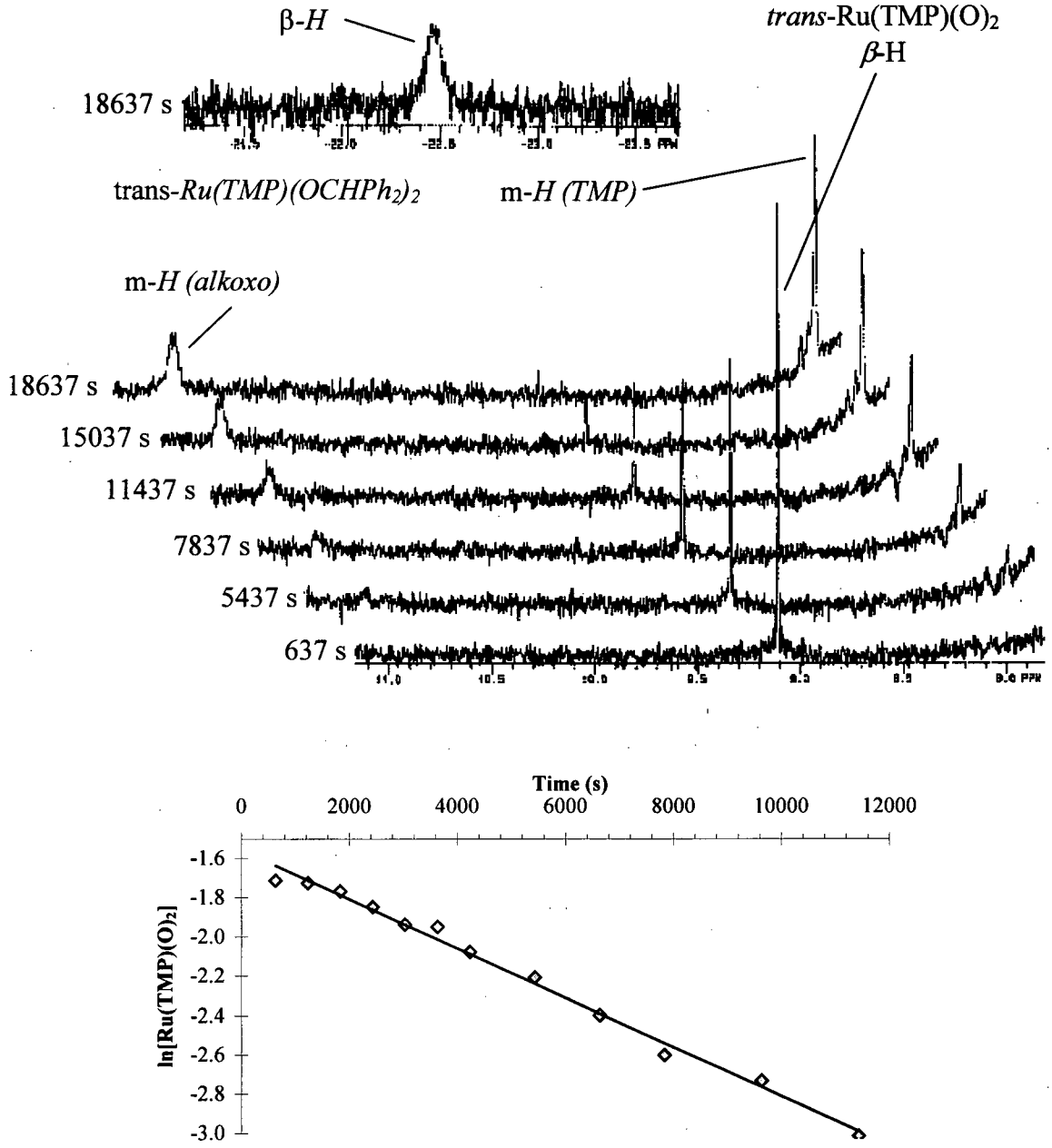

Figure III.3. Stoichiometric oxidation of Ph_2CHOH by *trans*-Ru(TMP)$(O)_2$ at 20°C followed by monitoring the loss in intensity of its β-H signal using the alcohol α-CH as an internal standard. The concentration of the Ru(VI)-dioxo species was determined from this ratio. Plots of ln[*trans*-Ru(TMP)$(O)_2$] versus time show straight lines. ([*trans*-Ru(TMP)$(O)_2]_o$ ~ 5 x 10^{-4} M, [Ph_2CHOH] = 0.015 M and $t_{1/2}$ = 5500 s). Peaks identified with regular font correspond to *trans*-Ru(TMP)$(O)_2$ with those labeled in italics corresponding to the *trans*-Ru(TMP)$(OCHPh_2)_2$ product.

Catalytic Aerobic Oxidations

A solution of *trans*-Ru(porp)$(O)_2$, from *m*-CPBA oxidation of Ru(porp)(CO), in benzene or $CHCl_3$ (1-2 mL), was added to a screw-top, 4 dram vial containing the solid alcohol, any additives and a small stir bar. The vial was tightly capped, shaken for 20 s to mix the reagents and placed in a 50°C oil-bath. The reactions were stirred at this temperature under 1 atm of air for 1-7 days and monitored at 24 h intervals by GC or ^{1}H-NMR spectroscopy. The identities of the products were determined by comparison with data for known standards (see Table II.2, p.28 for GC separation conditions). Percent conversion to products was determined by combining the peak areas for the alcohol and products and normalizing to 100%. From a knowledge of the initial catalyst concentration, calculated from UV-VIS spectroscopic data using known ε values,[32] and substrate concentration the catalyst turnover during the reaction could also be monitored. In all of the reactions the corresponding benzophenone was the only product of the benzhydrol oxidation.

Stoichiometric Oxidation of Benzhydrols by *trans*-Ru(TMP)$(O)_2$

In the absence of air, *trans*-Ru(TMP)$(O)_2$ oxidizes $(p\text{-R-}C_6H_4)_2CHOH$ to $(p\text{-R-}C_6H_4)_2CO$ according to the stoichiometry of eq. 3.1, the Ru(VI) species acting as an overall two-electron oxidant.

$$Ru^{VI}(O)_2 + 3\,(p\text{-R-}C_6H_4)_2CHOH \xrightarrow[R=H,\,F,\,OMe]{\text{under } N_2 \text{ in } C_6D_6} Ru^{IV}(OCH(p\text{-R-}C_6H_4)_2)_2 + 2\,H_2O + (p\text{-R-}C_6H_4)_2CO \qquad (3.1)$$

Ru = Ru(TMP)

The formation of one equivalent of the corresponding benzophenone is observed by ^{1}H-NMR spectroscopy when the Ru-dioxo oxidant reacts with an excess of the alcohol under N_2. Although no precautions were taken to ensure that the benzene was absolutely dry, the water stoichiometry was assumed to be the same as that for the oxidation of *i*PrOH to acetone, in which two equivalents of water were formed.[5,32] Bis(alkoxy)ruthenium(IV) products are obtained from the reactions and are characterized by the ^{1}H-NMR, UV-VIS and IR spectroscopic data (Chapter II). The presence of two alkoxy ligands is confirmed by ^{1}H-NMR spectral analysis of the *trans*-Ru(TMP)(OCH(*p*-MeO-C_6H_4)$_2$)$_2$ complex in which the *p*-CH_3 protons of TMP and the alkoxo *p*-OCH_3 protons both integrate to give 12 H-atoms (Figure III.4). Only one signal is seen for the *o*-CH_3 protons of the TMP ligand, indicating that the Ru(IV) complexes have D_{4h} symmetry.

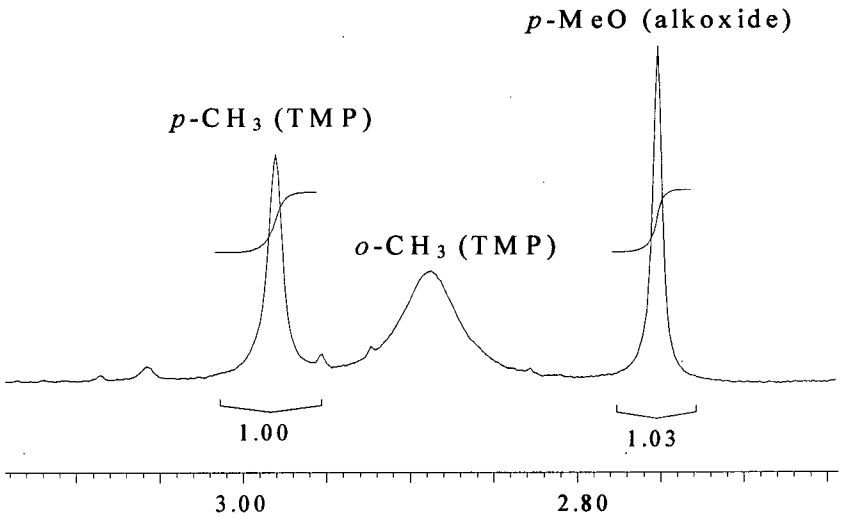

Figure III.4. ^{1}H-NMR spectral analysis of *trans*-Ru(TMP)(OCH(*p*-MeO-C_6H_4)$_2$)$_2$ illustrating that the integration of the *p*-CH_3 (TMP) signal and *p*-OCH_3 (alkoxy) signal is the same, showing that the Ru complex contains two alkoxo ligands.

The bis(alkoxo) complexes show paramagnetic shifts in TMS, CH_2Cl_2 and C_6F_6 peaks by ^{1}H- or ^{19}F-NMR spectroscopy; however, attempts to verify the number of unpaired electrons by the Evan's method[60b] yielded values for S ranging from 0.2 to 0.4, depending on the reference signal that was used. An S = 1 value, indicating 2 unpaired electrons, was expected given the previously reported results for the bis(isopropoxo) complex.[5,31] The lower measured magnetic susceptibility for the benzhydrol-based complexes possibly arises from exchange of the alkoxy ligands (see p.51) with slight amounts of excess alcohol in solution, required for stabilization of the complexes (see p.39). This alkoxo ligand exchange, seen as a broadening in the *o*-CH_3 signal, is still present at low temperatures (-40°C). The paramagnetic nature of the bis(alkoxo) complexes is also evident in the resonance of the β-H-atoms, found at δ -22 to -24, in comparison with chemical shifts in the region of δ 8-9 for diamagnetic Ru^{II}(porp)(CO) and *trans*-Ru^{VI}(porp)$(O)_2$ complexes. Similar paramagnetic shifts are noted for other Ru(IV)-bis(alkoxo) porphyrin species ranging from δ -12 for isopropoxo to δ -30 for phenoxo ligands.[32] Plots of TMP proton chemical shift against inverse temperature, for *trans*-Ru(TMP)$(OCHPh_2)_2$, show straight lines over -40 to +20°C indicating that the species exists in one paramagnetic spin state over this temperature range (Figure III.5). Unfortunately, due to decomposition of the complexes during purification by column chromatography, the compounds were not obtained in a pure enough form for elemental analysis. IR bands at 1010 and 1009 cm^{-1} are also indicative of a Ru(IV) centre [26,27] and crystals of the corresponding 2-propoxide, benzoxide and 1,3-dichloro-2-propoxide complexes have been isolated and characterized by X-ray crystallography.[31,36]

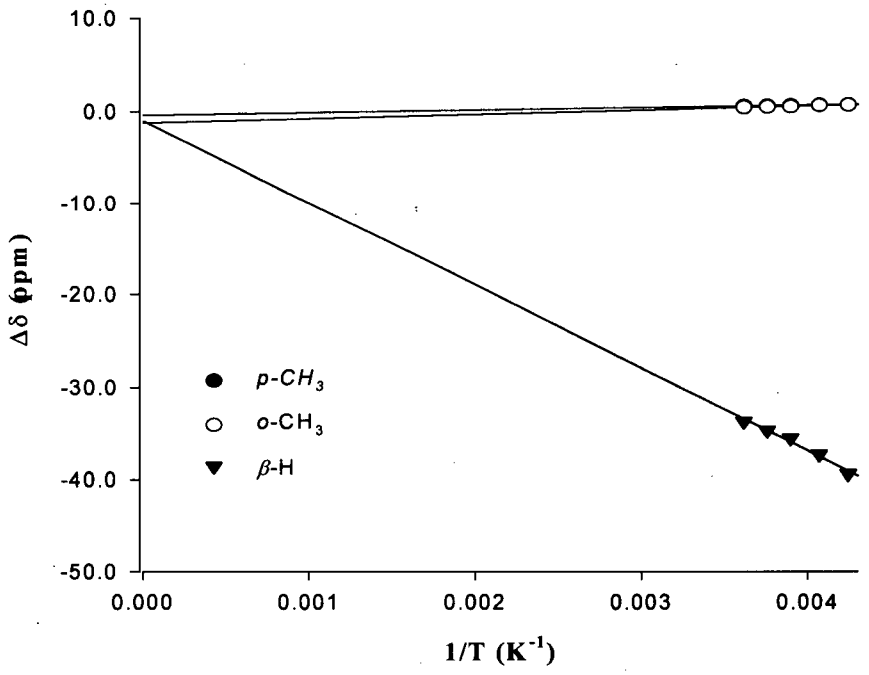

Figure III.5. Linear Curie plots of changes in chemical shift (TMP protons, cf. Ru(TMP)(MeCN)$_2$) versus 1/T indicating that the Ru(IV)-bis(alkoxo) species exists in a single spin state over the temperature range of -40 to +20°C.

The α-CH and *o*-CH protons could not be observed by ^{1}H-NMR spectroscopy in solution at 20°C due to exchange of the ligands with traces of the free alcohol remaining in solution, this causing these signals to broaden into the baseline. Addition of CD_3OD to a solution of Ru(TMP)(OCH(*p*-F-C_6H_4)$_2$)$_2$ confirms that this exchange occurs as all of the signals corresponding to the fluorinated complex disappear within 30 min of mixing. Analysis by ^{19}F-NMR shows the loss of the peak at δ -37.5 for the fluorinated bis(alkoxo) complex and an increase in the intensity of the alcohol peak at δ -39.0.

The kinetics for the stoichiometric oxidation of (p-F-$C_6H_4)_2$CHOH, (p-MeO-$C_6H_4)_2$CHOH and Ph_2CHOH were followed by UV-VIS spectroscopy under pseudo first-order conditions with a minimum 30 equiv. excess of the alcohol over the *trans*-Ru(TMP)$(O)_2$ oxidant. Plotting the natural logarithm of $A-A_\infty$ against time yields a straight line for over 75% of the reaction, indicating that the reaction is first order in Ru (Figure III.6). (A_∞ values were obtained from non-linear regression analysis of A versus t plots, see Figure III.1) Varying the initial concentration of the dioxo complex by a factor of 4 did not affect the value of the observed rate constant at [Ph_2CHOH] = 0.2 M, confirming this conclusion; at [*trans*-Ru(TMP)$(O)_2$] = 5×10^{-5} M, $k_{obs} = 1.5 \times 10^{-4}$ s^{-1} while at [*trans*-Ru(TMP)$(O)_2$] = 2×10^{-4} M, $k_{obs} = 1.6 \times 10^{-4}$ s^{-1}.

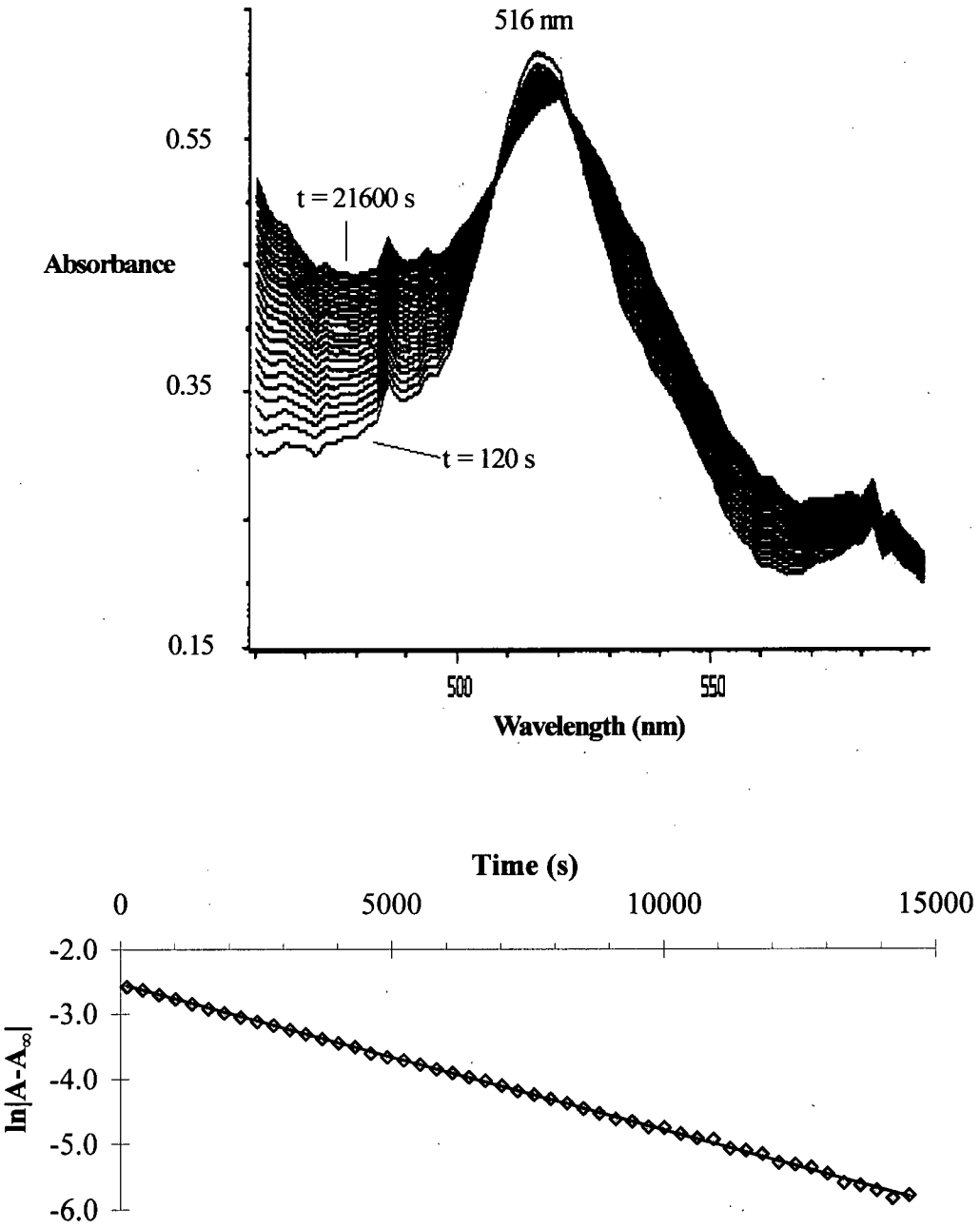

Figure III.6. Stoichiometric oxidation of Ph_2CHOH by *trans*-Ru(TMP)$(O)_2$ at 25°C under 1 atm of N_2 followed by UV-VIS spectroscopy over 450-600 nm. Each spectrum represents a 15 min time interval. The corresponding ln(A-A_∞) versus time plot, for absorbance changes at 490 nm, is linear for over 75% of the reaction; [*trans*-Ru(TMP)$(O)_2$] ~ 3 x 10^{-4} M, [Ph_2CHOH] = 0.40 M, and $t_{1/2}$ = 3090 s.

Plots of the pseudo first-order rate constants, k_{obs}, versus [alcohol] show the reaction rates leveling off at higher alcohol concentrations, indicating saturation kinetics (Figure III.7-Figure III.9). Rate law (eq. 3.2) was fit to the data using non-linear regression analysis and yielded the K and k_1 values listed in Table III.1; the K and k_1 values refer to a pre-equilibrium process, followed by a rate-determining k_1 step (see Figure III.11, p.63).

$$\text{rate} = -\frac{d[Ru(TMP)(O)_2]}{dt} = \frac{k_1 K[ROH]}{1+K[ROH]}[Ru(TMP)(O)_2] \qquad (3.2)$$

Previous studies with stoichiometric *i*PrOH oxidation by *trans*-Ru(TMP)$(O)_2$ also showed that the rate of oxidation leveled off at higher alcohol concentrations; however, this was attributed to solvent effects as the addition of the non-oxidizable alcohol *t*BuOH ([*t*BuOH] = 0.17 and 0.53 M) to the reaction mixture with [*i*PrOH] = 0.13 M slowed down the rate of alcohol oxidation by an order of magnitude.[32,36] Similar results are not obtained with this system, as oxidation of Ph_2CHOH (0.25 M and 0.54 M) in the presence of the non-oxidizable Ph_3COH (0.34 M) gave k_{obs} values which fit with the data obtained for Ph_2CHOH oxidation alone, Figure III.8. An explanation for the observance of saturation kinetics is the presence of a pre-association step, forming a {Ru-alcohol} adduct, prior to the actual oxidation step. At higher alcohol concentrations when the adduct is completely formed, the rate of oxidation is zero-order in the alcohol. Lower alcohol concentrations will result in partial formation of the {Ru-alcohol} adduct and the

rate of the reaction will show a dependence on the alcohol concentration. Unfortunately, evidence for the presence of the {Ru-alcohol} adduct was not seen by UV-VIS spectroscopy.

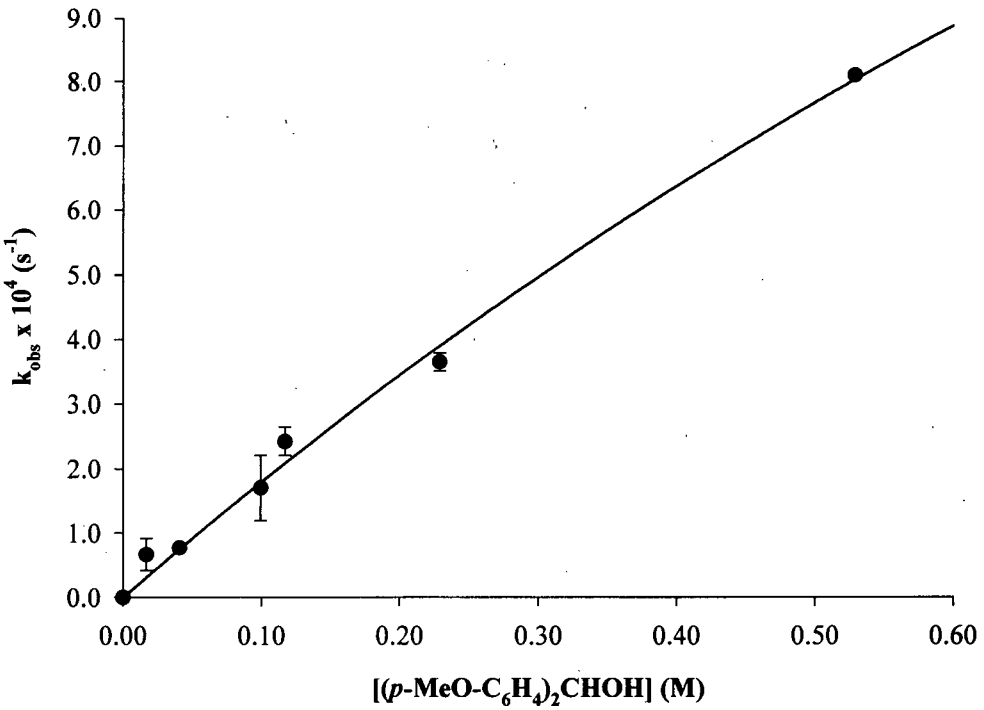

Figure III.7. Plot of k_{obs} (from UV-VIS spectroscopic data) versus alcohol concentration for the stoichiometric oxidation of (*p*-MeO-C_6H_4)$_2$CHOH by *trans*-Ru(TMP)$(O)_2$ in benzene at 25°C under 1 atm of N_2. Error bars indicate the range of k_{obs} values determined from a minimum of three repeat reactions. Instrumental error is within the range of the point size.

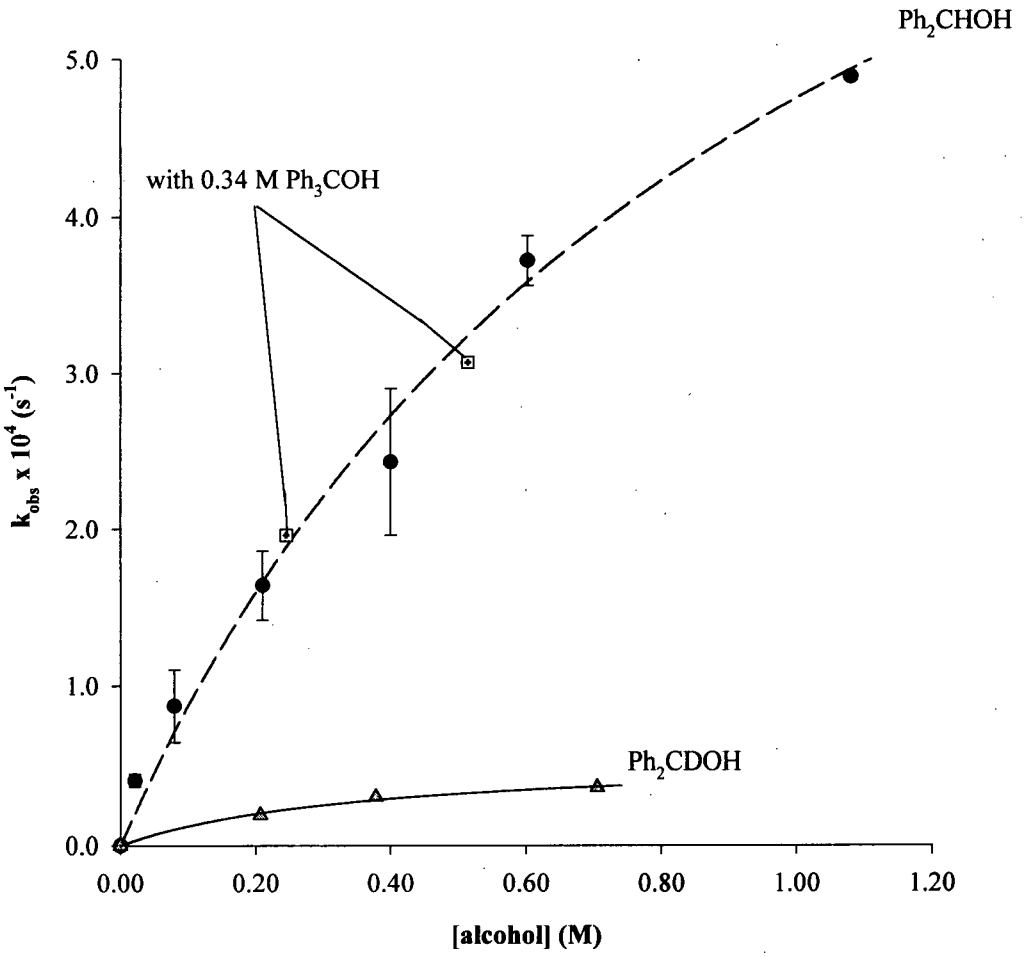

Figure III.8. Plot of k_{obs} (from UV-VIS spectroscopic data) versus alcohol concentration for the stoichiometric oxidation of Ph_2CHOH and Ph_2CDOH by *trans*-$Ru(TMP)(O)_2$ in benzene at 25°C under 1 atm of N_2. Error bars indicate the range of k_{obs} values determined from a minimum of three repeat reactions. Instrumental error is within the range of the point size.

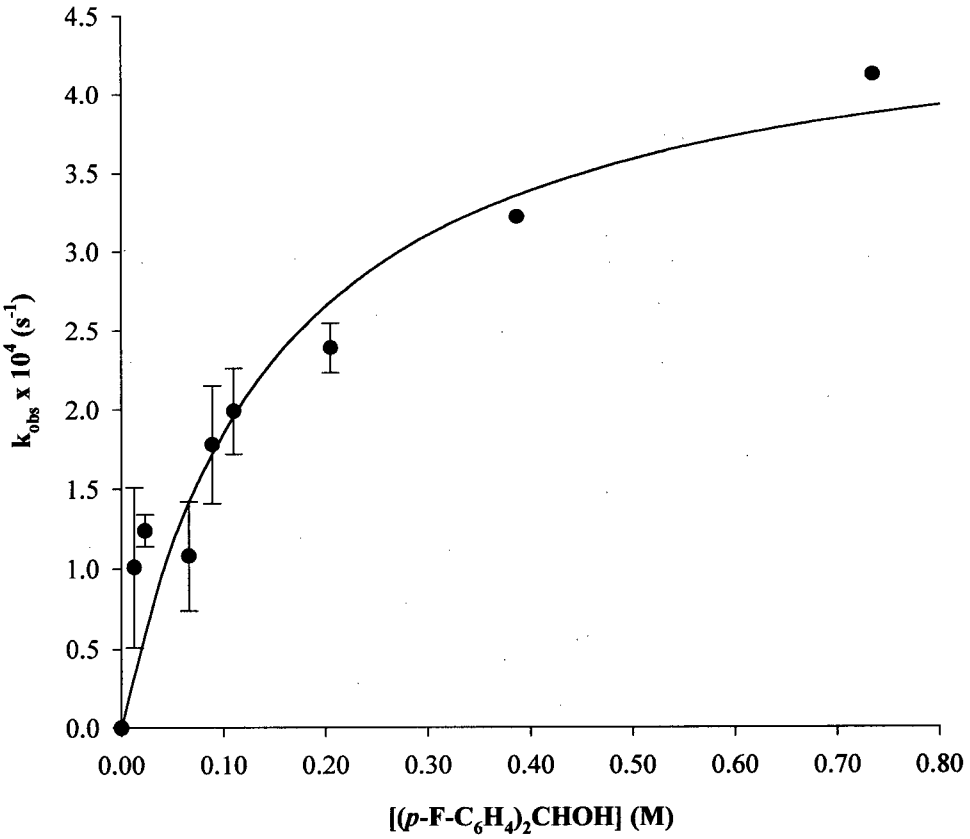

Figure III.9. Plot of k_{obs} (from UV-VIS spectroscopic data) versus alcohol concentration for the stoichiometric oxidation of (*p*-F-C_6H_4)$_2$CHOH by *trans*-Ru(TMP)$(O)_2$ in benzene at 25°C under 1 atm of N_2. Error bars indicate the range of k_{obs} values determined from a minimum of three repeat reactions. Instrumental error is within the range of the point size.

Adduct formation between Ru-oxo species and alcohols has been previously proposed by: Tony *et al.*[9] for the TPAP- and $[Ru^{VII}(O)_2(OCOR)Cl_2]^-$- catalyzed oxidation of alcohols in the presence of NMO in MeCN and CH_2Cl_2, respectively; Behari and co-authors[61] for the oxidation of cyclohexanol with RuO_4^{2-} in the presence of a $Fe(CN)_6^{3-}$ co-oxidant; and Bressan *et al.*[62] for the persulfate oxidation of alcohols catalyzed by Ru(II) species. In all three cases, the only evidence for the adduct formation was derived from kinetic data; no spectroscopic evidence for the presence of the adduct was reported. Lee and Congson[10] have proposed, based on theoretical calculations, that in the stoichiometric oxidation of alcohols by RuO_4^{2-} and RuO_4^- in 0.3 M NaOH a pre-equilibrium step occurs in which the α-CH bond of the alcohol oxidatively adds to the Ru=O bond (a 2 + 2 addition) to give a seven-coordinate Ru-hydroxo intermediate. Decomposition of this intermediate then occurs *via* a rate-determining step, leading to the synthesis of the ketone products. Once again, evidence for this pre-equilibrium step is based solely on kinetic data. As the sterics and rigidity of the porphyrin ligand would hinder formation of a seven-coordinate Ru system, it is likely that the {Ru-alcohol} adduct forms through weak bonding interactions between the Ru=O bond and the α-CH of the alcohol, similar to the "tight binding" between the alcohol α-CH and an *in situ* Ru-oxo species, as proposed by Bressen *et al.*[62]

Table III.1. K and k_1 Values for Stoichiometric Benzhydrol Oxidation by *trans*-Ru(TMP)$(O)_2$ in benzene.

Alcohol	K (M^{-1})	$k_1 \times 10^4$ (s^{-1})
(p-MeO-C_6H_4)$_2$CHOH[a]	0.45	42
(p-F-C_6H_4)$_2$CHOH[a]	6.5	4.7
Ph_2CHOH[a]	1.0	9.4
Ph_2CDOH[a]	1.3	0.77
Ph_2CHOH[b]	38	2.9
Ph_2CDOH[b]	68	0.20
Ph_2CHOD[b]	34	2.9

[a] Followed by UV-VIS spectroscopy at 490 nm, at 25°C under 1 atm N_2.
[b] Followed by ^{1}H-NMR spectroscopy at 20°C under 1 atm N_2.

The kinetics of the stoichiometric oxidation of Ph_2CHOH by *trans*-Ru(TMP)$(O)_2$ were also followed by ^{1}H-NMR spectroscopy. The reactions exhibit pseudo first-order kinetics and plots of ln[*trans*-Ru(TMP)$(O)_2$], determined from intensity changes in the β-H signal relative to that of the alcohol α-CH, versus time show straight lines over at least 2 half-lives (Figure III.3, p.47). As with the UV-VIS spectroscopic studies, the reaction exhibits saturation kinetics (Figure III.10); however, the values of k_1 and K determined from a non-linear regression fit of eq. 3.2 to a plot of k_{obs} versus [Ph_2CHOH] are significantly different (Table III.1, cf. Figure III.8, p.56). These differences possibly arise because of some light sensitivity of the reaction. Removal of the 200-450 nm filter from the UV-VIS spectrometer, which allows the sample to absorb light within the Soret region of the spectrum, increases the k_{obs} value for stoichiometric oxidation by a factor of ~ 2 (with the filter at 0.022 M Ph_2CHOH, $k_{obs} = 4.1 \times 10^{-5}$ s^{-1}, while in the absence of the filter at 0.027 M Ph_2CHOH, $k_{obs} = 1.0 \times 10^{-4}$ s^{-1}). The ^{1}H-NMR spectroscopic data are considered to pertain only to the thermal reactions.

Analysis of the spectra collected during the stoichiometric reactions shows three species to be present during the course of the reaction; *trans*-Ru(TMP)$(O)_2$, *trans*-Ru(TMP)$(OCHPh_2)_2$ and Ru(TMP)(O).[26] The intermediate Ru-oxo species grows in at the start of the reaction, remains at a low concentrations during the course of the reaction and then disappears at the end of the reaction (Figure III.2, p.46). Once again, no evidence for the presence of a {Ru-substrate} adduct was found, supporting the conclusion that the adduct is probably formed through non-covalent bonds between the Ru=O and the alcohol α-CH that presumably would not greatly disturb the electronic environment of the porphyrin protons. Media effects of high alcohol concentrations were also investigated by ^{1}H-NMR spectroscopy. The stoichiometric oxidation of benzhydrol (0.19 M) in the presence of Ph_3COH (0.41 M) gave $k_{obs} = 2.7 \times 10^{-4}$ s^{-1} which is within 8% of the k_{obs} value determined in the absence of Ph_3COH ($k_{obs} = 2.5 \times 10^{-4}$ s^{-1}). As k_{obs} typically varied by 10-15% for repeat experiments, this difference is not significant (Figure III.10).

Kinetic isotope effects were investigated by both UV-VIS and ^{1}H-NMR spectroscopies over a range of concentrations. A primary kinetic isotope effect of 12 ± 6 for k_1 and 0.7 ± 0.7 for K, determined from UV-VIS spectroscopy, is exhibited at the α-CH bond. Similar results are obtained from ^{1}H-NMR spectroscopy, giving $k_1^H/k_1^D = 15 \pm 1$ and $K^H/K^D = 0.6 \pm 0.2$ for Ph_2CDOH oxidation. The effect of using the -OD versus -OH alcohol was investigated only by the ^{1}H-NMR spectroscopic kinetics, which showed

$k_1^{OH}/k_1^{OD} = 1.0 \pm 0.1$ and $K^{OH}/K^{OD} = 1.1 \pm 0.7$, indicating that both the pre-association and rate-determining step are not significantly affected by O-deuteration. Previous work performed on the oxidation of *i*PrOH indicated a primary kinetic isotope effect of 1.9 ± 0.3 with the use of the fully deuterated *i*PrOD-d_8, in the initial first-order stage of the reaction ([*i*PrOH] < 0.3 M); at higher concentrations ([*i*PrOH] = 1.7 M), the k^H/k^D ratio decreased to about 1.[32,36] No isotope effects were noted for *i*PrOD oxidation.[32,36] Large kinetic isotope effects are typical for cleavage of α-CH bonds in alcohol oxidation by non-porphyrin Ru(IV)-oxo[2,63] and *trans*-Ru(VI)-dioxo[13a] oxidants, the values ranging from 8 for ethanol[13a] up to 50 for benzyl alcohol.[63]

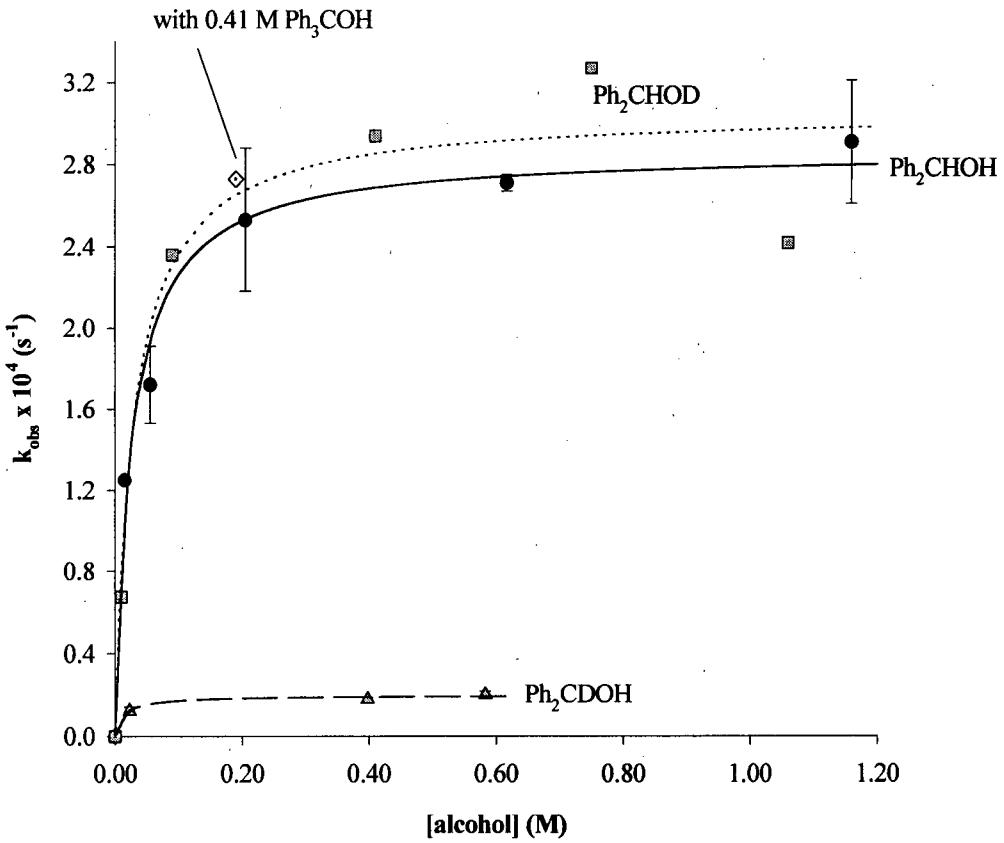

Figure III.10. Plot of k_{obs} (from ^{1}H-NMR spectroscopic data) versus alcohol concentration for the stoichiometric oxidation of Ph_2CHOH, Ph_2CDOH and Ph_2CHOD by *trans*-Ru(TMP)$(O)_2$ in benzene at 20°C under 1 atm of N_2. Error bars indicate the range of k_{obs} values determined from a minimum of three repeat reactions. Instrumental error is within the range of the point size.

Proposed Mechanism for Anaerobic, Stoichiometric Alcohol Oxidation

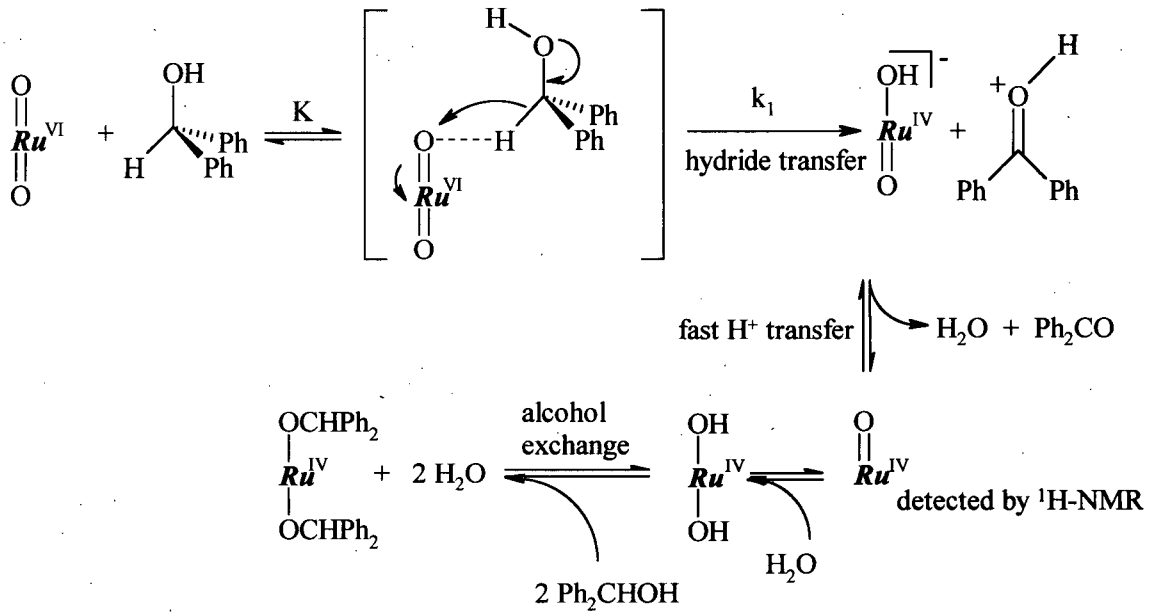

Figure III.11. Proposed mechanism for stoichiometric alcohol oxidation by *trans*-Ru(TMP)$(O)_2$, ***Ru*** = Ru(TMP).

Figure III.11 outlines a proposed mechanism (also considered earlier by members of this group)[32,36] for the stoichiometric alcohol oxidations (eq. 3.1, p.48). Saturation kinetics support the presence of a fast pre-equilibrium step forming a {Ru-alcohol} adduct, although no ^{1}H-NMR nor UV-VIS spectroscopic evidence has been seen for the formation of such a new Ru species. Something akin to hydrogen-bonding between the α-CH and the electrophilic Ru=O (but perhaps involving a hydride H-atom and an electrophilic O-atom) is thought to occur to form the adduct, followed by subsequent C-H bond breaking in the rate-determining step. The small isotope effect of α-CD on K indicates that deuteration at this site has little effect on the value of ΔH for adduct formation; the K^H/K^D value of 0.6 corresponds to only a 1-2 kJ/mol difference for the

interaction in the presence and absence of α-deuteration. This small change signifies that there is essentially no difference between the bond energies of the Ru=O---D and Ru=O---H moieties in the adduct, supporting the idea of a very weak hydrogen-bonding Ru=O and alcohol α-CH interaction. Formation of a 'stronger' bond between the Ru=O and the alcohol α-CH in the pre-equilibrium step would be expected to show a larger difference in ΔH, resulting in a larger isotope effect on K. Also, the large kinetic isotope effect on k_1, seen with Ph_2CDOH oxidation, indicates that cleavage of the α-CH bond occurs in the rate-determining step; O-deuteration does not change the value of K or k_1.

A comparison of the k_1 values determined from UV-VIS spectroscopy for different benzhydrols indicates that *p*-substitution of an electron-donating group on the benzene rings of the alcohol increases the rate of oxidation. With 4,4'-(N,N'-dimethylamino)benzhydrol[ζ] (1.0 M, σ_p = -0.63), complete loss of *trans*-Ru(TMP)$(O)_2$ occurs within 7 min at r.t. under 1 atm of N_2, compared with half-lives for *trans*-Ru(TMP)$(O)_2$ loss (under corresponding conditions with 1.0 M alcohol) of 29 min with $(p\text{-F-}C_6H_4)_2CHOH$ (σ_p = 0.15), 25 min with Ph_2CHOH (σ_p = 0) and 9 min with $(p\text{-MeO-}C_6H_4)_2CHOH$ (σ_p = -0.28). A Hammett plot of $\log(k_1^X/k_1^H)$ against $2\sigma_p$ for the *p*-MeO, *p*-F and *p*-H substrates shows a linear relationship with a slope ρ = -1.1 (Figure III.12), signifying that a transfer of electron density from the alcohol α-CH to the Ru oxidant

---

[ζ] K and k_1 values for $(p\text{-Me}_2\text{N-}C_6H_4)_2CHOH$ oxidation were not included in Table III.1 because the alcohol oxidation did not exhibit pseudo first-order spectral changes; plots of $\ln|A\text{-}A_\infty|$ versus time were not linear. This discrepancy may result from binding of the alcohol to the Ru centre through the N-atom, or from an enhanced light-sensitivity in the reaction. In the absence of water, in solution, $(p\text{-Me}_2\text{N-}C_6H_4)_2CHOH$ is blue in colour.

occurs in the formation of the transition state.[64] These results, in combination with a k_1^H/k_1^D ratio of ~ 15 for α-CH bond cleavage, support hydride transfer as the rate-determining step of the oxidation reaction. The rate of stoichiometric oxidation of *i*PrOH by *trans*-Ru(TMP)$(O)_2$ was previously found to increase in the presence of added KOH or KO*t*Bu, adding to the evidence in favour of a hydride transfer mechanism.[32,36] Of note, oxidation *via* hydrogen atom abstraction from the α-CH bond to form Ru^V(TMP)(O)(OH) and an in-cage organic radical $Ph_2C^{\bullet}$-OH, followed by rapid electron transfer to the Ru(V) species and subsequent H^+ loss from $Ph_2C{=}OH^+$ is also possible.

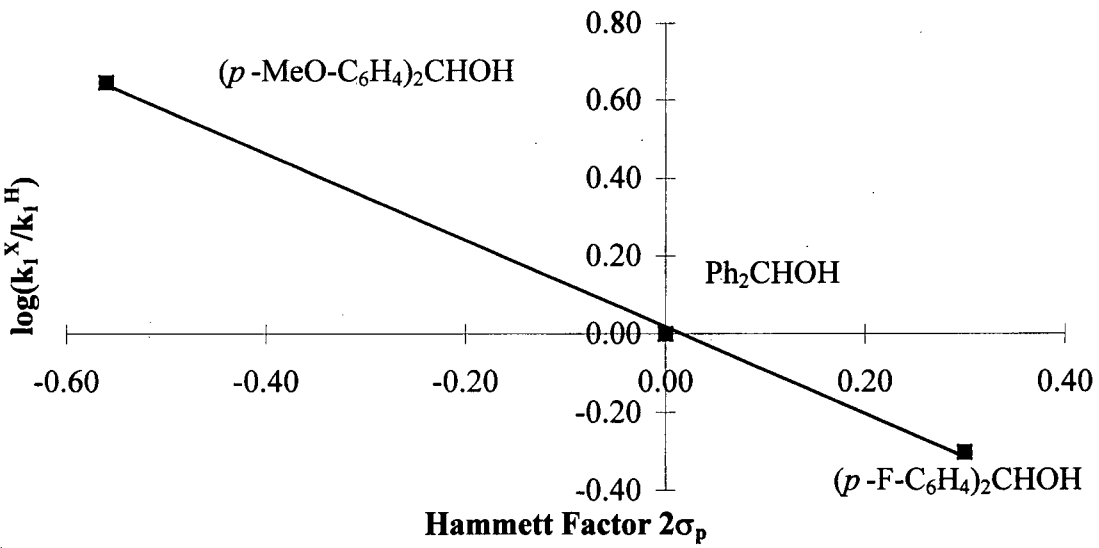

Figure III.12. Hammett plot for stoichiometric benzhydrol oxidation from UV-VIS spectroscopic data.

Formation of the bis(alkoxo) complexes almost certainly occurs through ligand exchange with an intermediate bis(hydroxo) species. Direct evidence for the formation of the Ru(IV)-bis(hydroxo) species in these alcohol systems is not available, though alkoxo ligand exchange with excess alcohol in solution has been observed (see p.51).[32] Recently

crystals of $Ru(OCP)(OH)_2$ have been isolated during the preparation of $Ru(OCP)(O)_2$ and analyzed by X-ray crystallography, providing indirect proof for the existence of $Ru(TMP)(OH)_2$ in solution.[65] Hydroxo intermediates are also proposed in alcohol oxidations with the non-porphyrin *trans*-$[Ru(O)_2L]^{2+}$ oxidants (L = 4-N donor macrocycles) where *trans*-$[Ru(O)L(OH_2)]^{2+}$ complexes are the final products detected by UV-VIS spectroscopy.[13a]

The stoichiometric oxidation of Ph_2CHOH by *trans*-$Ru(TMP)(O)_2$ was followed by ^{1}H-NMR spectroscopy at 35 and 50°C at a variety of alcohol concentrations in an effort to determine the reaction enthalpy for the pre-equilibrium step and the activation parameters for the rate-determining step. At ≥ 0.2 M Ph_2CHOH, the reaction exhibits zero-order dependence on the alcohol concentration (Figure III.13) allowing the values of $\Delta H_1^{\ddagger}$ and $\Delta S_1^{\ddagger}$, 58 ± 10 kJ/mol and -120 ± 30 J/(mol K), respectively, to be determined from an Eyring plot (Figure III.14). These values are comparable to the activation parameters (within a first-order kinetic regime in alcohol) measured for the oxidation of *i*PrOH and benzyl alcohol for both porphyrin ($\Delta H^{\ddagger}$, 45 ± 7 and 65 ± 11 kJ/mol; $\Delta S^{\ddagger}$ = -167 ± 10 and -70 ± 20 J/(mol K), respectively)[36] and non-porphyrin ($\Delta H^{\ddagger}$, 50 ± 4 and 42 ± 4 kJ/mol; $\Delta S^{\ddagger}$ = -117 ± 13 and -109 ± 13 J/(mol K), respectively)[13] *trans*-Ru(VI)-dioxo oxidants. In the current work, first-order dependence on alcohol concentration is seen in the 0.02 M Ph_2CHOH region, giving k_{obs} values of 2.9 x 10^{-4} s^{-1} at 35°C and 1.3 x 10^{-3} s^{-1} at 50°C. Using the k_1 values determined at from a best fit of the data in the [Ph_2CHOH] ≥ 0.2 M region, K values of ~ 42 and 57 M^{-1} at 35 and 50°C, respectively, can be calculated;

together with the value of 38 M^{-1} at 20°C, the data indicate that the formation of the {Ru-alcohol} adduct is essentially isenthalpic.

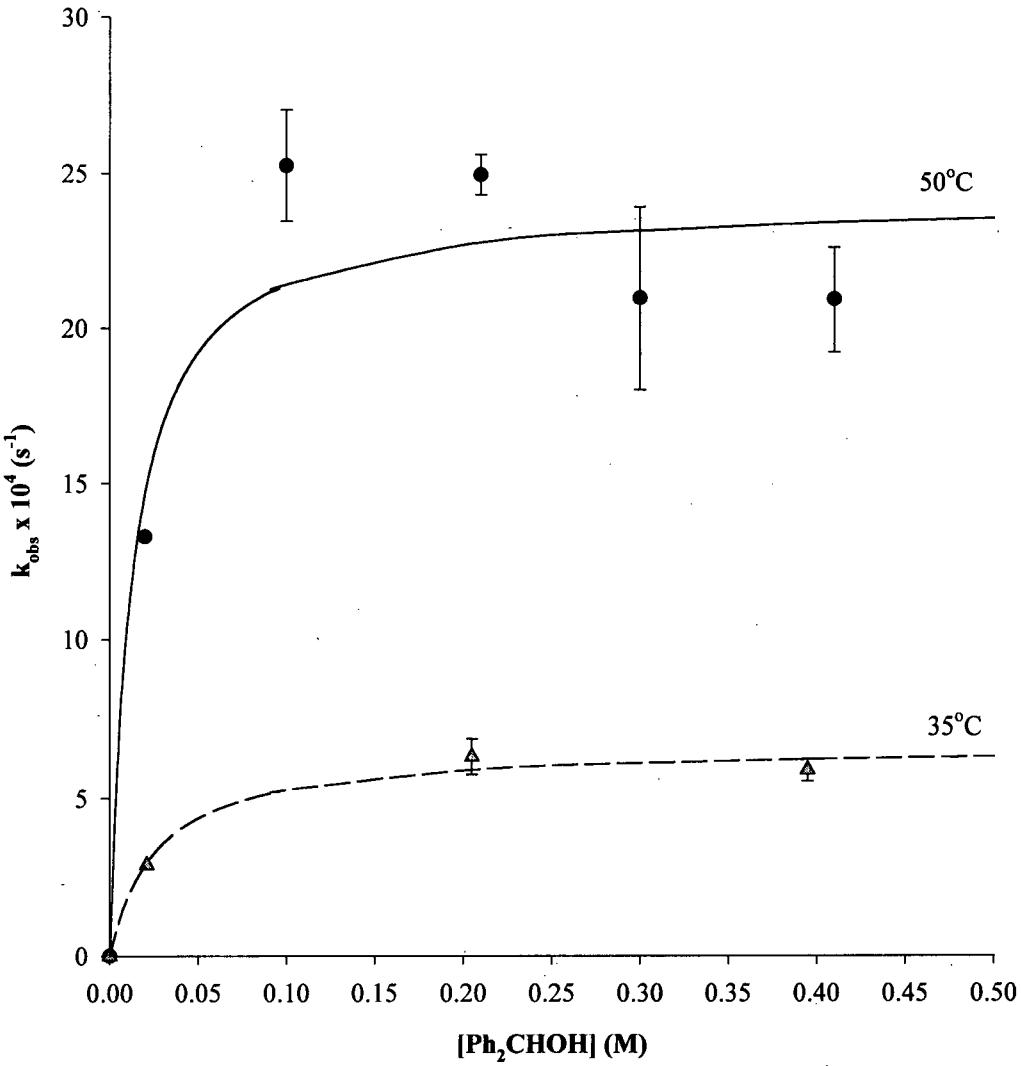

Figure III.13. Ph_2CHOH oxidation by *trans*-Ru(TMP)$(O)_2$ from ^{1}H-NMR spectroscopic data at 35 and 50°C under 1 atm of N_2 in C_6D_6.

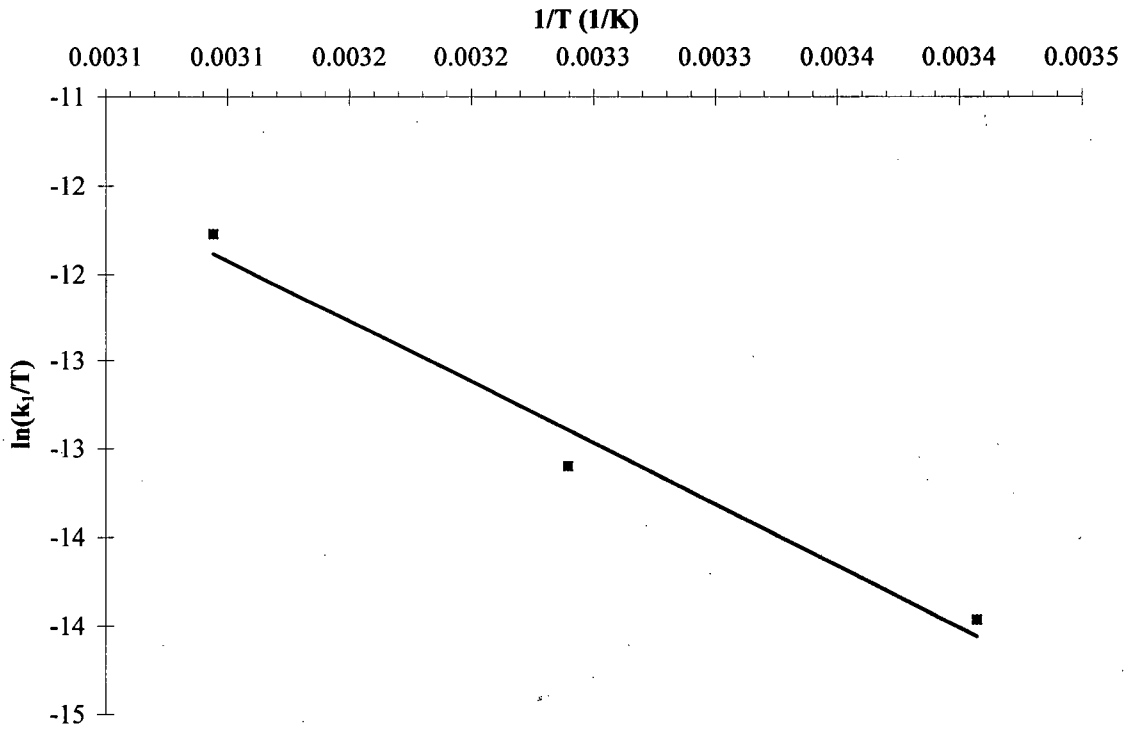

Figure III.14. Eyring plot for the stoichiometric oxidation of Ph_2CHOH (0.2 M) with *trans*-Ru(TMP)$(O)_2$ under 1 atm N_2 in C_6D_6.

Aerobic Oxidation of Benzhydrols Catalyzed by *trans*-Ru(porp)$(O)_2$

At 50°C under 1 atm of air in benzene *trans*-Ru(porp)$(O)_2$ (porp = TMP, OCP and OCP-Cl_8) catalyze the conversion of benzhydrols into benzophenones, though only in low turnovers (Table III.2). The addition of water to form a biphasic aqueous/benzene system increases the conversion to ketone products by a factor of 2-6 (Table III.3). In contrast to the results obtained with *i*PrOH oxidation,[32,36] the addition of NaOH to the reaction in aqueous benzene does not increase the % conversion of benzhydrol. Alkaline biphasic aqueous/benzene systems show an improved % conversion over straight benzene; however in comparison with neutral aqueous/benzene systems the % conversions are in

fact lower (Table III.3). The presence of mineral acids, either in concentrated or dilute solution (1N HCl) prevents any oxidation by *trans*-Ru(TMP)$(O)_2$ from occurring, almost certainly due to the formation of *trans*-Ru(TMP)Cl_2;[32] *trans*-Ru(porp)Cl_2 complexes do not shown catalytic aerobic oxidation activity.[32,54]

Table III.2. Oxidation of Benzhydrols Catalyzed by *trans*-Ru(TMP)$(O)_2$.

	Yield (%) and [Turnover][a]	
Alcohol	**45 h[b]**	**97 h[b]**
Ph_2CHOH	39 [10]	79 [21]
(*p*-Cl-C_6H_4)PhCHOH	22 [6]	63 [17]
(*p*-MeO-C_6H_4)PhCHOH	77 [21]	95 [25]
(*p*-MeO-$C_6H_4)_2$CHOH	86 [23]	96 [26]
(*p*-F-$C_6H_4)_2$CHOH	23 [6]	58 [16]
(*p*-Me_2N-$C_6H_4)_2$CHOH[c]	47 [13]	65 [18]

[a] Reaction conditions: 50°C, 1 mL benzene solvent under 1 atm of air. [*trans*-Ru(TMP)$(O)_2$] = 3.8×10^{-3} M, 27 equiv. alcohol.

[b] Determined by GC; see Table 2 (p.28) for separation conditions.

[c] Determined by ^{1}H-NMR spectroscopy based on *o*-H integration of ketone and α-CH integration of alcohol.

Table III.3. Oxidation of Benzhydrols by trans-Ru(porp)$(O)_2$: The Effect of Water, Base and the Porphyrin on Alcohol Conversion.

Porphyrin[b] (solvent)	**Yield (%) [Turnover] at ~19 h and *~45 h*[a]**		
	(*p*-MeO-C_6H_4)PhCHOH[c]	**Ph_2CHOH[c]**	**(*p*-Cl-C_6H_4)PhCHOH[c]**
TMP (C_6H_6)	not measured, *54 [14]*	not measured, *25 [6]*	not measured, *15 [4]*
TMP (C_6H_6/H_2O)	99 [25], *100 [25]*	73 [18], *96 [24]*	66 [16], *96 [24]*
TMP (C_6H_6/1N NaOH)	80 [20], *87 [22]*	41 [10], *47 [12]*	51 [13], *70 [18]*
OCP (C_6H_6)	9 [2], *17 [4]*	6 [1], *16 [4]*	8 [2], *10 [2]*
OCP (C_6H_6/H_2O)	23 [6], *63 [16]*	10 [3], *24 [10]*	14 [4], *39 [5]*
OCP-Cl_8 (C_6H_6)	46 [12], *56 [14]*	53 [13], *58 [14]*	34 [8], *43 [11]*
OCP-Cl_8 (C_6H_6/H_2O)	98 [24], *98 [25]*	98 [24], *99 [25]*	98 [24], *98 [25]*

[a] Reaction conditions: 50°C, 2 mL benzene solvent under 1 atm of air, biphasic reactions were in a 2:1 ratio by volume of benzene/aqueous phase.

[b] [*trans*-Ru(TMP)$(O)_2$] = 3.8 x 10^{-3} M, [*trans*-Ru(OCP)$(O)_2$] = 4.6 x 10^{-4} M, [*trans*-Ru(OCP-Cl_8)$(O)_2$] = 2.7 x 10^{-4} M, 25 equiv. of alcohol.

[c] Determined by GC; see Table 2 (p.28) for separation conditions.

Catalyst activity is also affected by the substituents on the porphyrin ligand. Chlorinating the *o*-positions of the *meso*-phenyl groups decreases the catalyst activity for oxidation in both benzene and biphasic systems. Substituting chlorine atoms at the *β*-

positions of the porphyrin ring, as in OCP-Cl_8, provides greater catalytic activity than either the TMP or OCP complexes; the degree of enhanced activity is reduced in biphasic systems (Table III.3). Catalyst deactivation occurs at 50°C and is evident, in the absence of added water, as insoluble solids are deposited on the sides of the reaction vials after 24 h. In the presence of added water, these deposits are not formed; however, catalyst deactivation still occurs as only 42-50% conversion is noted during the first 20 h after the OCP-Cl_8 based reactions are recharged with additional alcohol. Monitoring the reactions after 120 h by UV-VIS spectroscopy indicates the presence of Ru(porp)(CO), seen as a band at 414, 410 or 418 nm, respectively (porp = TMP, OCP or OCP-Cl_8).

Plotting $\log(\%\text{conversion}_X/\%\text{conversion}_H)$, for alcohol oxidation catalyzed by *trans*-Ru(TMP)$(O)_2$ in benzene at 50°C after 45 h (Table III.2), against the Hammett factor σ_p or $2\sigma_p$ for mono- or di-substituted alcohols, respectively, yields linear plots with slopes of -1.5 and -2.4 when data for (p-Me_2N-$C_6H_4)_2$CHOH (σ_p = -0.63) are excluded. The *p*-amino-substituted alcohol is not included in the plot because further work indicated that conversion of benzhydrols to benzophenones was inhibited by a factor of ~ 2-7 when a tertiary amine was introduced into the benzene solution (Table III.5, p.80); this indicates that the amino substituent of the alcohol could inhibit the alcohol oxidation. The presence of two singlets for both the NMe_2 and CH protons, attributed to free and N-coordinated alcohol, after 48 h at 50°C supports this conclusion. The negative ρ values determined from the slopes of the Hammett plots indicate that aerobic oxidation of

benzhydrols catalyzed by *trans*-Ru(porp)$(O)_2$ is also favoured by electron-donating substituents.

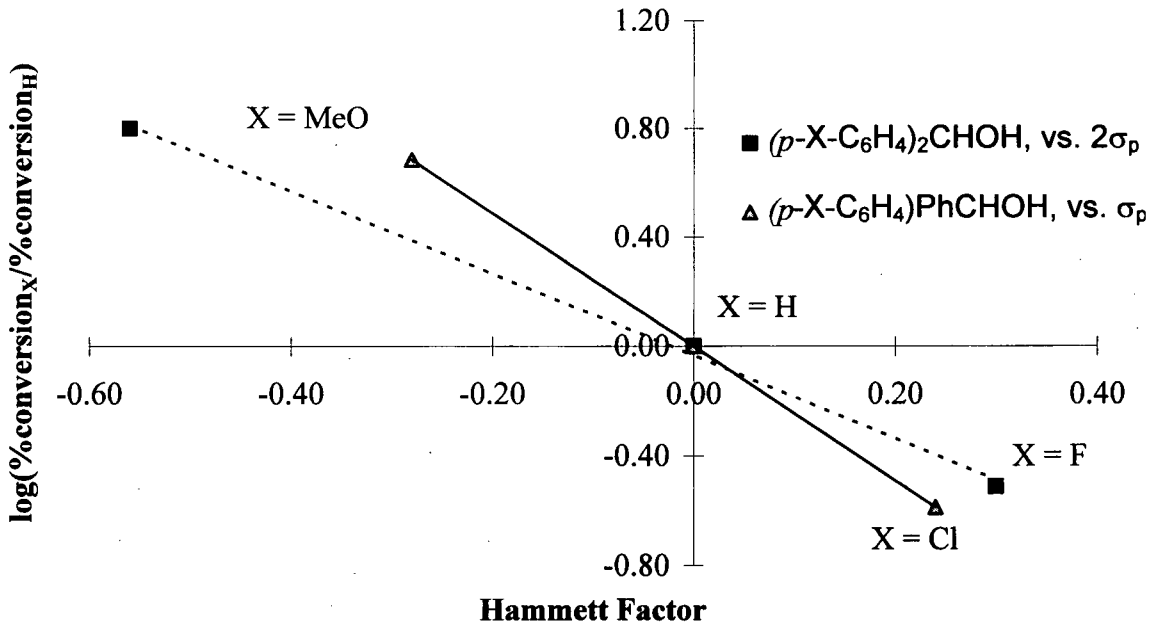

Figure III.15. Correlation of % conversion after 45 h at 50°C with the Hammett factor σ_p or $2\sigma_p$.

Finally, when the catalyst turnovers for the oxidation of benzhydrols at 50°C under 1 atm of air in benzene or biphasic benzene/water systems are compared with those for other alcohols, the following reactivity trends are noted (Table III.4): in the absence of added water, 1° benzylic > 2° alkylic > 2° benzylic alcohols, and in the presence of added water 1° benzylic > 2° benzylic > 2° alkylic alcohols.

Table III.4. Catalyst Turnover for Alcohol Oxidation Catalyzed by *trans*-Ru(TMP)$(O)_2$ Under 1 atm of Air at 50°C.

Substrate	Product	Turnover[a] (Benzene)	Turnover[b] (Biphasic System)
Benzhydrol	Benzophenone	6	18
4-Chlorobenzhydrol	4-Chlorobenzophenone	5	16
4-Methoxybenzhyrdrol	4-Methoxybenzophenone	14	25
Benzyl alcohol[32]	Benzaldehyde	26[c]	32
Isopropanol[32]	Acetone	6[c]	10

[a] Reactions were run in benzene; catalytic turnovers are quoted for reactions after 45 h (when the catalyst is still active).

[b] Reactions were run in a biphasic benzene/water system; catalytic turnovers are quoted for reactions after 19-24 h (when the catalyst is still active).

[c] Reactions were run in benzene; catalytic turnovers are quoted for reactions after 24 h (when the catalyst is still active).

Proposed Mechanism of Aerobic Benzhydrol Oxidation Catalyzed by* trans-*Ru(porp)$(O)_2$

The mechanism shown in eqs. 3.3-3.7 (which has been considered earlier by this group)[32,36] is proposed for the aerobic oxidation of alcohols catalyzed by *trans*-Ru(porp)$(O)_2$, where porp = TMP, OCP and OCP-Cl_8. Evidence for the outlined steps is discussed in the text below.

$$Ru^{VI}(O)_2 + 3Ph_2CHOH \longrightarrow Ru^{IV}(OCHPh_2)_2 + Ph_2CO + 2H_2O \qquad (3.3)$$

$$Ru^{IV}(OCHPh_2)_2 + 2H_2O \rightleftharpoons Ru^{IV}(OH)_2 + 2Ph_2CHOH \qquad (3.4)$$

$$Ru^{IV}(OH)_2 \rightleftharpoons Ru^{IV}(O) + H_2O \qquad (3.5)$$

$$2Ru^{IV}(O) \longrightarrow Ru^{VI}(O)_2 + Ru^{II} \qquad (3.6)$$

$$Ru^{II} + 1/2O_2 \longrightarrow Ru^{IV}(O) \qquad (3.7)$$

A study of the oxidation of Ph_2CHOH by *trans*-Ru(TMP)$(O)_2$ under air in benzene and biphasic water/benzene systems at 25°C using ^{1}H-NMR spectroscopy indicates the following: (i) Ru(IV)-bis(alkoxo) is the major species present in both solutions after 2 h; (ii) under 1 atm of air or dry O_2, and in benzene, the reaction exhibits pseudo first-order kinetics (Figure III.16) for the loss of *trans*-Ru(TMP)$(O)_2$ (in air with [Ph_2CHOH] = 0.071 M, $k_{obs} = 4.2 \times 10^{-4}$ s^{-1}, and in O_2 with [Ph_2CHOH] = 0.075 M, $k_{obs} = 3.4 \times 10^{-4}$ s^{-1}), the rate of this loss being ~ 2 times faster than noted in the stoichiometric reactions under N_2 at a similar alcohol concentration ([Ph_2CHOH] = 0.057 M, $k_{obs} = 1.7 \times 10^{-4}$ s^{-1}); (iii) after a 24 h reaction, no signals corresponding to the dioxo species are visible in the benzene solution, and under these conditions after 120 h only 3 equiv. of benzophenone are formed; (iv) addition of water prolongs the lifetime of *trans*-Ru(TMP)$(O)_2$ such that the dioxo species is still visible in solution after 24 h. These data imply that the initial step in the catalytic process is the formation of the Ru(IV)-bis(alkoxo) species during the first 24 h of reaction (eq. 3.3). Reactions run under dry O_2 or air were stirred at 25°C to ensure that the concentration of O_2 in solution remained constant; aliquots of solutions were monitored by ^{1}H-NMR spectroscopy to determine k_{obs} for *trans*-Ru(TMP)$(O)_2$ loss (for the experiments under N_2 no stirring was used). As it was necessary to use a different technique to monitor the reactions under O_2 or air (vs. N_2), and the k_{obs} values for the reactions under O_2 or air are similar (indicating no kinetic dependence on O_2 concentration), the two-fold increase in k_{obs} seen in the presence of O_2 (vs. N_2) is attributed to experimental effects and is not considered to be significant. Of note, pseudo

first-order kinetics are not observed for loss of *trans*-Ru(TMP)$(O)_2$ during the oxidation of Ph_2CHOH in a biphasic water/benzene system at 25°C under 1 atm of air.

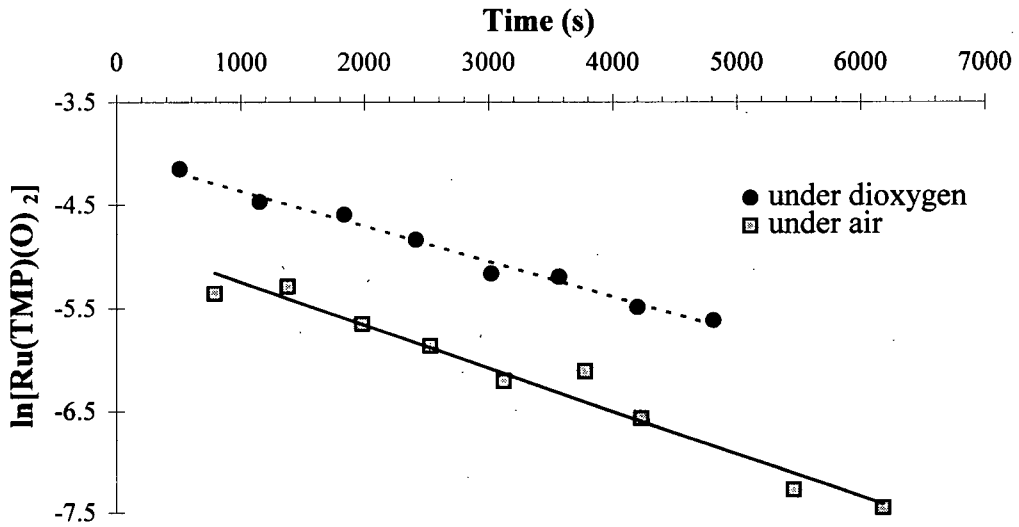

Figure III.16. Oxidation of Ph_2CHOH by *trans*-Ru(TMP)$(O)_2$ at 25°C under 1 atm of air or O_2 in C_6D_6. The loss of *trans*-Ru(TMP)$(O)_2$ was followed by measuring changes in the β-H signal intensity using the alcohol α-CH as an internal standard. Reactions were stirred under air or O_2 to ensure the concentration of O_2 in solution remained constant; [*trans*-Ru(TMP)$(O)_2$] ~ 5×10^{-3} M and [Ph_2CHOH] = 0.071 - 0.075 M.

Monitoring the oxidation of Ph_2CHOH by *trans*-Ru(TMP)$(O)_2$ in C_6D_6 at 50°C over 5 days, by ^{1}H-NMR spectroscopy, shows no detectable concentration of dioxo species present in solution after 24 h; only signals for the bis(alkoxo) species are visible. Yet, catalysis still occurs under these conditions as turnovers of 17, 21 and 25 for the oxidation of (p-Cl-C_6H_4)PhCHOH, Ph_2CHOH and (p-MeO-C_6H_4)PhCHOH, respectively, are found by GC analysis of reactions run in C_6H_6 after 97 h (see Table III.2, p.69).

Presumably, *trans*-Ru(TMP)$(O)_2$ that has been regenerated in a low, non-detectable, concentration is responsible for the oxidation. When a benzene solution of *trans*-Ru(TMP)$(OCH(p\text{-}MeO\text{-}C_6H_4)_2)_2$ is exposed to air at r.t., complete conversion to the dioxo-complex occurs after 1 day; $(p\text{-}MeO\text{-}C_6H_4)_2CO$ is formed as the co-product. However, when a C_6D_6 solution of *trans*-Ru(TMP)$(OCH(p\text{-}F\text{-}C_6H_4)_2)_2$ is exposed to air, after 2 days only 50% conversion to the Ru(VI)-dioxo complex has occurred; $(p\text{-}F\text{-}C_6H_4)_2CO$ is the co-product. This finding, along with the lower catalyst turnover of 17 for $(p\text{-}Cl\text{-}C_6H_4)PhCHOH$ versus 25 for $(p\text{-}MeO\text{-}C_6H_4)PhCHOH$ oxidation, indicates that (i) regeneration of *trans*-Ru(TMP)$(O)_2$ is also subject to the electronic effects of the *p*-substituents with more electron-donating substituents favouring reformation of the dioxo species, and (ii) subsequent to the formation of the Ru(IV)-bis(alkoxo) complexes, the catalytic process is limited by the rate of regeneration of the dioxo species. The Hammett plots shown in Figure III.15 (p.72) based on % conversion data after 45 h at 50°C probably illustrate, therefore, the electronic effect of changing *p*-substitution on the rate of *trans*-Ru(TMP)$(O)_2$ regeneration during the catalytic process. Previous work has shown that removal of water from the system, by using dry benzene and dry O_2, completely prevents the formation of the dioxo-complex from *trans*-Ru(TMP)$(O\text{i}Pr)_2$.[32] This result, when combined with point (iv) of above (p.74) and the increase in catalyst turnover in aqueous water/benzene systems (cf. Table III.3, p.69) indicates that water plays a key role in the regeneration of *trans*-Ru(porp)$(O)_2$ from Ru(IV)-bis(alkoxo) complexes. As proposed for the stoichiometric oxidation of alcohols by dioxo-ruthenium species (Figure III.11, p.63), alkoxo-hydroxo ligand exchange probably occurs to form a

Ru(IV)-bis(hydroxo) complex (eq. 3.4); this then reacts further through loss of one mole of water to form Ru(porp)(O) (eq. 3.5), which was still detected under the aerobic conditions at 25°C, but only in very low concentrations (Figure III.17). The generally accepted mechanism, though not fully established, for reformation of *trans*-Ru(porp)$(O)_2$ from Ru(porp)(O) is *via* disproportionation of the monooxo species (eq. 3.6).[30] Finally, rapid reaction of the 'bare' Ru(II)(porp)[28] with O_2 regenerates Ru(porp)(O) continuing the catalytic cycle (eq. 3.7). It has also been proposed that water accelerates the disproportionation reaction by increasing the rate of dioxo formation, eq. 3.8.[32]

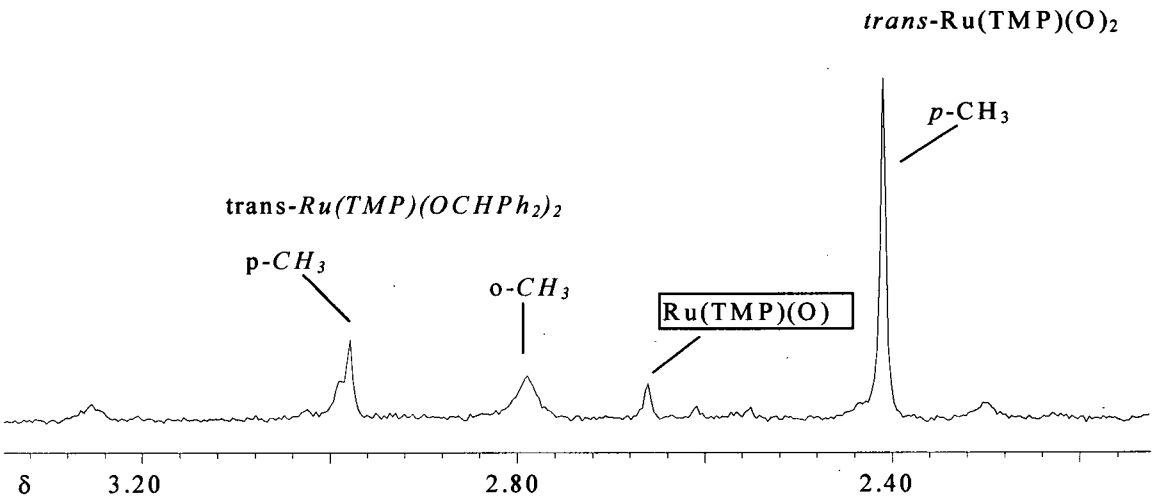

Figure III.17. ^{1}H-NMR spectrum obtained during Ph_2CHOH oxidation under 1 atm of air in benzene at 25°C. Signals corresponding to *trans*-Ru(TMP)$(OCHPh_2)_2$ are shown in italics while the *trans*-Ru(TMP)$(O)_2$ signals are indicated with a regular font.

$$\boldsymbol{Ru}^{IV}(O) + \boldsymbol{Ru}^{IV}(O)(OH_2) \rightarrow \boldsymbol{Ru}^{VI}(O)_2 + \boldsymbol{Ru}^{II}(OH_2) \qquad (3.8)$$

$\boldsymbol{Ru}$ = Ru(porp)

Evidence for the formation of Ru(II) species in the catalytic reaction was found when benzhydrols were oxidized in benzene under 1 atm of air at 50°C in the presence of

NEt_3 (8 equiv.). The conversion of benzhydrols to benzophenones using a *trans*-Ru(TMP)$(O)_2$ catalyst is decreased by a factor of 2-7 over the oxidations occurring in the absence of the amine (Table III.5, p.80). Studying the reaction, for (p-MeO-$C_6H_4)_2$CHOH oxidation in the presence of NEt_3 at 50°C under 1 atm of air in C_6D_6, by ^{1}H-NMR spectroscopy shows the lack of any significant concentration of Ru-bis(alkoxo) or -dioxo species after 24 h (Figure III.18). Presumably, in the absence of significant amounts of water, NEt_3 reacts with Ru(TMP) at a faster rate than O_2 does, and inhibits the regeneration of *trans*-Ru(TMP)$(O)_2$ *via* eq. 3.7, most likely by trapping the Ru as the stable *trans*-Ru(TMP)$(NEt_3)_2$ complex, δ 2.44 (p-CH_3) and 2.16 (o-CH_3) (evidenced by comparison with data for the Ru(II)-bis(benzylamine) complex, δ 2.35 (p-CH_3) and 2.26 (o-CH_3)).[33] Of interest, when the same reaction is run in a biphasic benzene/water (2:1) system at 50°C under 1 atm of air, the number of catalyst turnovers increases by a factor of 2.5 after 24 h of reaction (Figure III.19), indicating that water does affect catalytic turnover, possibly by accelerating the regeneration of Ru(IV)-oxo species from Ru(II) complexes (see eqs. 3.9 and 3.10). No significant concentration of *trans*-Ru(TMP)$(O)_2$ is noted in the presence of added water, under these conditions; however, signals corresponding to *trans*-Ru(TMP)(OCH-(p-$MeOC_6H_4)_2)_2$ are seen while those for *trans*-Ru(TMP)$(NEt_3)_2$ are absent (Figure III.19).

$$\boldsymbol{Ru}^{II}(L)_2 + 2\,H_2O \rightarrow \boldsymbol{Ru}^{II}(H_2O)_2 + 2\,L \qquad (3.9)$$

$$\boldsymbol{Ru}^{II}(H_2O)_2 + 1/2\,O_2 \rightarrow \boldsymbol{Ru}^{IV}(O)(H_2O) + H_2O \qquad (3.10)$$

L = alcohol or amine, ***Ru*** = Ru(porp)

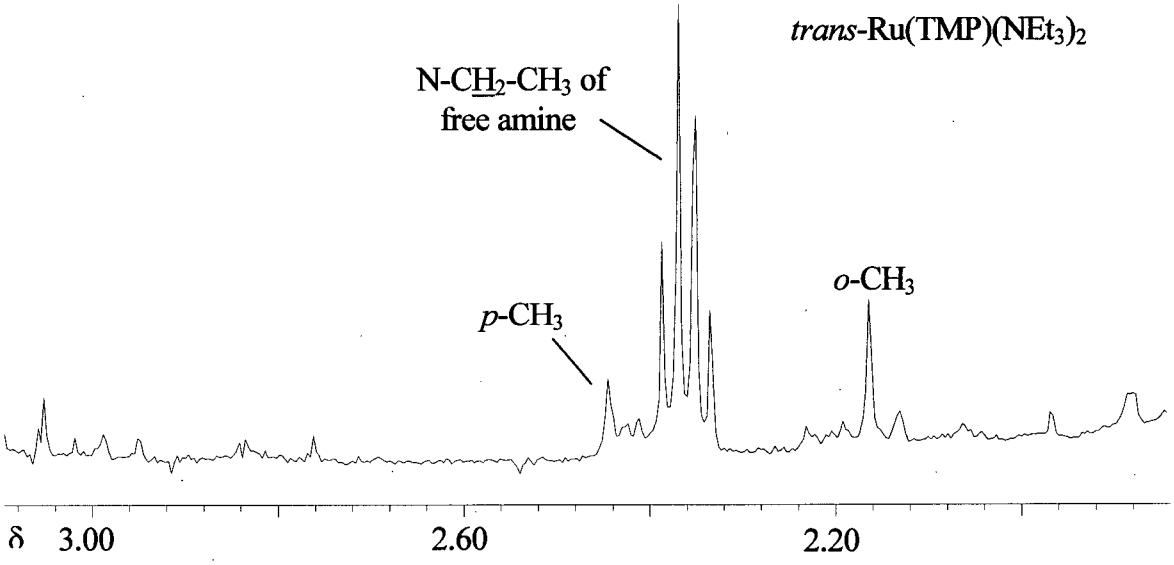

Figure III.18. ^{1}H-NMR spectra for (p-MeO-C_6H_4)$_2$CHOH oxidation by *trans*-Ru(TMP)$(O)_2$ in C_6D_6 under 1 atm of air at 50°C in the presence of NEt_3; [*trans*-Ru(TMP)$(O)_2$] = 4.8 x 10^{-4} M, [(p-MeO-C_6H_4)$_2$CHOH] = 0.075 M and [NEt_3] = 0.014 M; % conversion and [turnover] data after 24 h are: 8% and [13].

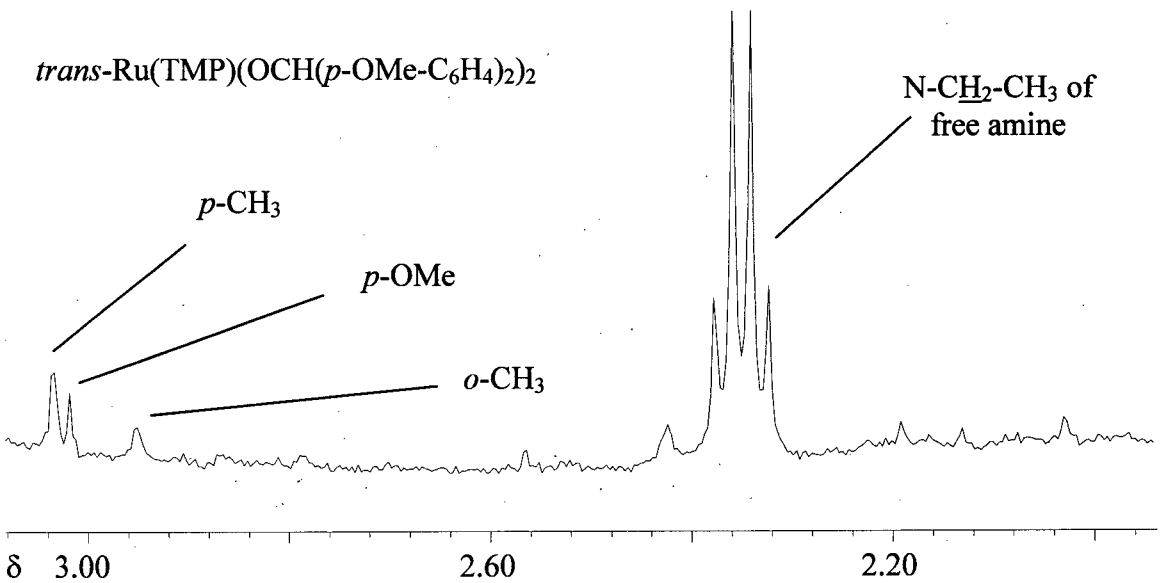

Figure III.19. ^{1}H-NMR spectra for (p-MeO-C_6H_4)$_2$CHOH oxidation by *trans*-Ru(TMP)$(O)_2$ in a biphasic C_6D_6/H_2O system under 1 atm of air at 50°C in the presence of NEt_3; [*trans*-Ru(TMP)$(O)_2$] = 4.8 x 10^{-4} M, [(p-MeO-C_6H_4)$_2$CHOH] = 0.072 M and [NEt_3] = 0.014 M; % conversion and [turnover] data after 24 h are: 21% and [31].

Finally, in an attempt to determine whether radical intermediates are formed during alcohol oxidations, BHT (2,6-di(*t*-butyl)-4-methylphenol) was added to the reactions in benzene. In the presence of 4 equiv. of BHT, based on Ru, the percent conversion of the benzhydrols is generally cut in half after 40 h, although in the $(p\text{-F-C}_6\text{H}_4)_2\text{CHOH}$ oxidation the conversion actually increased somewhat (Table III.5); however, when BHT is added to a benzene solution of *trans*-Ru(TMP)$(\text{O})_2$ in the absence of alcohol, loss of the TMP signals for the Ru(VI)-dioxo species occurs after 1 h. at r.t.. Subsequent heating of this solution to 50°C under air results in a decrease in signal intensity for the *t*-butyl H atoms of BHT and the formation of a large number of alkyl signals in the region of δ 0.7-1.0. These results indicate that the decrease in alcohol conversion in the presence of BHT probably results from the reaction of BHT with *trans*-Ru(TMP)$(\text{O})_2$, possibly to form a Ru(IV)-bis(phenoxo) complex, rather than through its action as a radical trap. Regeneration of the dioxo species from any such Ru-BHT complex must be slower than that from the bis(alkoxo) complexes (with the exception of *trans*-Ru(IV)(TMP)$(\text{OCH}(p\text{-F-C}_6\text{H}_4)_2)_2$), thus limiting the catalyst turnover. The fact that *trans*-Ru(TMP)$(\text{O})_2$ stoichiometrically oxidizes phenol to form a bis(phenoxo)ruthenium(IV) complex and *p*-hydrobenzoquinone,[5,32] implies that a reaction with BHT is not unexpected. Cyclobutanol, cyclopentanol and cyclohexanol are all converted to the corresponding cyclic ketones,[36] indicating that long-lived radical species are not formed during the catalytic cycle.

Table III.5. The Effect of BHT and NEt_3 on Benzhydrol Oxidation.

	Yield (%) and [Turnover][a]	
Alcohol	**40 h[b]**	**90 h[b]**
Ph_2CHOH	25 [7]	51 [14]
+ NEt_3	3 [1]	6 [2]
+ BHT	13 [4]	22 [6]
(*p*-Cl-C_6H_4)PhCHOH	15 [4]	21 [6]
+ NEt_3	6 [2]	10 [3]
(*p*-MeO-C_6H_4)PhCHOH	54 [15]	77 [21]
+ NEt_3	7 [2]	10 [3]
+ BHT	23 [6]	39 [10]
(*p*-MeO-C_6H_4)$_2$CHOH	85 [23]	95 [25]
+ NEt_3	42 [11]	36 [10]
+ BHT	23 [6]	60 [16]
(*p*-F-C_6H_4)$_2$CHOH	15 [4]	32 [9]
+ NEt_3	6 [1]	13 [4]
+ BHT	22 [6]	35 [9]

[a] Reaction conditions: 50°C, 1 mL benzene solvent under 1 atm of air. [*trans*-Ru(TMP)$(O)_2$] = 1.7×10^{-3} M, 27 equiv. alcohol, [NEt_3] = 1.4×10^{-2} M and [BHT] = 6.8×10^{-3} M.

[b] Determined by GC; see Table 2 (p.28) for separation conditions.

Conclusions

The ability of *trans*-Ru(TMP)$(O)_2$ to stoichiometrically oxidize benzhydrols was investigated in an effort to gain insight into the mechanism of the reaction. Intermediates of the type *trans*-Ru(TMP)$(OR)_2$ were isolated from the stoichiometric reactions and characterized by ^{1}H-NMR, IR and UV-VIS spectroscopies. Kinetic studies indicate that cleavage of the α-CH bond occurs in the rate-determining step, most likely *via* hydride transfer to the Ru=O moiety, though a slow hydrogen-atom transfer followed by a fast 1-electron transfer can not be ruled out. This conclusion is supported by a limited, linear Hammett correlation (ρ = -1.1) between $2\sigma_p$ and the stoichiometric rate constants k_1 determined by UV-VIS spectroscopy for the oxidation of *p*-substituted benzhydrols.

Trans-Ru(porp)$(O)_2$ complexes also catalyze the aerobic oxidation of benzhydrols into benzophenones. Studies of the system at 25 and 50°C by ^{1}H-NMR spectroscopy indicate that initially the catalytic process is limited by the rate at which the Ru(IV)-bis(alkoxo) species are formed (the first step in the catalytic cycle). Subsequently, the catalyst turnover is limited by the rate at which the dioxo species can be reformed. Added water is essential for higher catalytic activity and increases the % conversion to ketones by a factor of 2-6 after 45 h at 50°C (Table III.3). The role of water is complex: the water is thought to be involved in accelerating the regeneration of the Ru(VI)-dioxo catalyst through ligand exchange with the Ru(IV)-bis(alkoxo) complexes and by accelerating the reaction of Ru(II) with O_2 (eqs. 3.4, and 3.8-3.10). Very limited linear Hammett correlation plots between % conversion after 45 h and σ_p indicate that the conversion of

benzhydrols to benzophenones in benzene is accelerated in the presence of *p*-electron-donating groups. As complete conversion to the bis(alkoxo) complexes occurs within 24 h in the absence of added water, these Hammett plots presumably illustrate the effect of electron-donating groups on the regeneration of *trans*-Ru(porp)$(O)_2$. Finally, a comparison of catalyst turnover after 24 h at 50°C under 1 atm of air with those of other alcohols shows the following reactivity trend: 1° benzylic > 2° alkylic > 2° benzylic alcohols in the absence of added water, and 1° benzylic > 2° benzylic > 2° alkylic in the presence of added water.

CHAPTER IV

OXIDATION OF AMINES

Introduction

Recently, work in this laboratory has extended the use of *trans*-Ru(porp)$(O)_2$ oxidants to the catalytic and stoichiometric dehydrogenation of amines (see eqs. 4.1 and 4.2 for the stoichiometric reactions).[33]

$$Ru^{VI}(TMP)(O)_2 + 4\ RR'CHNH_2 \rightarrow Ru^{II}(TMP)(RR'CHNH_2)_2 + 2\ RR'C{=}NH + 2\ H_2O \quad (4.1)$$

(R and R′ = aryl or alkyl substituents), or

$$Ru^{VI}(TMP)(O)_2 + 3\ RCH_2NH_2 \rightarrow Ru^{II}(TMP)(RCH_2NH_2)_2 + RCN + 2\ H_2O \quad (4.2)$$

This is the first example of Ru-porphyrin catalyzed amine oxidation, though a few stoichiometric oxidations have been investigated also (Chapter I).[38,50] Understanding the mechanism of this reaction may provide greater knowledge of the metabolism of both naturally occurring amines and xenobiotics.[38] In an effort to gain insight into this mechanism, the kinetics of the stoichiometric oxidation of amines by *trans*-Ru(porp)$(O)_2$ (porp = TMP and OCP) were investigated as part of this thesis work. The catalytic reaction was also examined briefly in an attempt to determine the effect of changing the porphyrin ligand and reaction conditions on the catalyst turnover and % conversion of the amines.

Sample Preparation and Data Analysis

Stoichiometric Reactions

The stoichiometric oxidations of the amines Ph_2CHNH_2, racemic (*rac*-)$Ph(Me)CHNH_2$ and $iPrNH_2$, by *trans*-Ru(porp)$(O)_2$ (porp = OCP and TMP) were followed by UV-VIS spectroscopy. Some of the kinetic data amassed during these investigations are listed in Appendix B. *Trans*-Ru(OCP)$(O)_2$ was synthesized by *m*-CPBA oxidation of Ru(OCP)(CO) in benzene or $CHCl_3$ and purified, respectively, through a silica or basic alumina column. The corresponding TMP-based oxidant was synthesized through O_2 oxidation of *trans*-Ru(TMP)$(MeCN)_2$ in benzene. Reactions were run at 23°C in an anaerobic, UV-VIS spectroscopic cell (Figure II.1, p.25) with a 1.0 cm path length, monitored at 420 nm (the Soret maximum for *trans*-Ru(TMP)$(O)_2$), or a 0.1 cm path length, monitored at 506 for the *rac*-$Ph(Me)CHNH_2$ system, 508 for $iPrNH_2$ or 510 nm for Ph_2CHNH_2 (the respective α-band absorption maxima for the *trans*-Ru(II)-bis(amine) products).

The stoichiometric oxidations of amines by *trans*-Ru(porp)$(O)_2$ were examined using several different procedures. Two typical procedures, one for the OCP-based oxidant and the other for the TMP-based oxidant are described below, and any deviations from these procedures are noted, where necessary, in the text. The amines used in all of the experiments were liquid and were purified by distillation (Chapter II).

Procedure A: Trans-*Ru(OCP)(O)$_2$ Oxidant*

A freshly columned solution of *trans*-Ru(OCP)(O)$_2$ was transferred to a 1.0 cm or 0.1 cm path length, anaerobic, UV-VIS spectroscopic cell, the solvent removed *in vacuo*, and the system then placed under Ar. Meanwhile, a solution of Ph_2CHNH_2 in dry solvent (10^{-2} M) was purged with Ar for 20-30 min. The solid oxidant was then redissolved in a known amount of dry, Ar-saturated solvent (5-20 mL) and its concentration determined by UV-VIS spectroscopy using known ε values;[32] concentrations were typically 4-8 x 10^{-6} M for the 1.0 cm cell and 2-5 x 10^{-4} M for the 0.1 cm cell. By use of a syringe, the amine solution was transferred to the anaerobic cell and the two solutions mixed for 30 s, prior to the start of analysis. The final amine concentration in the reaction mixture ranged from 0.5-2 x 10^{-3} M for reactions in the 1.0 cm cell and 0.4-1 x 10^{-2} M for reactions in the 0.1 cm cell.

Procedure B: Trans-*Ru(TMP)(O)$_2$ Oxidant*

Solid *trans*-Ru(TMP)(MeCN)$_2$ (1 mg, 1.1 x 10^{-3} mmol) was placed in a 0.1 cm anaerobic cell and dissolved in dry benzene. Dioxygen was bubbled through the solution for 10 min and the solution monitored by UV-VIS spectroscopy to ensure complete conversion to the dioxo product. The solvent was removed under vacuum and the solid oxidant placed under an atmosphere of Ar. A solution of *i*PrNH$_2$ (2 mL, 2.6 x 10^{-2} M) in dry C_6H_6 or *rac*-Ph(Me)CHNH$_2$ (1.5 mL, 1.4 x 10^{-2} M) in C_6D_6 under Ar, degassed by 3 freeze-pump-thaw cycles, was transferred to the cell *via* canula and the two solutions mixed for 60 or 70 s before the reaction was monitored.

Catalytic Aerobic Oxidations

Solutions of *trans*-Ru(porp)$(O)_2$ (porp = TMP, OCP and OCP-Cl_8) in benzene were synthesized by *m*-CPBA oxidation of the carbonyl precursor and purified through a column of basic alumina. UV-VIS spectroscopy was used to determine the concentration of the oxidant (typically 0.1-1 x 10^{-3} M) using known ε values[32] and 20 equiv. of the amine were added to 1 mL of the Ru-dioxo solution in a vial (~ 15 mL) containing a stir bar. The vials were tightly capped and the solutions stirred at 50°C under 1 atm of air for 24 - 90 h. The solutions were then analyzed by GC and the identities of the products were determined by comparison with data for known standards (see Table II.1, p.27 for GC separation conditions). Substrate and product concentrations were determined using calibration curves of concentration versus peak area allowing percent conversion and catalyst turnover to be calculated.

Stoichiometric Oxidation of Amines with *trans*-Ru(porp)$(O)_2$

Initial investigations into the stoichiometric oxidation of amines commenced using *trans*-Ru(OCP)$(O)_2$ oxidant and Ph_2CHNH_2 as substrate. The reaction (eq. 4.1) was monitored in the Soret (420 nm) region of the spectrum at low Ru concentrations (~ 10^{-6} M) in dry benzene under Ar using a minimum 100 equiv. excess of the amine over 12 h. Spectral changes, monitored at 420 nm, are shown in Figure IV.1.[ζ] The natural logarithm of $A-A_\infty$ was plotted against time to determine the pseudo first-order rate constant, k_{obs}, for the reactions; A_∞ was determined from the spectrum at t = 12 h. The slopes of the line

[ζ] Absorbance values at 420 nm for benzene solutions of *trans*-Ru(OCP)$(O)_2$ (~ 10^{-6} M) under Ar or O_2, in the absence of added amine, remain essentially constant over 7200 s.

for the $\ln|A-A_\infty|$ versus time plots determined usually over the first 1500 s, gave k_{obs} values ranging from 2-10 x 10^{-4} s^{-1} for a range of amine concentrations from 0.5-8.5 x 10^{-3} M (Figure IV.2). Unfortunately, plots of k_{obs} against amine concentration showed non-reproducible results, with k_{obs} values varying by up to 200% for essentially repeat reactions run at the same amine concentration (Figure IV.3). Comparison of the shapes of the absorbance versus time plots, for spectral changes at 420 nm, also showed that the reactions were not reproducible (Figure IV.1).

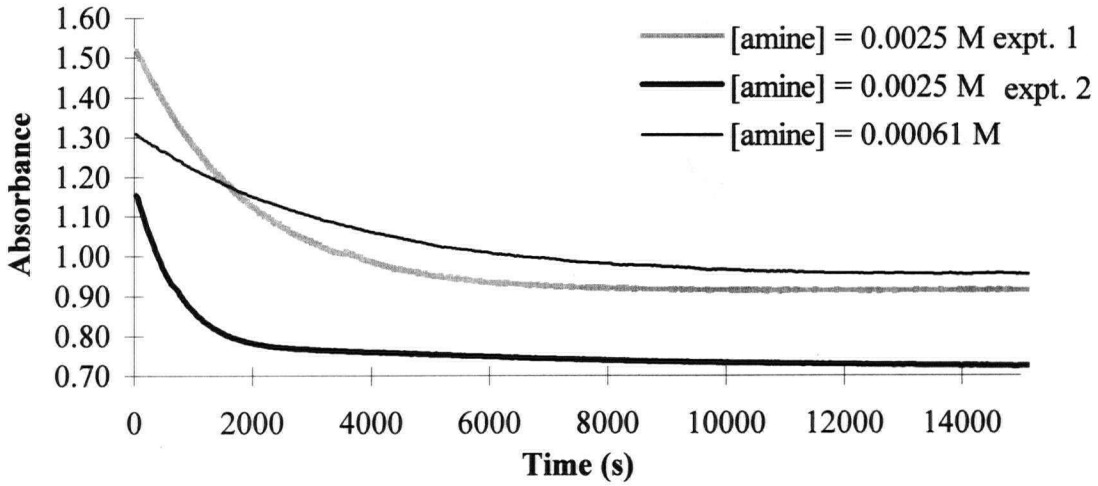

Figure IV.1. Plots of absorbance, at 420 nm, versus time for the stoichiometric oxidation of Ph_2CHNH_2 with *trans*-Ru(OCP)$(O)_2$ in dry benzene at 23°C under Ar. Essentially repeat experiments, run at the same amine concentration, do not show reproducible absorbance changes.

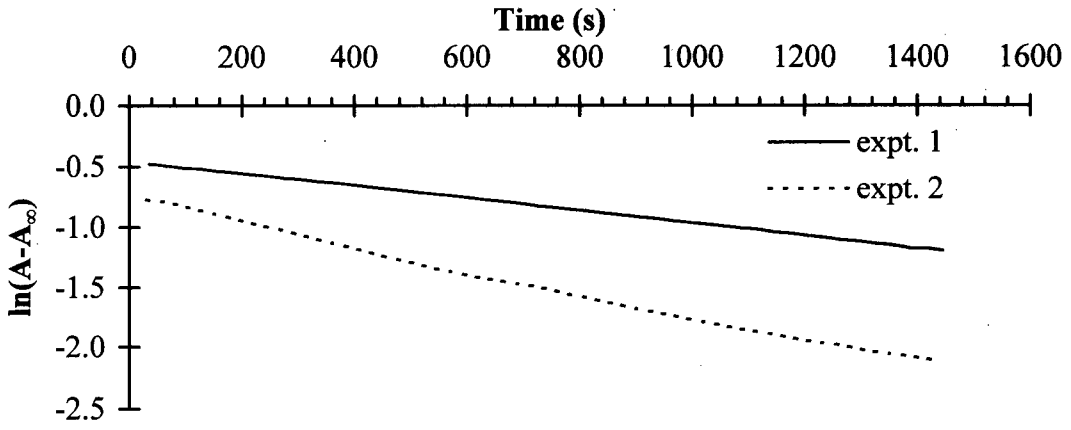

Figure IV.2. Pseudo first-order plots of $\ln|A-A_\infty|$ versus time for the stoichiometric oxidation of Ph_2CHNH_2 at 23°C under 1 atm of Ar; [*trans*-Ru(TMP)$(O)_2$] ~ 5 x 10^{-6} M and [Ph_2CHNH_2] = 0.0025 M.

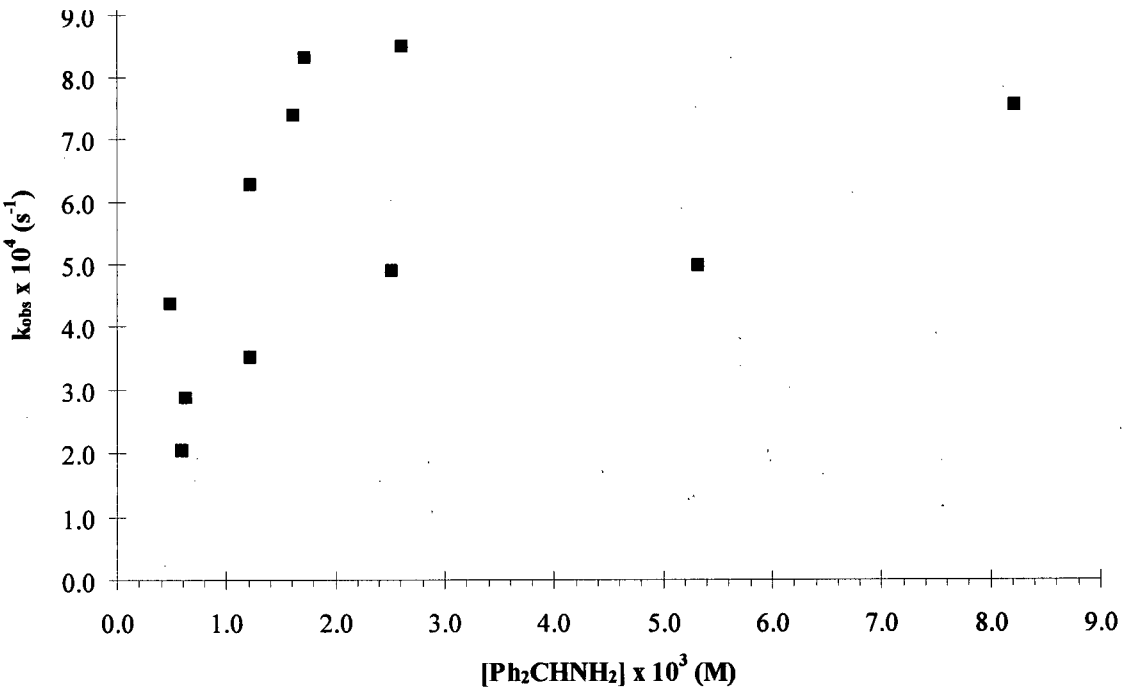

Figure IV.3. Plot of k_{obs} against [Ph_2CHNH_2] for reactions at 23°C under 1 atm Ar in dry benzene; non-reproducible results are evident. Instrumental error is within the size of the points.

Because of the possibility that very low concentrations of O_2 remaining in the solutions may have played a role in the irreproducibility, the reaction was repeated under an atmosphere of O_2. In these case, both the Ph_2CHNH_2 (0.3-1.3 x 10^{-3} M) and *trans*-Ru(OCP)$(O)_2$ (~ 10^{-6}M) solutions were purged with dry O_2 rather than dry Ar. Absorbance data were extracted at 420 nm and non-linear regression analysis of the absorbance versus time plots was used to determine both k_{obs} and A_∞ values (Figure IV.4). These k_{obs} values were compared with those determined from the Guggenheim method of analysis, and excellent agreement was found (see Figure B.1, Appendix B).

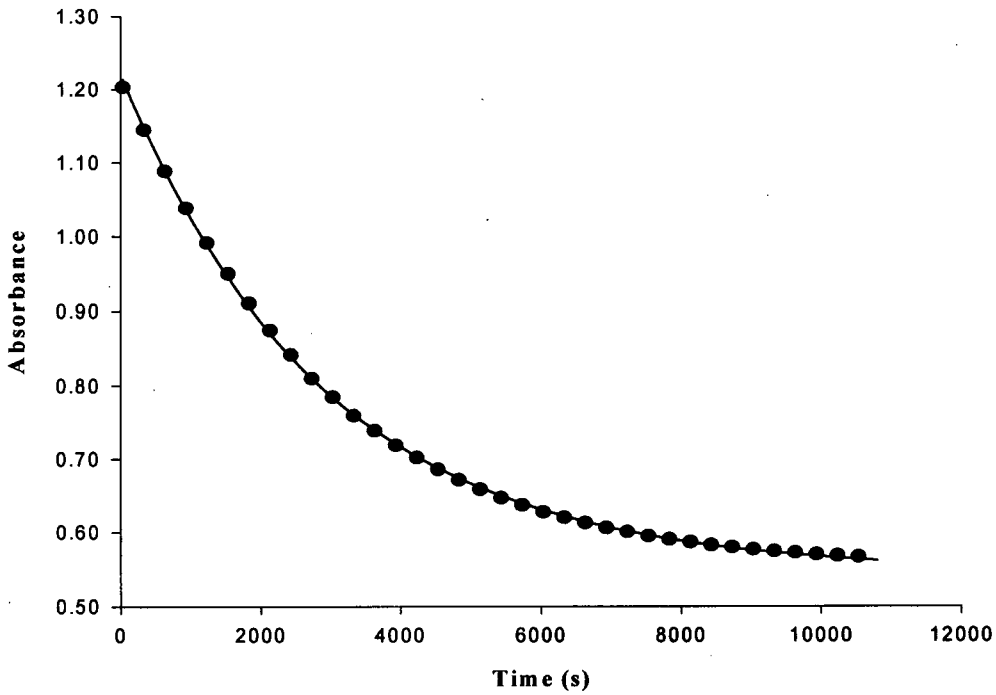

Figure IV.4. A typical absorbance (at 420 nm) versus time plot for Ph_2CHNH_2 oxidation with *trans*-Ru(OCP)$(O)_2$ under 1 atm of O_2 in dry benzene at 23°C. The line for pseudo first-order kinetics, $A = A_\infty + (A_o - A_\infty)\exp(-k_{obs}t)$, was fit to the data using non-linear regression analysis; [*trans*-Ru(OCP)$(O)_2$] = 5.1 x 10^{-6} M and [Ph_2CHNH_2] = 1.3 x 10^{-3} M.

Plots of k_{obs} against [amine] for the reactions under 1 atm of O_2 (Figure IV.5) again showed a similar scatter of points as for reactions performed under 1 atm of Ar. Similar k_{obs} values were obtained in the presence or absence of O_2, implying that low concentrations of O_2 remaining in solutions purged with Ar are not the source of the irreproducible results. This finding also indicates that the rate of regeneration of Ru(VI)-dioxo species (for the purposes of a catalytic process) is much slower than that of amine dehydrogenation at 23°C in benzene.

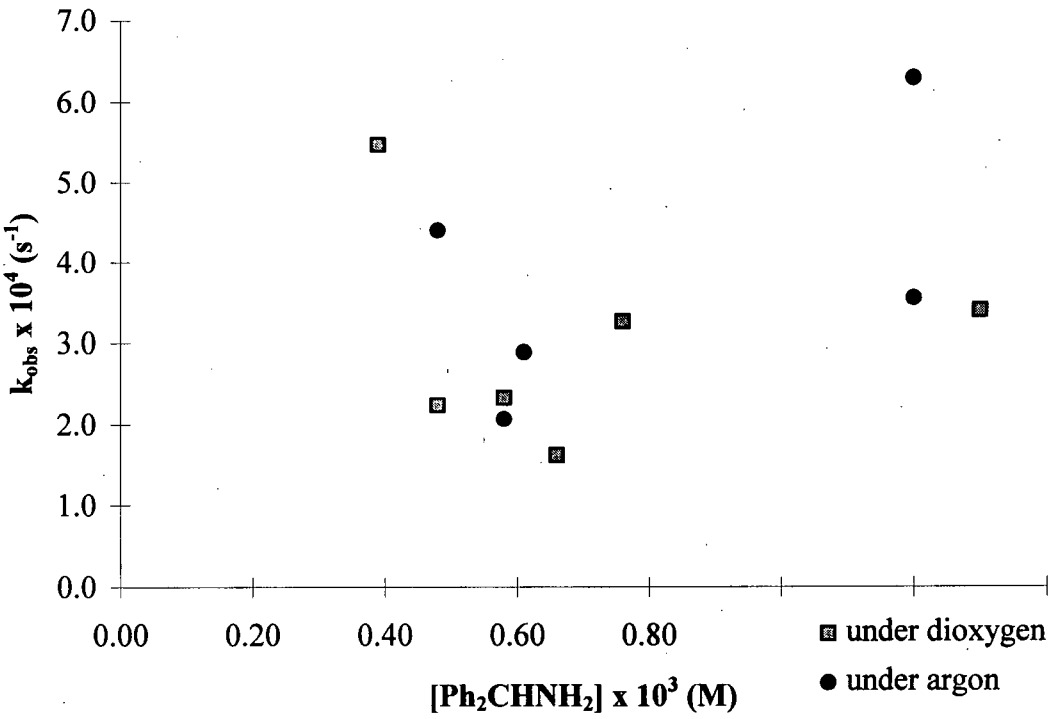

Figure IV.5. Plot of k_{obs} versus $[Ph_2CHNH_2]$ under O_2 and Ar in dry benzene at 23 °C. Instrumental error is within the size of the points.

It has been shown previously that low concentrations of *trans*-Ru(OCP-Cl_8)$(O)_2$ ($\leq 10^{-5}$ M) in neat alkane or alkene catalyze the aerobic oxidation of these compounds *via* free-radical pathways.[32] Perhaps a related stoichiometric reaction is occurring with benzene at low [*trans*-Ru(OCP)$(O)_2$] thus causing a loss of the oxidant that is not involved in amine oxidation. In an effort to rule out this possibility, the reactions were run at a higher Ru-oxidant concentration. Due to the low solubility of the oxidant in C_6H_6, the solvent was changed to $CHCl_3$ in order to reach concentrations of 10^{-4} M. The reactions were run following procedure A under Ar using a 0.1 cm path length cell; the first two reactions attempted did not exhibit typical pseudo first-order absorbance changes at 510 nm with time (Figure IV.6). Because the reaction might be light-sensitive, a filter was placed between the sample and source in order to block out light from 200-450 nm and prevent strong absorbance within the Soret region of the spectrum. The anaerobic cell was also wrapped in Al foil in an attempt to limit the effects from ambient light within the room. Plots of absorbance versus time collected under these conditions (Figure IV.7) now displayed typical pseudo first-order changes (Figure IV.8), and $\ln|A-A_\infty|$ showed a linear dependence on time over the first 3500 s of the reaction; A_∞ values were determined after 16 h. Examination of the k_{obs} values at an average amine concentration of 0.097 M shows irreproducibility once again; a range of 0.68-1.3 x 10^{-3} s^{-1} is found (Table IV.1). This finding indicates that low Ru-dioxo concentrations are not responsible for the irreproducible pseudo first-order kinetics. However, a comparison of Figure IV.6 and Figure IV.8 shows the reactions do exhibit a light-sensitivity at Ru-dioxo concentrations of 10^{-4}M .

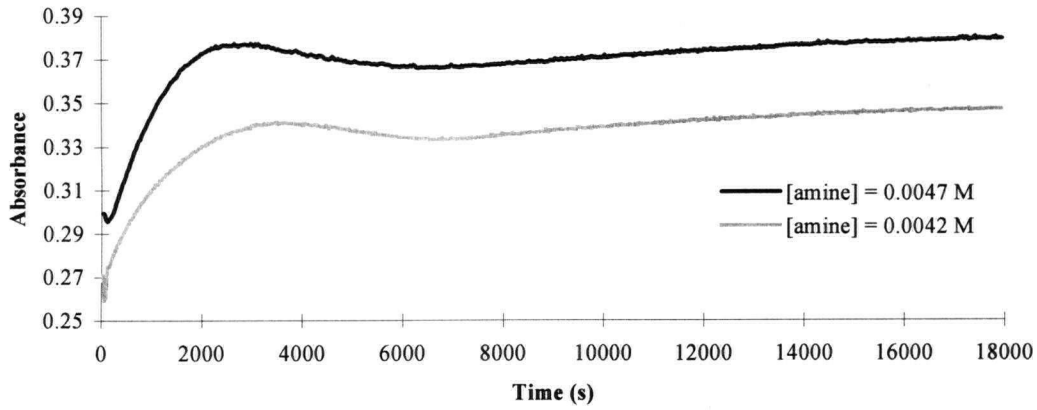

Figure IV.6. Absorbance changes at 510 nm monitored during the stoichiometric reaction of *trans*-Ru(OCP)$(O)_2$ with Ph_2CHNH_2 in $CHCl_3$ under 1 atm of Ar at 23°C; [*trans*-Ru(OCP)$(O)_2$] ~ 2 x 10^{-4} M.

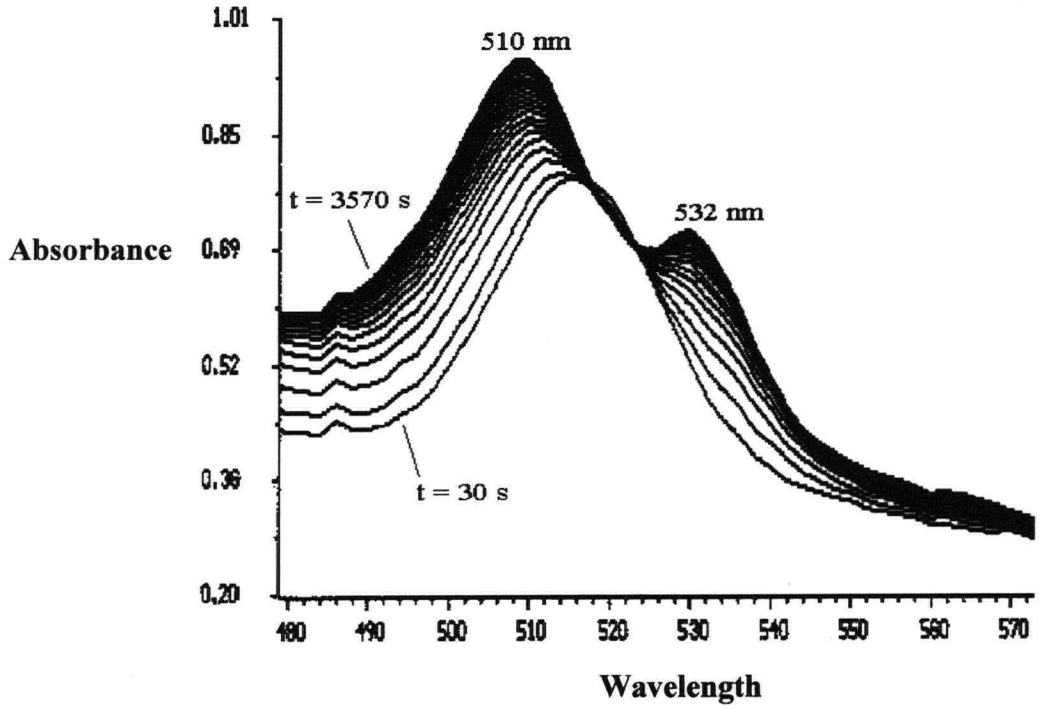

Figure IV.7. Typical spectral changes observed over 480-570 nm for the oxidation of Ph_2CHNH_2 by *trans*-Ru(OCP)$(O)_2$ under 1 atm of Ar at 23°C in $CHCl_3$. The reaction was run in the presence of a 200-450 nm filter and the UV-VIS cell was wrapped in Al foil to block out ambient light; [*trans*-Ru(OCP)$(O)_2$] = 4.9 x 10^{-4} M and [Ph_2CHNH_2] = 9.7 x 10^{-3}M

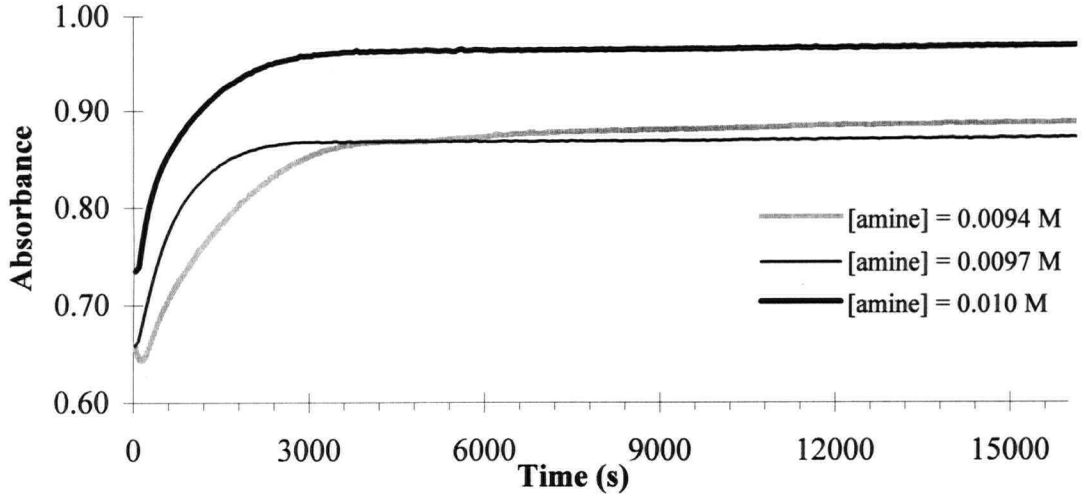

Figure IV.8. Absorbance changes at 510 nm during the stoichiometric reaction of *trans*-$Ru(OCP)(O)_2$ (5×10^{-4} M) with Ph_2CHNH_2 in $CHCl_3$ under 1 atm of Ar at 23°C. The anaerobic cell was wrapped in Al foil, and a 200-450 nm filter was placed between the source and sample in order to limit the effects of ambient room light and prevent absorbance within the Soret (420 nm) region of the spectrum.

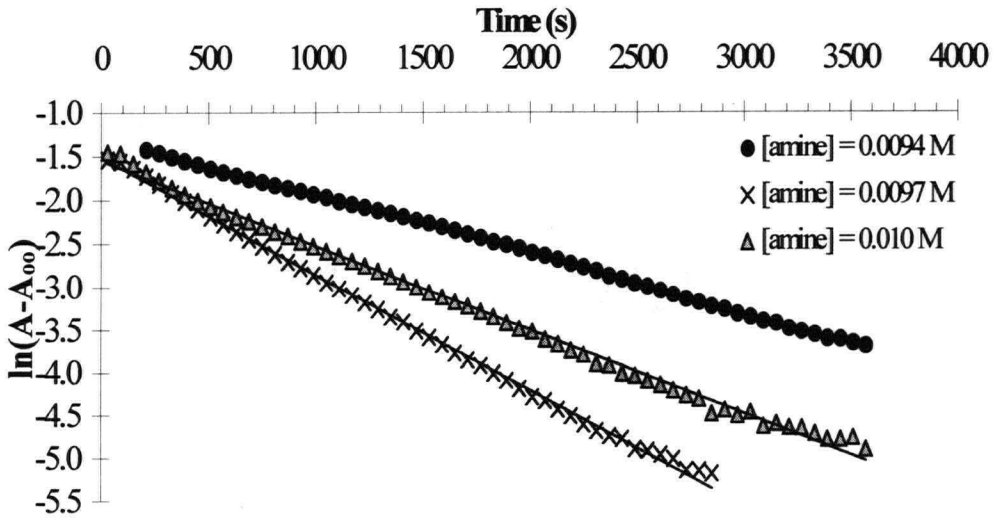

Figure IV.9. A $\ln|A-A_\infty|$ versus time plot based on absorbance data at 510 nm collected at $[Ph_2CHNH_2] \sim 0.0097$ M for amine dehydrogenation by *trans*-$Ru(OCP)(O)_2$ in $CHCl_3$.

Table IV.1. The Range of k_{obs} Values Determined for Stoichiometric Oxidation of Ph_2CHNH_2 by *trans*-Ru(OCP)$(O)_2$.

[*Trans*-Ru(OCP)$(O)_2$] x 10^4 (M)[a]	[Ph_2CHNH_2] x 10^3 (M)	k_{obs} x 10^3 (s^{-1})
4.7	9.4	0.68
4.9	9.7	1.3
5.1	10.1	0.98

[a] Reaction conditions: 23°C, 0.1 cm path length anaerobic cell, under 1 atm Ar in $CHCl_3$; with use of 200-450 nm filter.

As both O_2 and the oxidant concentration were thus ruled out as the source of irreproducibility, a few other possibilities were considered: (i) the amine itself was the source of the problems; (ii) there were traces of residual *m*-CPBA leftover from the *in situ* *trans*-Ru(OCP)$(O)_2$ synthesis that affected the results; or (iii) the reactions were extremely water-sensitive. In an effort to rule out (i) and (ii), the stoichiometric oxidation of $iPrNH_2$ was studied using an oxidant, *trans*-Ru(TMP)$(O)_2$, synthesized by O_2-oxidation of the bis(acetonitrile) complex (see procedure B). A box was used to shield the reactions from ambient light and a 200-450 nm filter prevented strong absorbance in the Soret (420 nm) region of the spectrum. Studying time-resolved absorbance traces for spectral changes at 508 nm showed once again that repeat reactions did not give the same results (Figure IV.10). Finally, in an effort to rule out water as a source of the problems, wet C_6D_6 (~ 10^{-3} M determined by ^{1}H-NMR spectroscopy) was used as the solvent to study the oxidation of *rac*-Ph(Me)$CHNH_2$ by *trans*-Ru(TMP)$(O)_2$. At this concentration, water is present in a 5-7 fold excess over Ru ([*trans*-Ru(TMP)$(O)_2$] = 1.8-2.8 x 10^{-4} M). Even under these conditions, repeat reactions did not show the same spectral changes at 506 nm (Figure IV.11).

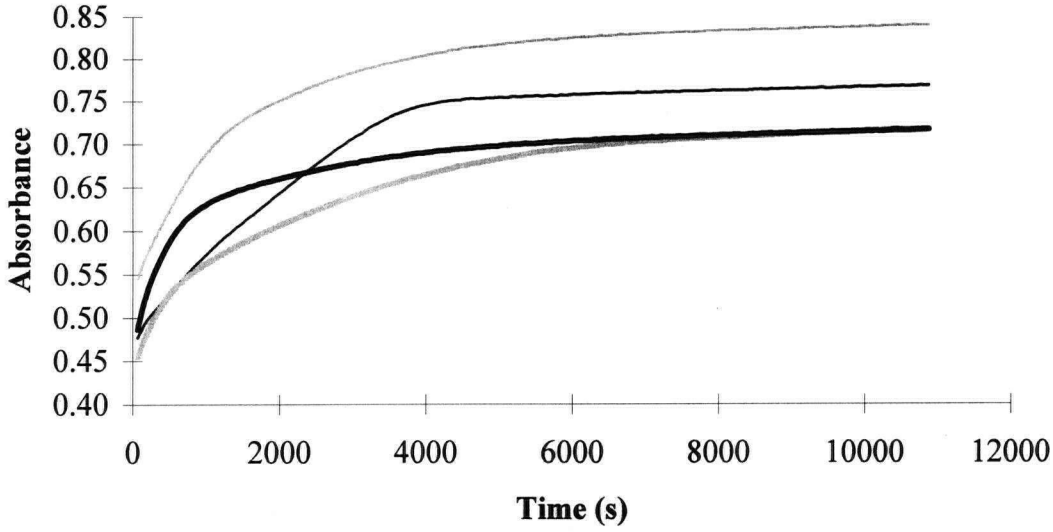

Figure IV.10. Absorbance at 508 nm versus time plots for the stoichiometric oxidation of *i*PrNH$_2$ by *trans*-Ru(TMP)(O)$_2$ at 23°C under 1 atm of Ar in dry C_6H_6; [*trans*-Ru(TMP)(O)$_2$] = 3.2-3.5 x 10^{-4} M and [*i*PrNH$_2$] = 7.8 x 10^{-3} M.

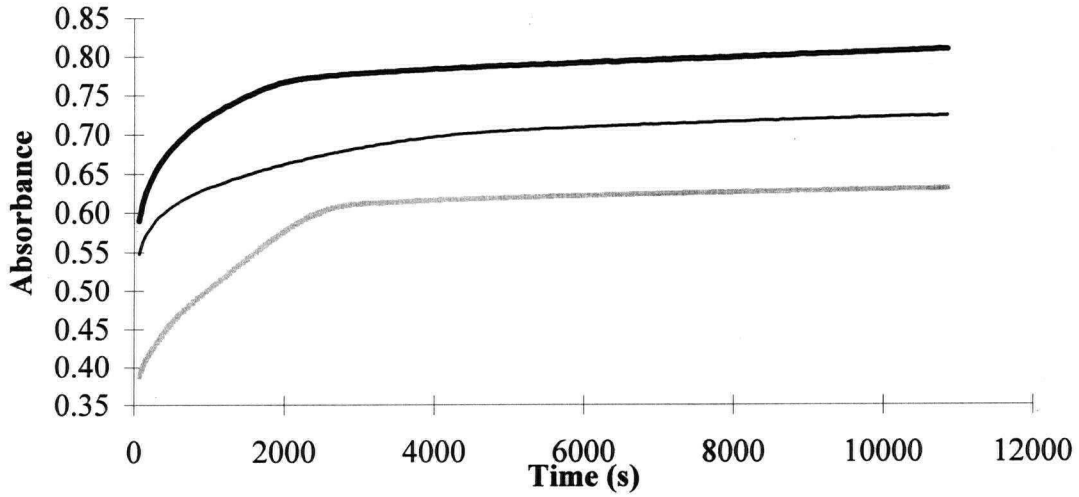

Figure IV.11. Absorbance at 506 nm versus time plots for the stoichiometric oxidation of *rac*-Ph(Me)CHNH$_2$ by *trans*-Ru(TMP)(O)$_2$ at 23°C under 1 atm of Ar in wet C_6D_6; [*trans*-Ru(TMP)(O)$_2$] = 1.8-2.8 x 10^{-4} M and [*rac*-Ph(Me)CHNH$_2$] = 1.4 x 10^{-2} M.

As trace air, low oxidant concentration, the amine, trace acid and water had been ruled out as the source of the problems, and no other possible sources could be thought of, it was concluded that the stoichiometric reaction could not be studied by UV-VIS spectroscopy. At this stage of the studies, Dr. M. Ezhova in this group found that the reaction could be studied successfully by ^{1}H-NMR spectroscopy (at concentrations about 10 times those used in the 0.1 cm path length UV-VIS studies). Thus, further reactions in attempts to study the stoichiometric amine oxidation using *trans*-Ru(porp)$(O)_2$ oxidants were not performed. The success of the NMR spectroscopic studies, where the reaction is monitored in the darkness of the NMR probe, implies perhaps an 'extreme' photosensitivity of the system.

Amine Dehydrogenation Catalyzed by *Trans*-Ru(porp)$(O)_2$ Complexes in Air; Porp = TMP, OCP or OCP-Cl_8

Previous work in this laboratory has demonstrated that *trans*-Ru(porp)$(O)_2$ catalyzes the dehydrogenation of amines to form imines and imine hydrolysis products, or nitriles. Detailed results had only been compiled for the TMP systems.[33] In an effort to study the effect of chlorinating the porphyrin, the reactions were studied using OCP- and OCP-Cl_8- as well as the TMP-based Ru-oxidants. Analysis of the results indicates that chlorinating the porphyrin ring has no significant effect on the yield of the dehydrogenated products or catalyst turnover (Table IV.2); more importantly the data show that the reactions are at best marginally catalytic, a result that contrasts with data previously reported.[33] Efforts were made to confirm the more substantial catalysis (100% conversion for a 20:1 amine/Ru ratio) by increasing the *trans*-Ru(TMP)$(O)_2$ and amine

concentrations by a factor of 10, and also stirring the reactions under O_2; however, there were negligible changes in the yield of dehydrogenated products after 24 h. Addition of water or a 1N NaOH (aq) solution to form a biphasic benzene/water (2:1) system does have a significant effect on catalyst turnover and the amine % conversion. In the biphasic systems, the catalyst turnover after 90 h at 50°C (Table IV.3) is increased by a factor of 5 over that for reactions run in benzene alone. Even in biphasic systems, a maximum of 8 turnovers or 39.8% conversion of Ph_2CHNH_2 after 24 h is seen (Table IV.3). The low catalytic activity of *trans*-Ru(porp)$(O)_2$ toward amine oxidation in benzene is not unexpected given the effect of NEt_3 on benzhydrol oxidation catalyzed by *trans*-Ru(TMP)$(O)_2$ (see Table III.5, p.79), i.e. within the difficulty of re-converting the Ru(II)-bis(amine) products to the *trans*-dioxo species. Previous studies have indicated that *trans*-Ru(II)(porp)$(amine)_2$ complexes were likely intermediates in the catalytic oxidation process,[33] and presumably, in the absence of water, regeneration of the dioxo species from these complexes is slow, thus limiting the catalyst turnover. This finding provides further support for the hypothesis presented in Chapter III that water increases the rate of regeneration of Ru(IV)-oxo species from Ru(II) complexes during the catalytic cycle (see eqs. 3.9 and 3.10, p.78). The reason for the discrepancy between the catalyst activity for amine dehydrogenation found in this thesis and the previously reported results[33] could not be elucidated.

Table IV.2. Product Yield and Catalyst Turnover after 24 h for Amine Dehydrogenation Catalyzed by *trans*-Ru(porp)$(O)_2$ Complexes in Air.[a]

		% Yield [Turnover] with Porphyrin Ligand			
Amine	**Product(s)**	**TMP[b]**	**TMP**	**OCP**	**OCP-Cl_8**
Ph_2CHNH_2	Ph_2C=NH	not used	7 [1]	7 [1]	1 [1]
Ph(Me)$CHNH_2$	Ph(Me)C=NH	90 [18]	4 [1]	15 [3]	8 [2]
$PhCH_2NH_2$	PhCN	100 [20]	11 [3]	could not be accurately determined[c]	could not be accurately determined[c]
$(PhCH_2)_2NH$	$PhCH{=}NCH_2Ph$	76 [15]	5 [2]	7 [2]	5 [3]
	PhCN	11	2	2	0
	PhCO	13	4	4	7

[a] Reaction Conditions: 1 mL of benzene solution containing the oxidant and 20 equiv. of the amine heated to 50°C in a sealed vial under 1 atm of air. [*Trans*-Ru(TMP)$(O)_2$] = 4.2 x 10^{-4} M, [*trans*-Ru(OCP)$(O)_2$] = 1.7 x 10^{-4} M and [*trans*-Ru(OCP-Cl_8)$(O)_2$] = 1.8 x 10^{-4} M. Yield and turnover were determined by GC; see Table II.1 (p.27) for separation conditions.

[b] Results previously determined.[33]

[c] Imine signal was to small to give an accurate concentration measurement.

Table IV.3. Aerobic Dehydrogenation of Ph_2CHNH_2 Catalyzed by *Trans*-Ru(TMP)$(O)_2$: The Effect of Neutral and Basic Aqueous/Benzene Biphasic Systems.

Solvent System[a]	**% Yield Ph_2C=NH (24 h, *90 h*)[b]**	**% Yield Ph_2C=O (24 h, *90 h*)[b]**	**Catalyst Turnover (24 h, *90 h*)[b]**
C_6H_6	7.6, *10.7*	3.6, *4*	2, *3*
C_6H_6/water	19.5, *52.4*	5.2, *13.8*	5, *14*
C_6H_6/1N NaOH	29.8, *66*	10, *7.1*	8, *15*

[a] Reaction conditions: 2 mL of a benzene solution containing the oxidant and 21 equiv. of amine were sealed in a vial and stirred at 50°C under 1 atm of air. Biphasic systems had aqueous and benzene phases in a 1:2 ratio by volume. [*Trans*-Ru(TMP)$(O)_2$] = 1.1 x 10^{-3} M.

[b] Yield and catalyst turnover were determined by GC on a HP-17 column; see Table II.1 (p.27) for separation conditions.

Conclusions

Attempts were made to investigate the kinetics of the stoichiometric dehydrogenation of amines by *trans*-Ru(porp)$(O)_2$ species in an effort to understand better the mechanism of these reactions. Unfortunately, repeat experiments gave irreproducible results as both k_{obs} values and absorbance traces at 420 nm or 506-510 nm were different for essentially repeat reactions run with the same amine and similar Ru concentrations (Figures IV.3, IV.5 and IV.7-IV.11). Traces of O_2 remaining in solution, low oxidant concentrations, traces of residual acid from oxidant synthesis, trace water and the amine used were eliminated as the sources of the non-reproducible results; the cause of the problem was not resolved. The reactions, however, did exhibit a light-sensitivity at *trans*-Ru(OCP)$(O)_2$ concentrations of ~ 10^{-4} M (cf. Figure IV.7 and Figure IV.8), the systems showing pseudo first-order absorbance changes at 510 nm for Ph_2CHNH_2 oxidation with *trans*-Ru(OCP)$(O)_2$ in $CHCl_3$, only when the ambient room light was blocked out and a 200-450 nm filter was used. Based on this light-sensitivity, and the problems in obtaining similar results with repeat experiments, it was concluded that stoichiometric amine oxidation by *trans*-Ru(porp)$(O)_2$ should not be studied by UV-VIS spectroscopy. Of note, reactions run under 1 atm of Ar and 1 atm of O_2 produced a similar range of k_{obs} values, indicating that, under the reaction conditions, regeneration of the Ru-dioxo complex from the Ru(II)-bis(amino) intermediate[33] is slower than the dehydrogenation of the amine (Figure IV.5).

The air-oxidation of amines catalyzed by *trans*-Ru(porp)$(O)_2$ with porp = TMP, OCP and OCP-Cl_8 was also investigated in order to determine the effect of chlorinating

the porphyrin ring on the catalyst turnover and yield of dehydrogenation products. Analysis of the reactions after 24 h at 50°C under 1 atm of air indicates that the type of porphyrin ligand used does not affect the catalyst turnover or amine conversion. In fact only 1-3 catalyst turnovers occurred during this time, a result that contradicts the 15-20 turnovers previously attained (Table IV.2).[33] Analysis after 90 h at 50°C did not show improved turnovers, nor did stirring the reactions or running them under 1 atm of O_2. Adding water or a 1N NaOH (aq) solution to the reaction mixture to create a biphasic system, however, yielded up to a 4-fold increase in catalyst turnover after 24 h and a 5-fold increase after 90 h for the oxidation of Ph_2CHNH_2 catalyzed by *trans*-Ru(TMP)$(O)_2$ (Table IV.3). These results support the conclusion found with alcohol oxidation that water accelerates the regeneration of the Ru(VI)-dioxo complex from Ru(II) complexes.

CHAPTER V

CONCLUSIONS AND FUTURE WORK

General Conclusions

The goals set for this thesis were:

1. To investigate the kinetics of the stoichiometric oxidation of *para*-substituted benzhydrols with *trans*-Ru(porp)$(O)_2$ oxidants, in order to help establish the mechanism of alcohol oxidation (porp = TMP, OCP or OCP-Cl_8).
2. As a subsection of goal 1, to determine the role that electronic changes in the alcohol have on the rates of stoichiometric and catalytic oxidations effected by *trans*-Ru(porp)$(O)_2$.
3. To investigate the mechanism of amine oxidation by *trans*-Ru(porp)$(O)_2$.

Kinetic analysis of the stoichiometric oxidation of benzhydrols by *trans*-Ru(TMP)$(O)_2$ reveals that the reaction mechanism proceeds through the formation of a {Ru-alcohol} adduct; subsequent cleavage of the alcohol α-CH bond, probably *via* hydride transfer to the Ru=O moiety, in a rate-determining step leads to the formation of Ru(IV)-bis(alkoxo) and ketone products. Adduct formation is essentially an isenthalpic process and k_1 is characterized by $\Delta H_1^{\ddagger} = 58 \pm 10$ kJ/mol and $\Delta S_1^{\ddagger} = -117 \pm 30$ J/(mol K). Electron-donating substituents favour benzhydrol dehydrogenation.

Oxidation of benzhydrols is catalyzed by *trans*-Ru(porp)$(O)_2$ under 1 atm of air at 50°C, and water is essential for higher catalyst activity. Up to 24 turnovers (98% conversion) is possible in biphasic water/benzene systems using an OCP-Cl_8-based catalyst. Catalytic activity shows a dependence on the type of porphyrin, giving the following order of reactivity: OCP-Cl_8 > TMP > OCP. Limited linear Hammett relationships indicate that electron-donating substituents also favour alcohol oxidation. A comparison of catalyst turnovers for various alchols[32,36] at 50°C under 1 atm of air show the following trends: 1° benzylic > 2° alkylic > 2° benzylic alcohols for reactions in benzene, and 1° benzylic > 2° benzylic > 2° alkylic alcohols in biphasic aqueous/benzene systems.

Information on the stoichiometric oxidation of amines by *trans*-Ru(OCP)$(O)_2$ and *trans*-Ru(TMP)$(O)_2$ could not be obtained as UV-VIS spectroscopic studies of the reaction gave irreproducible results. Trace oxygen, acid, water and the amine are ruled out as the sources of variable experimental results; however, the reactions are light-sensitive. Studies of the aerobic oxidation of amines by *trans*-Ru(porp)$(O)_2$ at 50°C indicate that the reactions are catalytic only in biphasic aqueous/benzene systems, giving ~ 15 catalyst turnovers for Ph_2CHNH_2 oxidation after 90 h; only 3 turnovers occur in the absence of added water. These findings are in a direct contrast to previously reported results,[33] but, the source of the discrepancy was not determined.

Future Work

As only limited Hammett relationships with k_1 and % alcohol conversion were obtained, further investigations of the stoichiometric and catalytic oxidation of other *m*- and *p*-substituted benzhydrols are required in order to establish fully the effect of electronic changes in the alcohol on oxidation.

Attempts to study the stoichiometric dehydrogenation of amines by *trans*-Ru(porp)$(O)_2$ by UV-VIS spectroscopy were not successful and further work using ^{1}H-NMR spectroscopy was continued in this group by Dr. M. Ezhova. The source of the discrepancy in results for aerobic amine oxidations catalyzed by *trans*-Ru(porp)$(O)_2$ must also be determined. If it can be determined, then it may be possible to extend the application of the oxidations to other organic substrates, and increase the catalyst turnover and % substrate conversion. Finally, attempts should be made to elucidate more clearly the role of water in the oxidation of both alcohols and amines catalyzed by *trans*-Ru(porp)$(O)_2$ complexes.

REFERENCES

(1) S. Murahashi, *Angew. Chem. Int. Ed. Engl.*, **1995**, *34*, 2443.

(2) J. G. Muller, J. H. Acquaye and K. J. Takeuchi, *Inorg. Chem.*, **1992**, *31*, 4552.

(3) B. Meunier, *Chem. Rev.*, **1992**, *92*, 1411.

(4) R. R. Engle and C. Djerassi, *J. Am. Chem. Soc.*, **1953**, *75*, 3838.

(5) N. Rajapakse, B. R. James and D. Dolphin, in *New Developments in Selective Oxidation*, eds. G. Centi and F. Trifiro, Elsevier Science Pub., Amsterdam, **1990**, p.109.

(6) W. P. Griffith, *Chem. Soc. Rev.*, **1992**, 179.

(7) W. P. Griffith, *Transition Met. Chem.*, **1990**, *15*, 251.

(8) C. -M. Che and V. W. -W. Yam, *Adv. Inorg. Chem.*, **1992**, *39*, 233.

(9) K. J. Tony, V. Mahadevan, J. Rajaram and C. S. Swamy, *React. Kinet. Catal. Lett.*, **1997**, *62(1)*, 105.

(10) D. G. Lee and L. N. Congson, *Can. J. Chem.*, **1990**, *68*, 1774.

(11) D. D. Agarwal, R. Jain, P. Sangha and R. Rastogi, *Indian J. Chem.*, **1993**, *32B*, 381.

(12) W. -H. Fung, W. -Y. Yu and C. -M. Che, *J. Org. Chem.*, **1998**, *63*, 2873.

(13) (a) C. -M. Che, W. -T. Tang, W. -O. Lee, K. -Y. Wong and T. -C. Lau, *J. Chem. Soc., Dalton Trans.*, **1992**, 1551.

(b) C. -M. Che, W. -H. Leung, C. -K. Li and C. -K. Poon, *J. Chem. Soc., Dalton Trans.*, **1991**, 379.

(c) C. -M. Che, W. -T. Tang, W. -O. Lee, W. -T. Wong and T. -F. Lai, *J. Chem. Soc., Dalton Trans.*, **1989**, 2011.

(d) C. -M. Che, T. -F. Lai and K. -Y. Wong, *Inorg. Chem.*, **1987**, *26*, 2289.

(14) A. J. Bailey, W. P. Griffith and P. Savage, *J. Chem. Soc., Dalton Trans.*, **1995**, 3537.

(15) A. E. M. Boelrijk, T. X. Neenan and J. Reedijk, *J. Chem. Soc., Dalton Trans.*, **1997**, 4561.

(16) R. Tang, S. E. Diamond, N. Neary and F. Mares, *J. Chem. Soc., Chem. Commun.*, **1978**, 562.

(17) M. Matsumoto and N. Watanabe, *J. Org. Chem.*, **1984**, *49*, 3436.

(18) C. Bilgrien, S. Davis and R. S. Drago, *J. Am. Chem. Soc.*, **1987**, *109*, 3786.

(19) R. Lenz and S. V. Ley, *J. Chem. Soc., Perkin Trans. 1*, **1997**, 3291.

(20) I. E. Markó, P. R. Giles, M. Tsukazaki, I. Chellé-Regnaut, C. J. Urch and S. M. Brown, *J. Am. Chem. Soc.*, **1997**, *119*, 12661.

(21) (a) G. -Z. Wang, U. Andreasson and J. -E. Bäckvall, *J. Chem. Soc., Chem. Commun.*, **1994**, 1037.

(b) J. -E. Bäckvall, R. L. Chowdhury and U. Karlsson, *J. Chem. Soc., Chem. Commun.*, **1991**, 473.

(22) (a) J. T. Groves and T. J. McMurry, in *Cytochrome P450: Structure, Mechanism and Biochemistry* (ed. P. R. Ortiz de Montellano), *Chapter 1*, Plenum Press, New York (**1995**).

(b) J. P. Collman, A. S. Chien, T. A. Eberspacher and J. I. Brauman, *J. Am. Chem. Soc.*, **1998**, *120*, 425.

(c) T. L. Poulos, B. C. Finzel and A. J. Howard, *J. Mol. Biol.*, **1987**, *195*, 687.

(23) B. Meunier, in *Metalloporphyrins Catalyzed Oxidations*, eds. F. Montanari and L. Casella, Kluwer Academic Publishers, Dordrecht, **1994**, p.1.

(24) (a) T. Mlodnicka and B. R. James, in *Metalloporphyrins Catalyzed Oxidations*, eds. F. Montanari and L. Casella, Kluwer Academic Publishers, Dordrecht, **1994**, p.121.

(b) D. Dolphin, T. G. Traylor and L. Y. Xie, *Acc. Chem. Res.*, **1997**, *30*, 251.

(25) E. F. Birnbaum, W. P. Schaefer, J. A. Labinger, J. E. Bercaw and H. B. Gray, *Inorg. Chem.*, **1995**, *34*, 1751.

(26) J. T. Groves and K. -H. Ahn, *Inorg. Chem.*, **1987**, *26*, 3833.

(27) J. T. Groves and R. Quinn, *J. Am. Chem. Soc.*, **1985**, *107*, 5790.

(28) M. J. Camenzind, B. R. James and D. Dolphin, *J. Chem. Soc., Chem. Commun.*, **1986**, 1137.

(29) J. T. Groves and J. S. Roman, *J. Am. Chem. Soc.*, **1995**, *117*, 5594.

(30) S. Y. S Cheng and B. R. James, *J. Mol. Catal. A.*, **1997**, *117*, 91.

(31) S. Y. S. Cheng, N. Rajapakse, S. J. Rettig and B. R. James, *J. Chem. Soc., Chem. Commun.*, **1994**, 2669.

(32) S. Y. S. Cheng, *Ph.D. Dissertation*, University of British Columbia, Vancouver, **1996**.

(33) A. J. Bailey and B. R. James, *J. Chem. Soc., Chem. Commun.*, **1996**, 2343.

(34) T. Higuchi, H. Ohtake and M. Hirobe, *Tetrahedron Lett.*, **1991**, *32*, 7435.

(35) H. Ohtake, T. Higuchi and M. Hirobe, *Heterocycles*, **1995**, *40*, 867.

(36) A. J. Bailey, S. Y. S. Cheng, B. R. James, S. J. Rettig and V. G. Young Jr. *to be published.*

(37) D. Mansuy and P. Battioni, in *Metalloporphyrins in Catalytic Oxidations*, ed. R. A. Sheldon, Marcel Dekker Inc., New York, **1994**, p.99.

(38) (a) C. Morice, P. Le Maux and G. Simonneaux, *Tetrahedron Lett.*, **1996**, *37*, 6701. (b) C. Morice, P. Le Maux, C. Moinet and G. Simonneaux, *Inorg. Chim. Acta*, **1998**, *273*, 142.

(39) A. Kamal, P. W. Howard, B. S. N. Reddy, B. S. P. Reddy and D. E. Thurston, *Tetrahedron*, **1997**, *53*, 3223.

(40) S. -I. Murahashi, T. Naota and K. Yonemura, *J. Am. Chem. Soc.*, **1988**, *110*, 8256.

(41) S. -I. Murahashi, T. Naota, N. Miyaguchi and T. Nakato, *Tetrahedron Lett.*, **1992**, *33*, 6991.

(42) S. -I. Murahashi, T. Naota and H. Taki, *J. Chem. Soc., Chem. Commun.*, **1985**, 613.

(43) P. Müller and D. M. Gilabert, *Tetrahedron*, **1988**, *44*, 7171.

(44) A. Goti, F. De Sarlo and M. Romani, *Tetrahedron Lett.*, **1994**, *35*, 6571.

(45) A. Goti and M. Romani, *Tetrahedron Lett.*, **1994**, *35*, 6567.

(46) J. Barrera, S. D. Orth and W. D. Harman, *J. Am. Chem. Soc.*, **1992**, *114*, 7316.

(47) S. Cenini, F. Porta and M. Pizzotti, *J. Mol. Catal.*, **1982**, *15*, 297.

(48) F. Porta, C. Crotti and S. Cenini, *J. Mol. Catal.*, **1989**, *50*, 333.

(49) R. A. Leising, J. S. Ohman, J. H. Acquaye and K. J. Takeuchi, *J. Chem. Soc., Chem. Commun.*, **1989**, 905.

(50) J. -S. Huang, C. -M. Che, Z. -Y Li and C. -K. Poon, *Inorg. Chem.*, **1992**, *31*, 1315.

(51) C. Shista, M. Ke, B. R. James and D. Dolphin, *J. Chem. Soc., Chem. Commun.*, **1986**, 787.

(52) (a)M. Ke, S. J. Rettig, B. R. James and D. Dolphin, *J. Chem. Soc., Chem. Commun.*, **1987**, 1110.

(b)J. P. Collman, P. J. Brothers, L. McElwee-White and E. Rose, *J. Am. Chem. Soc.*, **1985**, *107*, 6110.

(53) S. -M. Au, W. -H. Fung, M. -C. Cheng, C. -M. Che and S. -M. Peng, *J. Chem. Soc., Chem. Commun.*, **1997**, 1655.

(54) W. -H. Leung, T. S. M. Hun, H. -W. Hou and K. -Y. Wong, *J. Chem. Soc., Dalton Trans.*, **1997**, 237.

(55) J. -S. Huang, C. -M. Che and C. -K. Poon, *J. Chem. Soc., Chem. Commun.*, **1992**, 161.

(56) A. Mantovani and S. Cenini. *Inorg. Syn.*, **1976**, *16*, 47.

(57) C. J. Pouchert and J. R. Cambell, *Aldrich Library of NMR Spectra, vol. 4*, Aldrich Chemical Co., U.S., **1974**.

(58) C. J. Pouchert and J. Behnke, *Aldrich Library of ^{13}C and ^{1}H FT-NMR Spectra, edn. I, vol.1*, Aldrich Chemical Co., U.S., **1994.**

(59) J. S. Lindsey and R. Wagner. *J. Org. Chem.*, **1989**, *54*, 828.

(60) (a)D. P. Rillema, J. K. Nagle, L. F. Barringer Jr. and T. J. Meyer. *J. Am. Chem. Soc.*, **1981**, *103*, 56.

(b)D. F. Evans, *J. Am. Chem. Soc.*, **1959**, 2003.

(61) K. Behari, H. Narayan, R. S. Shukla and K. C. Gupta, *Int. J. Chem. Kinet.*, **1984**, *16*, 195.

(62) M. Bressan, L. Forti and F. Ghelfi, *J. Mol. Catal.*, **1993**, *79*, 85.

(63) L. Roecker and T. J. Meyer, *J. Am. Chem. Soc.*, **1987**, *109*, 746.

(64) J. March, *Advanced Organic Chemistry, 4 ed.*, John Wiley and Sons, New York, **1992**, p. 278-286.

(65) P. Dubourdeaux, M. Taverès, A. Grand, R. Ramasseul and J. -C. Marchon, *Inorg. Chim. Acta*, **1995**, *240*, 657.

APPENDIX A

ALCOHOL OXIDATION

UV-VIS Spectroscopic Data

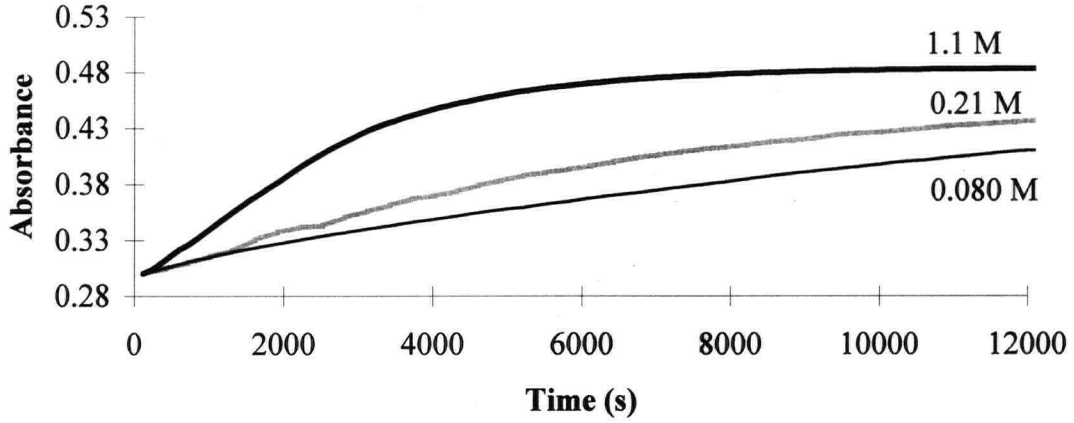

Figure A.1. Typical absorbance versus time plots for spectral changes at 490 nm measured by UV-VIS spectroscopy for the stoichiometric oxidation of Ph_2CHOH by *trans*-Ru(TMP)$(O)_2$ under 1 atm of N_2 in benzene at 25°C.

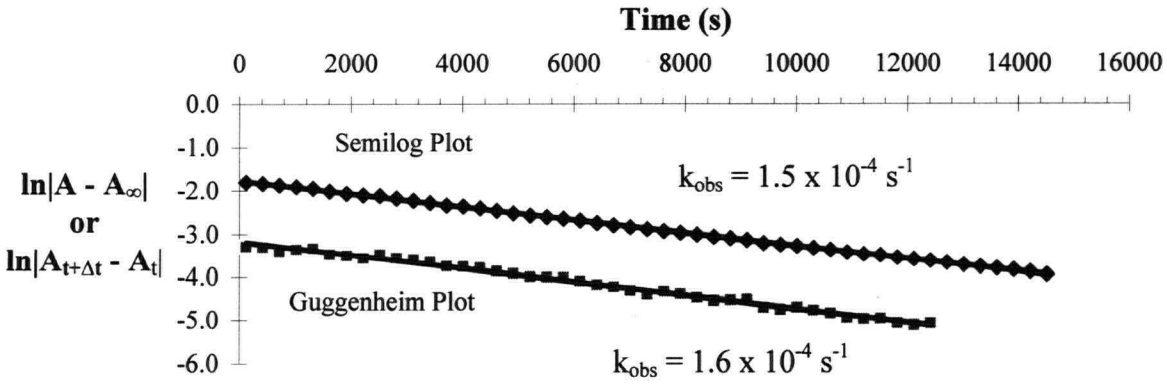

Figure A.2. Semilog and Guggenheim plots for the above reaction at $[Ph_2CHOH]$ = 0.211 M. A_∞ was determined from a computer fit of the absorbance versus time data (these A_∞ values were in agreement with those expected from the known extinction coefficients of the products).

Table A.1. k_{obs} Values for Stoichiometric Oxidation of Ph_2CHOH at 25°C under 1 atm of N_2 in Benzene.

[*Trans*-Ru(TMP)$(O)_2$] x 10^4 (M)	[Ph_2CHOH] (M)	k_{obs} x 10^4 (s^{-1})[a]
3.3	0.021	0.38
2.8	0.022	0.46
2.6	0.022	0.39
2.9	0.079	0.76
3.3	0.080	0.72
3.5	0.080	1.1
3.3	0.21	1.9
4.5	0.21	1.5
3.0	0.21	1.5
0.50[b]	0.20	1.5
2.3	0.40	2.1
1.7	0.40	2.2
2.0	0.40	3.0
2.9	0.60	3.8
3.1	0.60	3.6
3.4	1.1	4.9
0.60[c]	0.027	1.2
0.55[c]	0.027	1.1
0.79[c]	0.027	0.75
3.1[d]	0.25	2.0
3.6[d]	0.51	3.1

[a] Spectral changes were monitored at 490 nm in a 0.1 cm path length cell. A_∞ and k_{obs} were determined from a computer fit of A versus t data; using these A_∞ values gave straight line plots for $\ln|A-A_\infty|$ against time. k_{obs} values determined from Guggenheim plots were within 5% of the values determined by computer fit. A filter was placed between the sample and source in order to block light from 200 - 450 nm.

[b] Run in a 1.0 cm path length cell with the filter.

[c] Run in a 1.0 cm path length cell with no filter; monitored at 422 nm.

[d] Reactions run in the presence of Ph_3COH (0.34 M).

Table A.2. k_{obs} Values for Stoichiometric Oxidation of Ph_2CDOH at 25°C under 1 atm of N_2 in Benzene.

[*Trans*-Ru(TMP)$(O)_2$] x 10^4 (M)	[Ph_2CDOH] (M)	k_{obs} x 10^4 (s^{-1})[a]
2.7	0.21	0.15
2.6	0.21	0.13
2.6	0.38	0.30
2.3	0.70	0.36

[a] Spectral changes were monitored at 490 nm in a 0.1 cm path length cell. A_∞ and k_{obs} were determined from KMS plots of A_t versus $A_{t+\Delta t}$ where Δt = 600-5400 s. Plots of $\ln|A-A_\infty|$ against time, using an average A_∞ determined over Δt = 600-5400 s gave straight lines. k_{obs} values were verified by comparison with those determined from Guggenheim plots. A filter was placed between the sample and source in order to block light from 200 - 450 nm.

Table A.3. k_{obs} Values for Stoichiometric Oxidation of (p-MeO-$C_6H_4)_2CHOH$ at 25°C under 1 atm of N_2 in Benzene.

[*Trans*-Ru(TMP)$(O)_2$] x 10^4 (M)	[(p-MeO-$C_6H_4)_2CHOH$] (M)	k_{obs} x 10^4 (s^{-1})[a]
4.1	0.016	0.48
3.7	0.016	0.95
3.6	0.017	0.57
4.3	0.040	0.85
3.1	0.042	0.73
2.9	0.041	0.73
3.3	0.099	2.3
4.4	0.099	1.5
3.0	0.099	1.3
3.4	0.11	2.3
3.4	0.12	2.7
3.0	0.12	2.3
3.5	0.23	3.6
4.2	0.23	3.5
3.2	0.23	3.8
2.9	0.52	8.1

[a] Spectral changes were monitored at 490 nm in a 0.1 cm path length cell. A_∞ and k_{obs} were determined from a computer fit of A versus t data; using these A_∞ values gave straight line plots for $\ln|A-A_\infty|$ against time. k_{obs} values determined from Guggenheim plots were within 5% of the values determined by computer fit. A filter was placed between the sample and source in order to block light from 200 - 450 nm.

Table A.4. k_{obs} Values for Stoichiometric Oxidation of $(p\text{-F-C}_6\text{H}_4)_2\text{CHOH}$ at 25°C under 1 atm of N_2 in Benzene.

[*Trans*-Ru(TMP)$(O)_2$] x 10^4 (M)	[$(p\text{-F-C}_6\text{H}_4)_2$CHOH] (M)	k_{obs} x 10^4 (s^{-1})[a]
3.0	0.012	0.99
3.4	0.012	0.58
4.7	0.015	1.33
3.3	0.023	1.17
3.0	0.023	0.81
3.0	0.023	0.85
3.3	0.024	1.11
3.2	0.066	0.87
4.5	0.066	0.91
5.2	0.066	0.90
4.0	0.067	1.47
3.1	0.088	1.97
3.6	0.088	1.95
6.5	0.089	1.45
2.9	0.089	2.26
4.0	0.089	1.38
3.8	0.11	1.50
3.7	011	2.19
3.4	0.11	2.02
2.9	0.11	1.85
3.8	0.20	2.65
4.1	0.20	2.24
4.3	0.21	2.44
5.1	0.21	2.36
3.6	0.39	3.22
3.8	0.74	4.13

[a] Spectral changes were monitored at 490 nm in a 0.1 cm path length cell. A_∞ and k_{obs} were determined from a computer fit of A versus t data; using these A_∞ values gave straight line plots for $\ln|A - A_\infty|$ against time. k_{obs} values determined from Guggenheim plots were within 5% of the values determined by computer fit. A filter was placed between the sample and source in order to block light from 200 - 450 nm.

^{1}H-NMR Spectroscopic Data

The initial concentration of *trans*-Ru(TMP)$(O)_2$ was determined from UV-VIS spectroscopy by using a known ε value.[32] For all the reactions run with [alcohol] ≥ 0.02 M, [*trans*-Ru(TMP)$(O)_2$] = 5-7 x 10^{-4} M; for reactions run with [alcohol] ≤ 0.02 M, [*trans*-Ru(TMP)$(O)_2$] = 5 x 10^{-4} M. Unless otherwise mentioned, all of the oxidation reactions were performed under 1 atm of dry N_2.

Table A.5. 20°C, [Ph_2CHOH] = 0.015 M.

Time (s)	Relative intensity of β-H of *trans*-Ru(TMP)$(O)_2$	Relative intensity of Ph_2CHOH α-CH x 10^{-3}
637	59.2	0.329
1237	58.6	0.329
1837	59.9	0.351
2437	58.0	0.368
3037	53.8	0.373
3637	55.9	0.392
4237	49.4	0.394
5437	44.6	0.406
6637	36.7	0.404
7837	29.8	0.402
9637	27.4	0.423
11437	20.4	0.416

Table A.6. 20°C, [Ph_2CHOH] = 0.053 M.

Time (s)	Relative intensity of β-H of *trans*-Ru(TMP)$(O)_2$	Relative intensity of Ph_2CHOH α-CH x 10^{-3}
349	114	0.529
949	103	0.556
1549	93.4	0.558
2149	81.3	0.532

Table A.7. 20°C, [Ph_2CHOH] = 0.057 M.

Time (s)	Relative intensity of β-H of *trans*-Ru(TMP)$(O)_2$	Relative intensity of Ph_2CHOH α-CH x 10^{-3}
277	118	0.503
877	118	0.562
1477	115	0.621
2077	109	0.647
2677	104	0.667
3277	93.2	0.681
3877	86.4	0.695

Table A.8. 20°C, [Ph_2CHOH] = 0.057 M.

Time (s)	Relative intensity of β-H of *trans*-Ru(TMP)$(O)_2$	Relative intensity of Ph_2CHOH α-CH x 10^{-3}
228	132	0.553
828	126	0.553
1428	122	0.559
2028	116	0.564
2628	106	0.572
3228	97.9	0.585
3828	90.0	0.600
5028	68.7	0.603
6228	49.3	0.589
7428	33.4	0.546
8628	21.1	0.475
9828	14.9	0.421
11028	11.0	0.379

Table A.9. 20°C, [Ph_2CHOH] = 0.21 M.

Time (s)	Relative intensity of β-H of *trans*-Ru(TMP)$(O)_2$	Relative intensity of Ph_2CHOH α-CH x 10^{-3}
302	189	1.97
602	178	2.06
902	174	2.19
1202	164	2.27
1502	153	2.37
1802	140	2.39
2102	126	2.16
2702	93.1	1.76

Table A.10. 20°C, [Ph_2CHOH] = 0.21 M.

Time (s)	Relative intensity of β-H of *trans*-Ru(TMP)$(O)_2$	Relative intensity of Ph_2CHOH α-CH x 10^{-3}
352	115	1.71
652	144	1.94
952	137	2.03
1252	127	2.09
1552	119	2.15
1852	108	2.19
2152	94.3	2.20
2752	70.3	1.85

Table A.11. 20°C, [Ph_2CHOH] = 0.20 M.

Time (s)	Relative intensity of β-H of *trans*-Ru(TMP)$(O)_2$	Relative intensity of Ph_2CHOH α-CH x 10^{-3}
352	90.8	1.23
652	115	1.66
952	114	1.75
1252	109	1.79
1552	105	1.84
1852	101	1.87
2452	96.3	1.99
3052	85.1	2.01
3652	76.2	2.04
4252	63.5	2.08

Table A.12. 20°C, [Ph_2CHOH] = 0.62 M.

Time (s)	Relative intensity of β-H of *trans*-Ru(TMP)$(O)_2$	Relative intensity of Ph_2CHOH α-CH x 10^{-3}
302	81.3	3.95
602	77.8	4.27
902	72.8	4.31
1202	65.6	4.34
1502	61.7	4.36
2102	48.9	4.23
2702	40.2	4.09
3302	37.2	4.05
3902	29.6	3.97
4502	23.2	3.93
5102	21.1	3.93
5702	17.8	3.88

Table A.13. 20°C, [Ph_2CHOH] = 0.62 M.

Time (s)	Relative intensity of β-H of *trans*-Ru(TMP)$(O)_2$	Relative intensity of Ph_2CHOH α-CH x 10^{-3}
334	87.2	4.34
634	86.9	4.56
934	84.5	4.69
1234	78.5	4.82
1534	73.6	4.86
2134	65.3	4.97
2734	58.2	5.05
3334	51.2	5.15
3934	42.0	5.16
4534	36.5	5.21
5134	29.4	5.13
5734	23.6	5.07

Table A.14. 20°C, [Ph_2CHOH] = 0.61 M.

Time (s)	Relative intensity of β-H of *trans*-Ru(TMP)$(O)_2$	Relative intensity of Ph_2CHOH α-CH x 10^{-3}
233	84.3	4.64
533	78.4	4.78
833	78.6	4.92
1133	74.0	5.08
1433	71.3	5.18
2033	61.3	5.18
2633	51.0	5.13
3233	43.8	5.18
3833	38.7	5.17
4433	29.6	4.98
5033	26.8	5.02
5633	21.2	4.89
6233	17.0	4.78
6833	14.1	4.74

Table A.15. 20°C, [Ph_2CHOH] = 1.2 M.

Time (s)	Relative intensity of β-H of *trans*-Ru(TMP)$(O)_2$	Relative intensity of Ph_2CHOH α-CH x 10^{-3}
269	52.1	7.81
389	51.3	8.18
509	48.2	8.31
629	48.8	8.39
749	45.6	8.58
869	45.4	8.79
1169	41.4	8.69
1469	41.8	8.80
1769	36.0	9.01
2069	33.7	9.04
2369	31.5	9.02
2669	26.3	8.94
3269	25.0	9.03
3869	19.1	9.01

Table A.16. 20°C, [Ph_2CHOH] = 1.2 M.

Time (s)	Relative intensity of β-H of *trans*-Ru(TMP)$(O)_2$	Relative intensity of Ph_2CHOH α-CH x 10^{-3}
238	62.0	6.86
358	68.7	7.27
658	70.4	7.63
958	67.7	7.90
1258	61.7	7.99
1558	57.2	8.05
1858	55.2	7.97
2158	49.8	8.03
2458	43.0	8.01
3058	38.3	7.97
3658	32.0	7.95
4258	29.6	7.97
4858	24.9	7.79
5458	20.2	7.77

Table A.17. 20°C, [Ph_2CHOH] = 1.2 M.

Time (s)	Relative intensity of β-H of *trans*-Ru(TMP)$(O)_2$	Relative intensity of Ph_2CHOH α-CH x 10^{-3}
293	44.0	8.41
593	51.2	9.21
893	48.1	9.34
1193	38.6	9.22
1493	36.4	9.42
1793	34.9	9.24
2093	28.4	9.36

Table A.18. 20°C, [Ph_2CHOH] = 1.2 M.

Time (s)	Relative intensity of β-H of *trans*-Ru(TMP)$(O)_2$	Relative intensity of Ph_2CHOH α-CH x 10^{-3}
334	48.0	6.30
454	49.0	6.56
754	42.9	6.46
1054	37.8	6.48
1354	37.9	6.70
1654	34.7	6.60
1954	33.2	6.58
2254	28.9	6.57
2854	24.4	6.64
3454	19.4	6.63

Table A.19. 20°C, [Ph_2CHOH] = 0.20 M, [Ph_3CHOH] = 0.41 M .

Time (s)	Relative intensity of β-H of *trans*-Ru(TMP)$(O)_2$	Relative intensity of Ph_2CHOH α-CH x 10^{-3}
445	1.086	0.152
768	1.073	0.149
1040	0.941	0.150
1610	0.668	0.149
2409	0.585	0.148
3210	0.448	0.150
4004	0.361	0.150
4841	0.299	0.150
5637	0.283	0.141

Table A.20. 20°C, [Ph_2CDOH] = 0.022 M.

Time (s)	Relative intensity of β-H of *trans*-Ru(TMP)$(O)_2$	Relative intensity of Ph_2CDOH OH x 10^{-3}
447	68.6	0.642
4047	65.9	0.622
7647	61.2	0.616
11247	64.3	0.644
14847	61.7	0.644
18447	57.2	0.635
22047	55.6	0.642
25647	54.0	0.641
29247	50.5	0.629
32847	51.8	0.644
36447	47.9	0.639
40047	46.7	0.638
43647	43.1	0.633
47247	40.4	0.629

Table A.21. 20°C, [Ph_2CDOH] = 0.024 M.

Time (s)	Relative intensity of β-H of *trans*-Ru(TMP)$(O)_2$	Relative intensity of Ph_2CDOH OH x 10^{-3}
3240	45.7	0.329
6840	43.5	0.338
10440	41.2	0.340
14040	40.0	0.343
17640	37.5	0.339
21240	36.7	0.344
24840	34.0	0.338
28440	31.6	0.336
32040	30.7	0.337
35640	29.8	0.332
39240	27.5	0.325
42840	25.6	0.331
46440	24.7	0.329
50040	23.0	0.325

Table A.22. 20°C, [Ph_2CDOH] = 0.40 M.

Time (s)	Relative intensity of β-H of *trans*-Ru(TMP)$(O)_2$	Relative intensity of Ph_2CDOH OH x 10^{-3}
969	97.8	2.70
4569	97.6	2.83
8169	87.0	2.80
11769	83.5	2.78
15369	74.0	2.84
18969	76.3	2.89
22569	71.7	2.95
26169	66.0	2.97
29769	64.5	2.96
33369	60.9	2.91
36969	53.3	2.96

Table A.23. 20°C, [Ph_2CDOH] = 0.40 M.

Time (s)	Relative intensity of β-H of *trans*-Ru(TMP)$(O)_2$	Relative intensity of Ph_2CDOH OH x 10^{-3}
2007	35.8	1.20
9207	34.1	1.29
12807	32.2	1.27
16407	31.0	1.29
20007	28.4	1.28
23607	27.8	1.29
27207	26.6	1.30
30807	21.5	1.24
34407	21.8	1.26

Table A.24. 20°C, [Ph_2CDOH] = 0.58 M.

Time (s)	Relative intensity of β-H of *trans*-Ru(TMP)$(O)_2$	Relative intensity of Ph_2CDOH OH x 10^{-3}
395	55.4	2.70
3995	58.3	2.83
7595	53.4	2.80
11195	48.5	2.78
14795	45.9	2.84
18395	43.4	2.89
21995	40.2	2.95
25595	37.1	2.97
29195	34.4	2.96
32795	30.6	2.91
36395	29.7	2.96
38195	28.1	2.96

Table A.25. 20°C, [Ph_2CDOH] = 0.58 M.

Time (s)	Relative intensity of β-H of *trans*-Ru(TMP)$(O)_2$	Relative intensity of Ph_2CDOH OH x 10^{-3}
685	56.6	1.74
4285	52.1	1.80
7885	48.6	1.79
11485	46.9	1.80
15085	44.9	1.82
18685	41.3	1.79
22285	38.1	1.79
25885	35.9	1.81
29485	34.8	1.82
33085	31.7	1.80
36685	28.3	1.79
40285	27.1	1.78
43885	26.4	1.80
47485	23.9	1.78

Table A.26. 20°C, [Ph_2CDOH] = 0.58 M.

Time (s)	Relative intensity of β-H of *trans*-Ru(TMP)$(O)_2$	Relative intensity of Ph_2CDOH OH x 10^{-3}
316	87.1	3.93
3916	82.8	4.01
7516	76.8	3.97
11116	72.0	3.97
14716	66.2	3.96
18316	60.3	3.94
21916	57.0	3.91
25516	53.4	3.93
29116	49.3	3.95
32716	45.6	3.92

Table A.27. 20°C, [Ph_2CHOD] = 0.011 M.

Time (s)	Relative intensity of β-H of *trans*-Ru(TMP)$(O)_2$	Relative intensity of Ph_2CHOD α-CH x 10^{-3}
2833	21.3	0.139
3382	24.6	0.139
4228	21.4	0.141
5062	19.7	0.142

Table A.28. 20°C, [Ph_2CHOD] = 0.093 M.

Time (s)	Relative intensity of β-H of *trans*-Ru(TMP)$(O)_2$	Relative intensity of Ph_2CHOD α-CH x 10^{-3}
754	70.7	0.505
1054	71.7	0.532
1354	67.6	0.551
1954	63.0	0.594
2554	60.1	0.625
3154	52.4	0.601
3754	48.5	0.535
4354	43.0	0.507
5554	31.0	0.528
6754	20.7	0.616
7954	12.7	0.585
9154	9.63	0.531
10354	6.90	0.475
11554	6.14	0.435

Table A.29. 20°C, [Ph_2CHOD] = 0.41 M.

Time (s)	Relative intensity of β-H of *trans*-Ru(TMP)$(O)_2$	Relative intensity of Ph_2CHOD α-CH x 10^{-3}
506	1.68	0.139
981	1.61	0.143
1405	1.21	0.136
1828	1.15	0.137
2245	1.07	0.140
3325	0.648	0.127
3959	0.581	0.136
4543	0.468	0.127
5133	0.376	0.130
5908	0.313	0.130

Table A.30. 20°C, [Ph_2CHOD] = 0.74 M.

Time (s)	Relative intensity of β-H of *trans*-Ru(TMP)$(O)_2$	Relative intensity of Ph_2CHOD α-CH x 10^{-3}
508	2.38	0.152
1292	1.63	0.149
1791	1.42	0.150
2340	1.12	0.149
2922	0.893	0.148
3593	0.771	0.150
4243	0.595	0.150
5264	0.427	0.150
7430	0.228	0.141

Table A.31. 20°C, [Ph_2CHOD] = 1.1 M.

Time (s)	Relative intensity of β-H of *trans*-Ru(TMP)$(O)_2$	Relative intensity of Ph_2CHOD α-CH x 10^{-3}
643	61.1	7.32
943	57.4	7.41
1243	51.7	7.40
1843	46.0	7.33
2443	37.5	7.18
3043	29.4	7.22
3643	23.8	7.08
4243	23.0	7.23
4843	20.0	7.13
5443	17.9	7.12
6043	16.6	7.18
6643	13.3	7.17
7843	10.7	7.19

Table A.32. 35.5°C, [Ph_2CHOH] = 0.021 M.

Time (s)	Relative intensity of β-H of *trans*-Ru(TMP)$(O)_2$	Relative intensity of Ph_2CHOH α-CH x 10^{-3}
277	94.4	0.445
469	90.5	0.439
661	87.8	0.444
1003	82.9	0.475
1345	76.0	0.489
1687	68.9	0.493
2029	58.2	0.448
2371	52.5	0.427
2713	43.9	0.392
3055	34.9	0.379

Table A.33. 35.5°C, [Ph_2CHOH] = 0.21 M.

Time (s)	Relative intensity of β-H of *trans*-Ru(TMP)$(O)_2$	Relative intensity of Ph_2CHOH α-CH x 10^{-3}
256	54.1	1.16
598	45.0	1.27
940	39.8	1.32
1282	32.4	1.32
1624	25.5	1.27
1966	20.1	1.20

Table A.34. 35.5°C, [Ph_2CHOH] = 0.20 M.

Time (s)	Relative intensity of β-H of *trans*-Ru(TMP)$(O)_2$	Relative intensity of Ph_2CHOH α-CH x 10^{-3}
248	62.7	1.29
590	56.6	1.51
932	53.0	1.62
1274	47.3	1.70
1616	38.8	1.75
1958	30.7	1.75
2300	25.4	1.77
2942	13.8	1.71
3584	8.43	1.53
4226	8.41	1.50

Table A.35. 35.5°C, [Ph_2CHOH] = 0.20 M.

Time (s)	Relative intensity of β-H of *trans*-Ru(TMP)$(O)_2$	Relative intensity of Ph_2CHOH α-CH x 10^{-3}
253	81.0	1.27
595	79.9	1.44
937	66.3	1.52
1279	57.0	1.57
1621	41.1	1.49
1963	32.2	1.52
2305	24.5	1.57
2947	14.5	1.40
3589	9.68	1.21
4231	8.03	1.17

Table A.36. 35.5°C, [Ph_2CHOH] = 0.40 M.

Time (s)	Relative intensity of β-H of *trans*-Ru(TMP)$(O)_2$	Relative intensity of Ph_2CHOH α-CH x 10^{-3}
309	62.4	3.20
651	49.5	3.24
993	41.1	3.33
1335	33.6	3.34
1677	26.9	3.33
2019	21.6	3.23
2361	16.5	3.14
3003	11.5	2.95
3645	7.01	2.81
4287	4.03	2.63

Table A.37. 35.5°C, [Ph_2CHOH] = 0.40 M.

Time (s)	Relative intensity of β-H of *trans*-Ru(TMP)$(O)_2$	Relative intensity of Ph_2CHOH α-CH x 10^{-3}
350	144	6.92
542	141	7.32
734	128	7.35
1076	114	7.52
1418	101	7.80
1760	84.6	7.82
2402	59.3	7.84
3044	37.7	7.73
4286	16.2	6.71
5528	6.19	6.04

Table A.38. 35.5°C, [Ph_2CHOH] = 0.39 M.

Time (s)	Relative intensity of β-H of *trans*-Ru(TMP)$(O)_2$	Relative intensity of Ph_2CHOH α-CH x 10^{-3}
286	106	4.52
628	80.8	4.43
970	65.2	4.47
1312	57.9	4.60
1654	21.3	3.05

Table A.39. 35.5°C, [Ph_2CHOH] = 0.39 M.

Time (s)	Relative intensity of β-H of *trans*-Ru(TMP)$(O)_2$	Relative intensity of Ph_2CHOH α-CH x 10^{-3}
245	77.982	2.88
587	58.917	3
929	51.609	3.15
1271	45.279	3.15
1613	36.22	3.11
1955	25.998	2.96
2297	20.616	2.81
2939	13.86	2.65
3581	9.894	2.5
4223	7.29	2.38

Table A.40. 50.0°C, [Ph_2CHOH] = 0.021 M.

Time (s)	Relative intensity of β-H of *trans*-Ru(TMP)$(O)_2$	Relative intensity of Ph_2CHOH α-CH x 10^{-3}
275	125	0.731
446	200	1.36
617	159	1.45
788	125	1.41
959	102	1.34
1130	75.3	1.26
1301	52.9	1.26

Table A.41. 50.0°C, [Ph_2CHOH] = 0.10 M.

Time (s)	Relative intensity of β-H of *trans*-Ru(TMP)$(O)_2$	Relative intensity of Ph_2CHOH α-CH x 10^{-3}
257	104	1.44
398	73.9	1.37
539	60.3	1.45
680	44.0	1.33
821	28.1	1.27
962	15.9	1.32

Table A.42. 50.0°C, [Ph_2CHOH] = 0.11 M.

Time (s)	Relative intensity of β-H of *trans*-Ru(TMP)$(O)_2$	Relative intensity of Ph_2CHOH α-CH x 10^{-3}
235	73.6	1.17
376	46.4	1.18
517	31.5	1.23
658	22.7	1.15
799	13.8	1.08
940	10.9	1.14

Table A.43. 50.0°C, [Ph_2CHOH] = 0.20 M.

Time (s)	Relative intensity of β-H of *trans*-Ru(TMP)$(O)_2$	Relative intensity of Ph_2CHOH α-CH x 10^{-3}
234	60.1	1.10
375	43.1	1.71
516	37.1	1.86
657	26.8	1.81
798	20.5	1.80
939	12.3	1.80
1080	7.73	1.74
1221	5.60	1.68
1362	3.64	1.64

Table A.44. 50.0°C, [Ph_2CHOH] = 0.21 M.

Time (s)	Relative intensity of β-H of *trans*-Ru(TMP)$(O)_2$	Relative intensity of Ph_2CHOH α-CH x 10^{-3}
260	96.2	3.24
401	66.8	3.22
542	41.7	3.27
683	30.0	3.21
824	23.8	3.17
965	15.2	3.12
1106	12.1	3.02
1247	6.86	2.89

Table A.45. 50.0°C, [Ph_2CHOH] = 0.31 M.

Time (s)	Relative intensity of β-H of *trans*-Ru(TMP)$(O)_2$	Relative intensity of Ph_2CHOH α-CH x 10^{-3}
272	109	7.97
413	68.8	7.10
554	51.3	6.70
695	37.5	6.57
836	31.6	6.58
977	21.4	6.16
1118	18.6	6.24

Table A.46. 50.0°C, [Ph_2CHOH] = 0.30 M.

Time (s)	Relative intensity of β-H of *trans*-Ru(TMP)$(O)_2$	Relative intensity of Ph_2CHOH α-CH x 10^{-3}
272	129	1.14
413	98.1	1.11
554	73.4	1.10
695	57.7	1.07
836	46.6	1.05
977	36.9	1.00
1118	27.3	0.993

Table A.47. 50.0°C, [Ph_2CHOH] = 0.30 M.

Time (s)	Relative intensity of β-H of *trans*-Ru(TMP)$(O)_2$	Relative intensity of Ph_2CHOH α-CH x 10^{-3}
335	34.7	0.465
476	18.2	0.430
617	12.1	0.411
758	10.3	0.426
899	8.85	0.398

Table A.48. 50.0°C, [Ph_2CHOH] = 0.42 M.

Time (s)	Relative intensity of β-H of *trans*-Ru(TMP)$(O)_2$	Relative intensity of Ph_2CHOH α-CH x 10^{-3}
355	83.4	1.26
496	96.3	1.44
637	58.0	1.44
778	49.5	1.40
919	26.0	1.40

Table A.49. 50.0°C, [Ph_2CHOH] = 0.40 M.

Time (s)	Relative intensity of β-H of *trans*-Ru(TMP)$(O)_2$	Relative intensity of Ph_2CHOH α-CH x 10^{-3}
296	107	1.10
437	89.8	1.11
578	64.6	1.11
719	48.9	1.13
860	40.0	1.10
1001	28.7	1.09
1142	20.2	1.06

Table A.50. 50.0°C, [Ph_2CHOH] = 0.40 M.

Time (s)	Relative intensity of β-H of *trans*-Ru(TMP)$(O)_2$	Relative intensity of Ph_2CHOH α-CH x 10^{-3}
312	93.7	1.59
453	71.9	1.57
594	50.3	1.53
735	45.7	1.52
876	26.7	1.50
1017	19.6	1.47
1158	6.74	1.49

Table A.51. 25°C, [Ph_2CHOH] = 0.71 M, under 1 atm of air.

Time (s)	Relative intensity of β-H of *trans*-Ru(TMP)$(O)_2$	Relative intensity of Ph_2CHOH α-CH x 10^{-3}
788	12.4	0.158
1380	12.5	0.149
1980	9.03	0.155
2530	7.35	0.156
3120	5.25	0.156
3775	5.44	0.148
4230	3.53	0.151
5459	1.73	0.150
6180	1.44	0.150

Table A.52. 25°C, [Ph_2CHOH] = 0.075 M, under 1 atm of dry O_2.

Time (s)	Relative intensity of β-H of *trans*-Ru(TMP)$(O)_2$	Relative intensity of Ph_2CHOH α-CH x 10^{-3}
509	5.72	0.022
1152	4.24	0.022
1836	3.34	0.020
2414	2.79	0.021
3019	2.09	0.022
3566	2.19	0.024
4198	1.53	0.022
4813	1.29	0.021

Table A.53. k_{obs} Values for Stoichiometric Oxidation of Ph_2CHOH under 1 atm of N_2 in Benzene-d_6.

Temperature (°C)	[Ph_2CHOH] (M)	k_{obs} x 10^4 (s^{-1})[a]
20.0	0.015	1.2
	0.053	1.9
	0.057	1.7
	0.057	1.5
	0.20	2.2
	0.21	2.6
	0.21	2.8
	0.61	2.7
	0.62	2.8
	0.62	2.7
	1.2	3.0
	1.2	2.9
	1.2	2.5
	1.2	3.2
35.5	0.021	2.9
	0.20	6.1
	0.20	7.0
	0.21	5.9
	0.39	6.2
	0.39	5.5
	0.40	5.8
	0.40	6.2
50.0	0.021	13
	0.10	24
	0.11	26
	0.20	25
	0.21	24
	0.30	21
	0.30	18
	0.30	24
	0.40	19
	0.40	21
	0.42	23

[a] Values were determined from a plot of ln[*trans*-Ru(TMP)$(O)_2$], determined from the changes in signal intensity of the β-H-atoms of the TMP ring using the alcohol CH signal intensity as an internal standard, versus time. Plots were linear over at least two half-lives.

Table A.54. k_{obs} Values for Stoichiometric Oxidation of Ph_2CDOH at 20°C under 1 atm of N_2 in Benzene-d_6.

[Ph_2CDOH] (M)	**k_{obs} x 10^4 (s^{-1})[a]**
0.022	0.11
0.024	0.13
0.40	0.18
0.40	0.17
0.58	0.22
0.58	0.18
0.58	0.20

[a] Values were determined from a plot of ln[*trans*-Ru(TMP)$(O)_2$], determined from the changes in signal intensity of the β-H-atoms of the TMP ring using the alcohol CH signal intensity as an internal standard, versus time. Plots were linear over at least two half-lives.

Table A.55. k_{obs} Values for Stoichiometric Oxidation of Ph_2CHOD at 20°C under 1 atm of N_2 in Benzene-d_6.

[Ph_2CHOD] (M)	**k_{obs} x 10^4 (s^{-1})[a]**
0.011	0.67
0.093	2.4
0.41	3.1
0.74	3.2
1.1	2.4

[a] Values were determined from a plot of ln[*trans*-Ru(TMP)$(O)_2$], determined from the changes in signal intensity of the β-H-atoms of the TMP ring using the alcohol CH signal intensity as an internal standard, versus time. Plots were linear over at least two half-lives.

APPENDIX B

AMINE OXIDATION

UV-VIS Spectroscopic Data

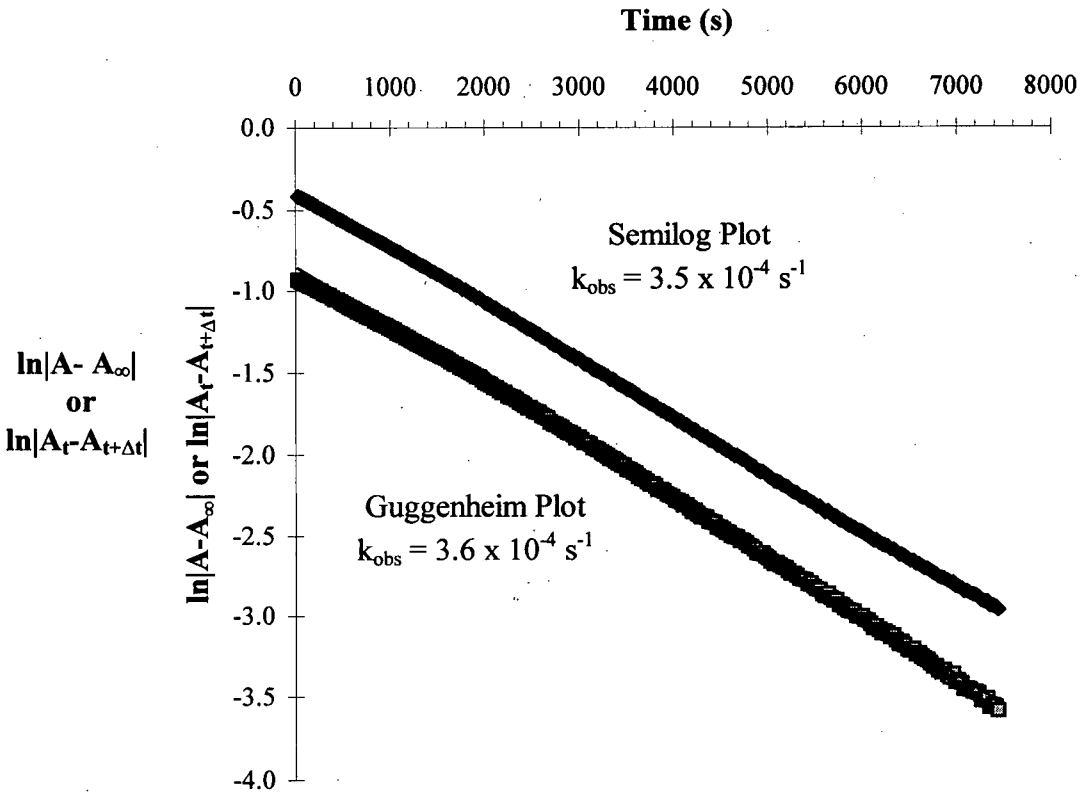

Figure B.1. Comparison of a $\ln|A-A_\infty|$ versus time plot (A_∞ determined from non-linear regression analysis of an absorbance at 420 nm versus time plot) with a Guggenheim analysis of the absorbance data for the oxidation of Ph_2CHOH by *trans*-$Ru(OCP)(O)_2$ under 1 atm of O_2 in dry benzene at 23°C.

Table B.1. Stoichiometric Oxidation of Ph_2CHNH_2 by *trans*-Ru(OCP)$(O)_2$ Under 1 atm Ar at 23°C.

[*trans*-Ru(OCP)$(O)_2$] x 10^6 (M)	[Ph_2CHNH_2] x 10^3 (M)	k_{obs} x 10^4 (s^{-1})[a]
4.7	0.48	4.4
6.3	0.58	2.1
5.7	0.61	2.9
9.2	1.2	3.6
4.5	1.2	6.3
3.7	1.6	7.4
6.8	1.7	8.3
not measured	2.5	4.9
5.1	2.5	9.8
5.2	2.6	8.5
5.8	3.1	9.3
5.8	5.3	5.0
5.8	8.2	7.6

[a] Spectral changes were monitored at 420 nm for reactions occurring in a 1.0 cm path length cell under 1 atm of Ar at 23°C in dry benzene. k_{obs} was determined from the slope of $\ln|A - A_\infty|$ versus time plots; A_∞ was the absorbance at 420 nm at t = 12 h.

Table B.2. Stoichiometric Oxidation of Ph_2CHNH_2 by *trans*-Ru(OCP)$(O)_2$ under 1 atm of O_2.

[*trans*-Ru(OCP)$(O)_2$] x 10^6 (M)	[Ph_2CHNH_2] x 10^3 (M)	k_{obs} x 10^4 (s^{-1})[a]
1.5	0.39	5.47
4.7	0.48	2.24
5.8	0.58	2.33
6.6	0.66	1.62
7.6	0.76	3.26
5.1	1.3	3.4

[a] Spectral changes were monitored at 420 nm for reactions occurring in a 1.0 cm path length cell under 1 atm of O_2 at 23°C in dry benzene. k_{obs} and A_∞ were determined from a non-linear regression fit of $A = A_\infty + (A_o - A_\infty)\exp\{-k_{obs}t\}$ to the A versus t data. These values for k_{obs} were verified by comparison to those determined from a Guggenheim analysis of the absorbance data.

Table B.3. Stoichiometric Oxidation of Ph_2CHNH_2 by *trans*-Ru(OCP)$(O)_2$ at High Concentrations.

[*trans*-Ru(OCP)$(O)_2$] x 10^4 (M)	[Ph_2CHNH_2] x 10^3 (M)	k_{obs} x 10^4 (s^{-1})[a]
4.7	9.4	7.3
4.8	9.6	22
4.9	9.7	16
5.1	10.1	12

[a] Spectral changes were monitored at 510 nm for reactions occurring in a 1.0 cm path length cell under 1 atm of O_2 at 23°C in $CHCl_3$. k_{obs} was determined from the slope of $\ln|A - A_\infty|$ versus time plots; A_∞ was the absorbance at 510 nm at t = 1 h. The reaction vessel was wrapped in Al foil and a filter was placed between the sample and source in order to block out light from 200 - 450 nm.

The amount of absorbance versus time data collected for the stoichiometric oxidations of *i*$PrNH_2$ and *rac*-Ph(Me)$CHNH_2$ by *trans*-Ru(TMP)$(O)_2$ is too large to be reproduced in this appendix. Please see the plots of absorbance versus time in Chapter IV for a pictorial representation of the spectral changes, at 506 and 508 nm respectively, that occurred during the reactions (Figures IV.10 and IV.11).